

**THE ROLE OF SIRT1 IN EXERCISE- AND  
RESVERATROL-INDUCED MUSCLE MITOCHONDRIAL  
BIOGENESIS**

**KEIR J. MENZIES**

A DISSERTATION SUBMITTED TO THE FACULTY OF GRADUATE STUDIES  
IN PARTIAL FULFILMENT OF THE REQUIREMENTS  
FOR THE DEGREE OF

**DOCTOR OF PHILOSOPHY**

GRADUATE PROGRAM IN BIOLOGY,  
MUSCLE HEALTH RESEARCH CENTRE,  
YORK UNIVERSITY,  
TORONTO, ONTARIO

JUNE 2012



Library and Archives  
Canada

Published Heritage  
Branch

395 Wellington Street  
Ottawa ON K1A 0N4  
Canada

Bibliothèque et  
Archives Canada

Direction du  
Patrimoine de l'édition

395, rue Wellington  
Ottawa ON K1A 0N4  
Canada

*Your file Votre référence*

*ISBN: 978-0-494-90350-6*

*Our file Notre référence*

*ISBN: 978-0-494-90350-6*

#### NOTICE:

The author has granted a non-exclusive license allowing Library and Archives Canada to reproduce, publish, archive, preserve, conserve, communicate to the public by telecommunication or on the Internet, loan, distribute and sell theses worldwide, for commercial or non-commercial purposes, in microform, paper, electronic and/or any other formats.

The author retains copyright ownership and moral rights in this thesis. Neither the thesis nor substantial extracts from it may be printed or otherwise reproduced without the author's permission.

#### AVIS:

L'auteur a accordé une licence non exclusive permettant à la Bibliothèque et Archives Canada de reproduire, publier, archiver, sauvegarder, conserver, transmettre au public par télécommunication ou par l'Internet, prêter, distribuer et vendre des thèses partout dans le monde, à des fins commerciales ou autres, sur support microforme, papier, électronique et/ou autres formats.

L'auteur conserve la propriété du droit d'auteur et des droits moraux qui protègent cette thèse. Ni la thèse ni des extraits substantiels de celle-ci ne doivent être imprimés ou autrement reproduits sans son autorisation.

---

In compliance with the Canadian Privacy Act some supporting forms may have been removed from this thesis.

While these forms may be included in the document page count, their removal does not represent any loss of content from the thesis.

Conformément à la loi canadienne sur la protection de la vie privée, quelques formulaires secondaires ont été enlevés de cette thèse.

Bien que ces formulaires aient inclus dans la pagination, il n'y aura aucun contenu manquant.

Canada

## ABSTRACT

The histone deacetylase SirT1 has recently been demonstrated to play a pivotal in cellular metabolic sensing. In response to elevations in  $\text{NAD}^+$ , a key cellular metabolite, SirT1 deacetylates and activates proteins that regulate metabolic pathways and mitochondrial biogenesis. The dysregulation of these SirT1 effects can lead to obesity, diabetes, cancer and cardiovascular disease. Using both cell culture and *in vivo* approaches, we compared the treatment of resveratrol (RSV), an activator of SirT1, to that of exercise to induce mitochondrial biogenesis.

In Chapter 2, the ability of exercise to induce mitochondrial biogenesis was examined with chronic contractile activity (CCA) of C2C12 mouse myotubes through electrical stimulation. The induction of mitochondrial biogenesis with CCA in C2C12 myotubes was then compared to those treated with RSV, or the combination CCA and RSV. Our results demonstrated that CCA produced a more robust induction than RSV treatment. In addition, the combination of CCA and RSV resulted in a synergistic effect on mitochondrial biogenesis. We found that this synergistic effect may be the result of the combined increase in PGC-1 $\alpha$  protein by CCA, and the activation of SirT1 by RSV.

In Chapter 3, we further examined the role of SirT1 in mitochondrial biogenesis through the generation of skeletal muscle-specific SirT1-KO mice. We used voluntary wheel-running exercise, dietary RSV, or a combination of these two treatments to examine role of SirT1 in the induction of mitochondrial biogenesis. These experiments demonstrated that SirT1 plays a modest role in maintaining basal mitochondrial content, and a larger role in preserving mitochondrial function. Voluntary exercise and RSV

treatment induced mitochondrial biogenesis in a SirT1-independent manner. However, when RSV and exercise were combined, a SirT1-dependent synergistic effect was evident, leading to the stimulation of mitochondrial biogenesis.

These data uniquely suggest that SirT1 protein is partly responsible for the maintenance of mitochondria in muscle, in addition to lowering mitochondrial ROS generation and lessening the rate of fatigue. In addition, the therapeutic potential of RSV for the induction of mitochondrial biogenesis and function may rely on the presence of a cellular environment created by repeated energy demands.

## **ACKNOWLEDGEMENTS**

I am thankful to my supervisor Dr. David Hood for his mentorship throughout my PhD candidacy; his support and guidance were essential for my success. Also, thank you to my wonderful labmates who helped me with many conceptual ideas, and provided generous donations of time and expert technical assistance. Most importantly, I would like to thank my family and friends for their continued support, and for excusing my absences from various important events and celebrations. Last but not least, this dissertation is dedicated to my Mother and Grandmother. They both valiantly fought and succumbed to cancer. I miss them and thank them for always being there for me.

## TABLE OF CONTENTS

<b>ABSTRACT</b> .....	iv
<b>ACKNOWLEDGEMENTS</b> .....	vi
<b>TABLE OF CONTENTS</b> .....	vii
<b>LIST OF ABBREVIATIONS</b> .....	xii
<b>DISSERTATION INTRODUCTION AND PURPOSE</b> .....	1
<b>CHAPTER 1: REVIEW OF LITERATURE</b> .....	4
1.1. INTRODUCTION TO SKELETAL MUSCLE.....	5
1.1.1. SLOW AND FAST FIBER TYPES.....	7
1.1.2. SKELETAL MUSCLE MITOCHONDRIAL SUBFRACTIONS.....	9
1.1.3. CELLULAR RESPIRATION .....	11
<i>1.1.3.1. GLYCOLYSIS</i> .....	12
<i>1.1.3.2. KREBS' CYCLE</i> .....	13
<i>1.1.3.3. OXIDATIVE PHOSPHORYLATION</i> .....	14
1.1.4. SKELETAL MUSCLE FATIGUE.....	16
1.2. INTRODUCTION TO SIRT1 .....	19
1.2.1. SIRT1 AND MITOCHONDRIAL TURNOVER .....	19
1.2.2. SIRT1.....	21
<i>1.2.2.1. SIRT1 AND LONGEVITY</i> .....	22
<i>1.2.2.2. SIRT1 ACTIVATION AND TRANSCRIPTION</i> .....	25
<i>1.2.2.3. EXERCISE AND SIRT1</i> .....	26
1.3. NAMPT MODULATION OF NAD <sup>+</sup> AVAILABILITY .....	27
1.4. AMPK .....	29

1.5. METABOLIC SENSING BY THE AMPK-NAMPT-SIRT1 PATHWAY .....	33
1.6. SIRT1-REGULATED MITOCHONDRIAL TURNOVER: BIOGENESIS, AUTOPHAGY AND CIRCADIAN RHYTHM .....	34
1.6.1. MITOCHONDRIAL BIOGENESIS .....	34
1.6.2. AMPK-NAMPT-SIRT1 PATHWAY INDUCED MITOCHONDRIAL BIOGENESIS .....	37
1.6.3. SIRT1 IN AUTOPHAGY .....	39
1.6.4. SIRT1 IN CIRCADIAN RHYTHM.....	44
1.6.5. CONCLUSION .....	49
1.7. DISSERTATION PURPOSES .....	49
1.8. REFERENCES.....	51
<b>CHAPTER 2: CONTRACTILE ACTIVITY AND RESVERATROL EXERT A SYNERGISTIC EFFECT ON MITOCHONDRIAL CONTENT .....</b>	<b>83</b>
Rationale for Chapter 2 .....	84
Abstract.....	87
Introduction .....	88
Methods.....	90
Results .....	93
Discussion .....	103
Acknowledgements.....	108
References .....	109
<b>CHAPTER 3: SIRT1-MEDIATED EFFECTS OF EXERCISE AND RESVERATROL ON MITOCHONDRIAL BIOGENESIS .....</b>	<b>117</b>
Rationale for Chapter 3 .....	118
Abstract .....	120
Introduction.....	122

Methods.....	124
Results .....	129
Discussion .....	138
Acknowledgements .....	144
References .....	145
<b>CHAPTER 4.....</b>	<b>153</b>
Dissertation Summary .....	154
References .....	159
<b>CHAPTER 5: APPENDICIES.....</b>	<b>162</b>
<b>APPENDIX I: ADDITIONAL DATA.....</b>	<b>163</b>
<b>APPENDIX II: PROTOCOLS .....</b>	<b>172</b>
BREEDING STRATEGY TO CREATE MUSCLE-SPECIFIC SIRT1-KO MICE ...	173
GENOTYPING MUSCLE-SPECIFIC SIRT1-KO MICE .....	175
IMMUNOFLUORESCENCE EXPERIMENTS WITH C2C12 MYOTUBES .....	181
MITOCHONDRIAL ISOLATION PROCEDURE FROM SKELETAL MUSCLE..	184
MITOCHONDRIAL RESPIRATION.....	188
ASSESSMENT OF ROS PRODUCTION FROM ISOLATED MITOCHONDRIA.	191
CYTOCHROME C OXIDASE ASSAY FOR MICROPLATE READER.....	197
WESTERN BLOT .....	201
SUMMARY OF SIRT1 ADENOVIRAL WORK .....	209
IN SITU MUSCLE STIMULATION (FATIGUE ASSAY).....	210
NUCLEAR AND CYTOSOLIC FRACTIONATION FROM TISSUE .....	212
<b>APPENDIX III: OTHER PROGRESS DURING PHD CANDIDACY .....</b>	<b>214</b>



## LIST OF FIGURES

<b>CHAPTER 1: REVIEW OF LITERATURE</b> .....	4
Figure 1.1. Schematic of the NAD <sup>+</sup> salvage pathway .....	29
Figure 1.2. The role of SirT1 in muscle mitochondrial turnover.....	35
Figure 1.3. The process of mitophagy .....	41
Figure 1.4. The influence of SirT1 on circadian rhythm .....	46
<b>CHAPTER 2: CONTRACTILE ACTIVITY AND RESVERATROL EXERT A SYNERGISTIC EFFECT ON MITOCHONDRIAL CONTENT</b> .....	83
Figure 1. Acute effect of RSV on C2C12 myotubes .....	97
Figure 2. SirT1 and PGC-1 $\alpha$ expression.....	98
Figure 3. Changes in mitochondrial content.....	99
Figure 4. ROS production and MnSOD expression .....	100
Figure 5. SirT1 and PGC-1 $\alpha$ nuclear localization.....	101
Figure 6. Schematic representation of RSV and CCA induced mitochondrial biogenesis through the activation of PGC-1 $\alpha$ .....	102
<b>CHAPTER 3: SIRT1-MEDIATED EFFECTS OF EXERCISE AND RESVERATROL ON MITOCHONDRIAL BIOGENESIS</b> .....	117
Figure 1. Fatigue response and running distance of WT and SirT1-KO animals.....	133
Figure 2. Total consumption of control or RSV diet and total wet muscle, body and heart weights .....	134
Figure 3. PGC-1 $\alpha$ and Nampt protein expression.....	135
Figure 4. Skeletal muscle COX activity and cytochrome c protein expression .....	136
Figure 5. State 4 and 3 rates of oxygen consumption and reactive oxygen species production in SS mitochondria.....	137
<b>APPENDIX I: ADDITIONAL DATA</b> .....	163
Figure 1. SirT1 activity, SDH and COX histochemical stains, Glucose Tolerance test, COXIV protein and PGC-1 $\alpha$ nuclear localization in SirT1-KO muscle .....	164
Figure 2. pAMPK expression in gastrocnemius muscle following acute stimulation in	

SirT1-KO muscle .....	165
Figure 3. Measurements of autophagy in whole muscle extracts from SirT1-KO mice	166
Figure 4. Indicators for mitophagy measured in whole muscle extracts from SirT1-KO mice .....	167
Figure 5. LC3II protein expression from isolated mitochondria was measured as an indicator of mitophagy in SirT1-KO animals.....	168
Figure 6. Schematic shows a summary of steps for the creation of the SirT1-Flag adenovirus .....	169
Figure 7. SirT1-Flag adenovirus infected C2C12 cells stained with an anti-hexon antibody .....	170
Figure 8. Development of immunoprecipitation protocol to examine PGC-1 $\alpha$ acetylation as a measure of SirT1 deacetylase activity.....	171

## **LIST OF ABBREVIATIONS**

[Ca<sup>2+</sup>]<sub>i</sub> - concentration of intracellular calcium  
[Pi] - concentration of inorganic phosphate  
ACC - acetyl-CoA carboxylase  
AMPK - AMP-activated protein kinase  
AMPKK - AMPK kinase  
ANT - adenine nucleotide translocase  
CaMKK $\beta$  - calcium calmodulin dependent kinase kinase  $\beta$   
CCA - contractile activity  
CK - creatine kinase  
CK - creatine kinase  
COX - cytochrome c oxidase  
COXIV - COX subunit IV  
CR - caloric restriction  
CRY1 and CRY2 - cryptochrome 1 and 2  
CtBP - Carboxylterminal Binding Protein  
DHPR - dihydropyridine receptor  
DMEM - Dulbecco's modified Eagle's medium  
DNA - deoxyribonucleic acid  
e-c coupling - excitation-contraction coupling  
eNOS - endothelial nitric oxide synthase  
ESA - essential for SirT1 activity  
ETC - electron transport chain  
FADH<sub>2</sub> - flavin adenine dinucleotide  
FoxO - forkhead transcription factors  
FTR - fast-twitch red fibers  
FTW - fast-twitch white fibers  
GAPDH - Glyceraldehyde-3-phosphate dehydrogenase  
H<sub>2</sub>DCFDA - 2',7'-dichlorodihydrofluorescein diacetate  
HIC1 - Hypermethylated in Cancer  
HS - horse serum  
IMF - intermyofibrillar  
LKB1 - liver kinase B1  
MHC - myosin heavy chain  
MLC - myosin light chain  
MnSOD - *manganese superoxide dismutase*  
MO25 - Mouse protein 25

mtDNA - mitochondrial DNA  
MTGFM - MitoTracker Green FM  
mtPTP - mitochondrial permeability pore  
*NAD*<sup>+</sup> - Nicotinamide adenine dinucleotide  
NADH - Nicotinamide adenine dinucleotide - reduced form  
NAM - nicotinamide  
Namt - Nicotinamide phosphoribosyltransferase (or visfatin)  
NES - nuclear export sequences  
NLS - nuclear localization sequences  
Nmnat - nicotinamide mononucleotide adenylyltransferase  
NRF-1 and NRF-2 - nuclear respiratory factors 1 and 2  
NUGEMPS - nuclear genes encoding mitochondrial proteins  
O<sub>2</sub><sup>-</sup> - superoxide  
pAMPK - phospho-AMP-activated protein kinase  
pAMPK - phospho-AMP-activated protein kinase  
PCr - phosphocreatine  
PDK4 - pyruvate dehydrogenase kinase 4  
PER1, PER2 and PER3 - Period 1, 2 and 3  
PFK-2 - 6-phosphofructo-2-kinase  
PGC-1 $\alpha$  peroxisome proliferator-activated receptor-gamma coactivator 1 $\alpha$   
RCR - Respiratory Control Ratio  
ROS - reactive oxygen species  
RSV - resveratrol  
RZR - ryanodine receptor  
SCN - suprachiasmatic nucleus  
SERCA1 and SERCA2 - sarco/endoplasmic reticulum Ca<sup>2+</sup>-ATPase 1 or 2  
Sir2 - silent information regulator 2  
SirT1 - Silent mating type information regulator 2 homolog 1  
SR - sarcoplasmic reticulum  
SS - subsarcolemmal  
STR - slow-twitch red fibers  
STRAD - Sterile-20-related adaptor  
TA - tibialis anterior  
TFAM - transcription factor A of the mitochondria  
VO<sub>2</sub> - oxygen consumption  
YY1 - ying-yang 1

**DISSERTATION INTRODUCTION AND PURPOSE  
(PREFACE)**

## **Dissertation Introduction and Purpose**

As the largest organ in the human body, skeletal muscle has demonstrated great adaptive potential in response to physiological and pathophysiological stressors. The most dramatic examples of muscle plasticity occur in mitochondria following exercise training for the maintenance of energy homeostasis. It is the turnover of mitochondria, or the biogenesis and clearance of damaged mitochondria, that promotes healthy muscle. This, in turn, can prevent imbalances in energy homeostasis leading to obesity, diabetes and cardiovascular disease and potentially aging (92; 143). The research interests in our laboratory lie in the molecular mechanisms that govern the process of mitochondrial biogenesis. Despite the vast number of studies on the topic of organelle biogenesis following exercise, many of the detailed cellular pathways remain to be identified. Recently, a conserved family of proteins named sirtuins was shown to regulate various metabolic pathways, and these proteins have emerged as important sensors of energy status. Accumulating evidence indicates that SirT1, a mammalian member of the sirtuin family, may play an important role in the induction of mitochondrial biogenesis following metabolic stress, such as exercise training, and may be an essential link for the prevention of metabolic and age-related diseases. An understanding of how SirT1 is involved in skeletal muscle mitochondrial function and biogenesis forms the main purpose of this project. To address this purpose, we used both a cell culture and *in vivo* model of skeletal muscle to examine the effects of exercise and RSV, a natural phytoestrogen, on SirT1-mediated mitochondrial biogenesis. Using C2C12 mouse

skeletal muscle myotubes we a) examined the ability of RSV to induce mitochondrial biogenesis, and compared this effect to that of chronic contractile activity (CCA), a cell culture model of exercise, b) further delineated the molecular pathways for each of these treatments and their corresponding reliance on PGC-1 $\alpha$  or SirT1 expression and nuclear localization, and c) determined the possibility for a competitive, additive or synergistic response on mitochondrial biogenesis following a combined treatment of CCA and RSV.

To specifically examine SirT1-mediated mitochondrial biogenesis with exercise or RSV treatment, we generated muscle-specific SirT1-KO mice. These mice were either fed dietary RSV, or submitted to a voluntary wheel running protocol. In addition, we combined these two treatments to examine the potential for an ergogenic effect. We hypothesized that both RSV and exercise may act in both a SirT1-dependent, and -independent manner to regulate mitochondrial biogenesis. Therefore, the specific aims of this *in vivo* study were a) to examine the effects of SirT1 protein on basal mitochondrial biogenesis by comparing muscle-specific SirT1-KO to WT animals, b) to determine the role that SirT1 plays in exercise-induced mitochondrial biogenesis, and c) to address the current contention in the literature concerning the dependency of the RSV effect on SirT1.

## **CHAPTER 1: REVIEW OF LITERATURE**

## 1.1. INTRODUCTION TO SKELETAL MUSCLE

Skeletal muscle often performs movements that are a result of a very complex set of interactions that depends on various systems and organs of the body. During a contraction there are many intercellular and intracellular events that ultimately dictate the specific dynamic nature of the muscle. For instance, muscle is composed of an array of fiber types that range from the slow-oxidative to the fast-fatigable types, each having different contractile properties and cellular energetics. Contraction of skeletal muscle requires voluntary activation achieved by a series of action potentials sent from the motor cortex down through the spinal cord to the peripheral nerves via the  $\alpha$ -motoneuron. Activation of this motoneuron results in the release of acetylcholine at the neuromuscular junction and subsequent depolarization of the muscle surface membrane, the sarcolemma. This depolarization causes muscle activation through a process known as *excitation-contraction coupling* (e-c coupling). The key to this activation is the interaction between the voltage-sensing dihydropyridine receptor (DHPR), and the ryanodine receptor (RYR), a  $\text{Ca}^{2+}$  channel in the sarcoplasmic reticulum (SR) that releases  $\text{Ca}^{2+}$  from its storage site in the SR. It is through the increase in  $[\text{Ca}^{2+}]_i$  via the SR that activation of muscle contraction occurs. The resulting magnitude of muscle fiber shortening and force production initiated by calcium binding to troponin and rapidly cycling crossbridges between actin and myosin are controlled by the frequency of nerve firing and the exact oscillatory changes in intracellular  $\text{Ca}^{2+}$  that result. The muscle fibers and the single  $\alpha$ -

motoneuron that innervates them is named a motor unit. During delicate and precise muscle movements, minute gradations of force are achieved by recruiting smaller motor units composed of motoneurons controlling a small number of fibers. In opposition, during activities such as jogging, the body requires larger motor units and during sprinting relies on the activation of all motor units for maximal force production. This recruitment occurs from the smallest to the largest motor unit. In addition, to sustain a prolonged period of force output an asynchronous activation of motor units and a rotation between motor units occurs in order to maintain force output while preventing fatigue. The frequency of motor neuron firing determines the rate of muscle fiber activation. There are therefore three main types of motor units including slow, fast fatigue-resistant, and fast-fatigable. Slow motor units are smaller and are activated at 10-20 pulses per second (Hz), while fast fatigue-resistant and fast-fatigable motor units are activated at 40-80 Hz and 70-250 Hz, respectively.

Being the largest organ of the body, skeletal muscle is not only responsible for locomotion but also for the regulation of fat metabolism and glucose uptake. Under exhaustive physical workloads, fatty acids and glucose act as substrates for aerobic metabolism and ATP production. However, muscles can also depend on glucose as a substrate for anaerobic energy production. Following a meal and the release of insulin, skeletal muscles account for approximately 80% of the total blood glucose uptake, and about half of this is then stored as glycogen.

### **1.1.1. SLOW AND FAST FIBER TYPES**

There are three classes of fiber types that compose skeletal muscle, based on their metabolic and contractile properties. These are designated as slow-twitch red (STR) fibers, fast-twitch red (FTR) fibers and fast-twitch white (FTW) fibers. The slow oxidative STR fibers contain mostly myosin heavy chain (MHC) type I isoform and are resistant to fatigue. FTR fibers possess mainly MHC type IIa isoform and are fast oxidative, but less fatigue resistant than STR fibers. The fast glycolytic and fatigable FTW fibers are composed of mostly MHC type IIb or IIx isoforms. Rodents express all four MHC isoforms, whereas humans do not express type IIb MHC. The majority of skeletal muscles contain a mixture of slow and fast fiber types, with varying biases towards one type depending on the physiological requirements of that particular muscle in the body. The soleus muscle in mice contains approximately 25% STR, 25% FTW and 50% FTR fibers (157). From an energy metabolism perspective, the classification of muscle fiber types based on MHC isoform expression is important because the cross-bridges of fast MHC isoforms consume ATP more rapidly than the slow isoform. In coordination, the fast MHC isoform has a higher rate of cross-bridge cycling compared to the slow isoform. However, despite a pattern of gene expression that goes along with each particular MHC isoform, there is still variation in the intracellular “slow” or “fast” isoforms of other proteins that is controlled by multiple interacting mechanisms (172). For example, the other major ATP consuming protein in skeletal muscle, the

sarcoplasmic reticulum (SR)  $\text{Ca}^{2+}$  pumps, exists in several isoforms. SERCA1 is found in fast type II fibers and SERCA2 in slow type I fibers, with a higher density of pumps in slow fibers (29; 146). Another major factor that affects the oxidative capacity of muscle revolves around mitochondrial content. In humans, there is a larger volume of mitochondria in STR, followed by FTR then FTW fibers (82). There are however, differences in the distribution of mitochondria in fiber types amongst different animal species. For example, in rodents FTR fibers have a higher mitochondrial volume than STR fibers (49; 99). In addition, evidence shows that with the activation of peroxisome proliferator-activated receptor-gamma coactivator 1 $\alpha$  (PGC-1 $\alpha$ ) there is synchronized nuclear and mitochondrial gene expression that coordinates both mitochondrial oxidative capacity and fiber type switching in skeletal muscle (154; 157). However, despite these observations in humans, rats and other species, there has been some recent contention that these events are not linearly associated to each other and are therefore not as coordinated as once thought. This was demonstrated in mice with a global PGC-1 $\alpha$  KO that do not exhibit a change in the fiber-type distribution in skeletal muscle (14; 200) despite having a significant shift from oxidative toward glycolytic muscle fibers (68). Hence, the main phenotypic alterations that occur with higher oxidative capacity, and are not contentious, include a higher percentage of mitochondrial content, capillaries and myoglobin (18; 49; 147; 170; 172).

### **1.1.2. SKELETAL MUSCLE MITOCHONDRIAL SUBFRACTIONS**

Unlike other mammalian organelles, mitochondria originate from other mitochondria since they contain their own DNA. In addition, they contain their own transcriptional and translational machinery. Many mitochondrial components such as ribosomes, transfer RNA molecules and components of their membrane are similar to those of bacteria. It is for these and other similar observations that an extracellular origin for mitochondria was proposed (124; 125). From punctate to reticular, mitochondria vary considerably in shape and size, yet maintain a similar internal architecture. They all have outer membranes surrounding a convoluted inner membrane also known as cristae. This creates two compartments, namely the intermembrane space between these two membranes, and the interior of the mitochondria called the matrix.

Mitochondria convert energy from fats, carbohydrates and proteins into a form that the body can use. They have this ability with the help of 37 genes encoded by mitochondrial DNA (mtDNA) which spans approximately 16,500 base pairs, in addition to 1,500 other genes encoded by nuclear DNA. Of the mitochondrial genes, 13 are necessary for the generation of ATP through oxidative phosphorylation (41). Mitochondria also encode for 22 tRNAs and 2 rRNAs (41).

Mitochondria in skeletal muscle have been subdivided into two functionally and biochemically distinct subfractions named subsarcolemmal (SS) and intermyofibrillar (IMF) mitochondria. As one might assume, SS mitochondria are found beneath the

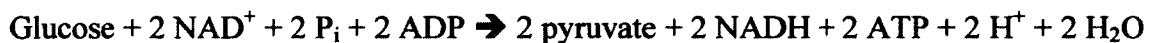
muscle membrane and are proximal to the myonuclei, which are normally found on the periphery of the muscle fiber (81). IMF mitochondria are interspersed between the contractile machinery (81). It has been established that these subpopulations of mitochondria differ functionally in several ways. In rats, they have been shown to have different protein and lipid contents, differential rates of ATP synthesis and protein import, as well as alternate capacities for mitochondrial respiration and endogenous protein synthesis (4; 179). Greater levels of oxidative phosphorylation subunits, carbohydrate metabolism and transport proteins, such as VDAC, are observed in IMF mitochondria (50). In addition, since IMF mitochondria have greater oxidative phosphorylation activity and a higher protein-to-mtDNA ratio, it is hypothesized that this subpopulation is specialized for ATP production, which is necessary to support local myofibrillar ATP demands (50). Alternatively, SS mitochondria express higher levels of chaperone proteins and therefore potentially have a greater capacity for roles against cellular stress and adaptation (4; 50). Both of these subpopulations demonstrate altered oxidative phosphorylation capacity and mitochondrial matrix protein stoichiometry following exercise (3; 81; 105) or muscle disuse (3; 105; 140), however, various studies have shown that with the ensuing metabolic perturbations the SS mitochondrial subpopulation exhibit a more dynamic adaptive response.

### **1.1.3. CELLULAR RESPIRATION**

Cellular reactions that consume energy rely on the conversion of organic carbon structures into usable high energy phosphate bonds of adenosine tri-phosphate (ATP) through a process called cellular respiration. Cellular respiration consists of catabolic reactions that include both the glycolytic and Krebs' cycle pathways, and mitochondrial oxidative phosphorylation. Nutrients are often reducing agents such as carbohydrates, fatty acids and amino acids that can form energy in cells in coordination with the oxidizing agent, or electron acceptor, oxygen. As a result, organisms that consume oxygen as a final electron acceptor in the process of cellular respiration are called aerobic. The final energy storage product of respiration, ATP, is then used to perform biochemical reactions. It has been estimated that ~90% of mammalian oxygen consumption in a normal state is mitochondrial. Of this 90%, approximately 20% is uncoupled by a mitochondrial proton leak and 80% is coupled to ATP synthesis. As for the 80% of oxygen coupled to ATP synthesis, ~25-30% is utilized during protein synthesis, 19-28% is consumed by the  $\text{Na}^+\text{-K}^+\text{-ATPase}$ , 4-8% is used by the  $\text{Ca}^+\text{-ATPase}$ , 7-10% is expended by gluconeogenesis, 2-8% is consumed by actinomyosin ATPase, and 3% is used by ureagenesis, while mRNA synthesis and substrate cycling also take portions of the ATP generated (165). However, these properties differ in a tissue-specific manner and during different physiological stresses.

### 1.1.3.1. GLYCOLYSIS

Glycolysis is a metabolic pathway that converts one molecule of glucose to two molecules of pyruvate in the cytosol of cells. In this anaerobic process, one glucose molecule produces four ATP molecules, in addition to two  $\text{NAD}^+$  molecules that are reduced to NADH, a molecule that can later release energy through aerobic metabolism. However, to prepare glucose for cleavage into two pyruvate molecules the cell must first hydrolyze two ATP molecules to phosphorylate glucose. Therefore, there is a net production of two ATP molecules. This enzymatic reaction involves 9 steps to produce the following equation (165):



This reaction is a preparatory phase for the oxidization of pyruvate that occurs within the matrix of the mitochondria as a prelude to Krebs' cycle. In an aerobic process each pyruvate is oxidized to one acetyl-CoA, an NADH molecule and a  $\text{CO}_2$  molecule by the pyruvate dehydrogenase complex. However, skeletal muscle can also rely on glycolysis as a major source of energy for the cell under anaerobic conditions. In this scenario pyruvate molecules are no longer oxidized in the mitochondria but are instead converted to lactic acid in the sarcoplasm in order to recycle  $\text{NAD}^+$  so that glycolysis can persist. If the rate of lactate production exceeds the rate of lactate removal then there will be a

reduction in cellular pH which more recently has been assigned new roles as a mobile fuel for aerobic metabolism, a mediator of redox state among compartments within and between cells, and an important intermediate for the process of wound repair and regeneration (60). There has been some debate on whether or not lactate anion plays a role in the development of fatigue. More recently, studies examining skinned mammalian muscle fibers have reported only minimal (5%) effects of lactate anion on muscle contractility (151). However, further studies on intact systems are required.

#### *1.1.3.2. KREBS' CYCLE*

Krebs' cycle is also known as the citric acid, or tricarboxylic acid cycle. This process was originally postulated by Hans Krebs, a German biochemist, in 1937 (104). This metabolic cycle is an 8-step process that occurs inside the mitochondrial matrix and involves 18 different enzymes (103). The two acetyl-CoA molecules that arise from the pyruvate dehydrogenase reaction within the cytosol are then metabolized by the Krebs cycle. The pyruvate molecules used to create acetyl-CoA often arise from glucose, however, fatty acids and some amino acids are also used in this cycle once converted into acetyl-CoA or certain other intermediates of Krebs' cycle. Following each turn of Krebs' cycle, three molecules of NADH and one molecule of reduced flavin adenine dinucleotide (FADH<sub>2</sub>) are formed (103; 165). The energy that is trapped as electrons may then later be donated in oxidative phosphorylation to drive ATP synthesis. In

addition to NADH and FADH<sub>2</sub>, one GTP molecule is produced, which may subsequently be utilized by nucleoside-diphosphate kinase to form one molecule of ATP. Waste produced from this reaction includes two molecules of CO<sub>2</sub>, which may diffuse from the mitochondria to leave the cell.

#### *1.1.3.3. OXIDATIVE PHOSPHORYLATION*

Generation of ATP is the purpose of the oxidative phosphorylation machinery. In 1948, Albert Lehninger and Eugene Kennedy discovered that oxidative phosphorylation occurs within mitochondria in eukaryotes. This work led Lehninger and others to describe the specific location of this machinery, on the inner mitochondrial membrane, along with a description of its components, the electron transport chain (ETC) and an ATP synthesizing enzyme. Several substrates fuel oxidative phosphorylation by feeding electrons into the ETC, including NADH and FADH<sub>2</sub>. The result of electron transfer through the ETC is the generation of a potential across the inner mitochondrial membrane. It is through ETC complexes I (NADH dehydrogenase), III (bc<sub>1</sub> complex), and IV (cytochrome c oxidase) that protons are pumped from the matrix into the intermembrane space thus creating the membrane potential. This membrane potential is essential for the production of ATP by the F<sub>0</sub>-F<sub>1</sub> ATP synthase (complex V). As electrons are passed down the ETC, oxygen is reduced to H<sub>2</sub>O by complex IV and ATP is generated by complex V. Oxygen can also be converted into superoxide (O<sub>2</sub><sup>-</sup>), which is a

highly reactive oxygen containing molecule called a free radical, or a reactive oxygen species (ROS). ROS are essential signalling molecules (113), however large quantities of ROS can be harmful to the cell. ROS can cause damage to macromolecules such as DNA, lipids and proteins. In particular, mtDNA is the most susceptible to incur damage from ROS as a result of its close proximity to the ETC. Mutations arise about 10-times more often in mtDNA compared to nuclear DNA (190). These somatic mutations accumulate with age reducing mitochondrial energy production and controlling the aging clock (189). Mutations can also cause, or further the progression of mitochondrial disease, causing the disruption of mitochondrial biogenesis and function.

At the end of the ETC, oxygen accepts the electrons that are passed along and combines with hydrogen to form water. Terminal electron acceptance and cellular oxygen consumption ( $\text{VO}_2$ ) occur at complex IV. The fifth complex of the ETC, the  $\text{F}_0\text{-F}_1$  ATP synthase, is the final multi-subunit complex of the ETC. Located within the inner mitochondrial membrane, this molecular rotary engine generates ATP from ADP and inorganic phosphate ( $\text{P}_i$ ), provided there is a sufficient protonmotive force. The transmembrane protonmotive force is generated through electron transport and is coupled mechanically to the ATP synthase by inducing a rotation of the molecule at a rate of about 100 times per second. Each of these rotations, generated by the movement of 9 protons through the complex, produces 3 ATP molecules. In addition, one proton is used to drive a phosphate translocase, which is a necessary substrate for the generation of ATP. Thus, a total of 4 protons are required for the generation of one ATP molecule.

ADP is also translocated from the cytosol to the mitochondrial matrix as a substrate for ATP synthase. This occurs through an ATP/ADP antiporter called the adenine nucleotide translocase (ANT). Once newly synthesized ATP is formed, it is translocated from the mitochondrion to the cytosol by the carrier protein ANT or by ANT complexed with the outer mitochondrial membrane channel, porin, which form the mitochondrial permeability pore (mtPTP) assembly.

#### **1.1.4. SKELETAL MUSCLE FATIGUE**

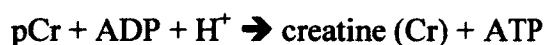
The activity-induced decline in muscle performance as a result of fatigue is highly dependent on the capacity of the aerobic metabolic system. The first form of fatigue, called central fatigue, occurs as a consequence of impaired  $\alpha$ -motor neuron activation and does not rely on the intracellular events within the muscle itself (55). Central fatigue is of greater likelihood during prolonged low-intensity activities since metabolic changes within muscle cells are more limited, while intramuscular factors appear to be important during activities of higher intensity (150). Although not well understood, central fatigue is a central nervous system response to reduce the intensity of exercise under certain circumstances, such as, when body temperatures become high or when glycogen stores are low. Peripheral fatigue is the second form of fatigue that relates to factors within the muscle that impair contractile function during intense exercise. Fatigue can adversely affect all steps of e-c coupling and can manifest as decreased isometric force production,

reduced shortening speed, altered force-velocity relationship, and slowed relaxation (6). Whether it is decreased force production or slowed shortening there would be a decrease in the frequency at which alternating muscle movements can be performed (91). Part of fatigue and the decrease in isometric force is a result of the reduced ability of cross-bridges to generate force and decreased myofibrillar  $\text{Ca}^{2+}$  sensitivity. There is a decrease in  $[\text{Ca}^{2+}]_i$  during fatigue which acts as a safety mechanism. If SR  $\text{Ca}^{2+}$  release remained high, [ATP] would fall to a severely low level that could result in a non-functional muscle cell. When  $[\text{Ca}^{2+}]_i$  declines there is a decrease in cross-bridge energy consumption and the amount of energy required to pump  $\text{Ca}^{2+}$  back into the SR thereby protecting the integrity of the muscle cell.

Acidosis results as a consequence of the anaerobic breakdown of glucosyl units to lactate and hydrogen ions. This was classically known as the main reason for reduced contractile function. However, recent results have shown that acidosis, of the magnitude seen in severely fatigued muscles (approximately 0.5 pH-units), does not have a significant impact on force production, contractile speed, or the rate of fatigue development at physiological temperatures (2; 6; 193; 194). Despite these findings, lactate is still a good indicator of the extent of anaerobic metabolism used by muscles following exercise.

Another consequence of increased energy consumption during anaerobic metabolism is the breakdown of phosphocreatine (PCr), which creates a rise in inorganic phosphate [Pi]. Increases in [Pi] account for approximately 10% of the decline in

maximal force production by decreasing myofibrillar  $\text{Ca}^{2+}$  sensitivity though the reduction of force generating cross-bridges (46). During periods of intense activity, changes in the [ATP]:[ADP] ratio are minimized by the creatine kinase (CK) reaction (22):



Experiments have demonstrated that if there is a lack of CK in muscle fibers there will be no breakdown of PCr (48). Animals lacking CK also show a decline in  $[\text{Ca}^{2+}]_i$  and force produced in muscle fibers during high-intensity stimulation. However, during prolonged lower intensity stimulation these muscle fibers are markedly more fatigue resistant than wild-type fibers (48). This demonstrates that the creation of ATP through the breakdown of pCr by CK may have an integral role in fatigue under conditions of high anaerobic metabolism in skeletal muscle (6).

During increased energy consumption there is an increase in ROS production, which may have adverse effects on muscle function (152). Elevated ROS levels have been proposed to induce fatigue by reducing maximum  $\text{Ca}^{2+}$ -activated force,  $\text{Ca}^+$  sensitivity and SR  $\text{Ca}^{2+}$  release (6; 152). However, low concentrations of ROS production can have important downstream effects to induce beneficial cellular adaptations such as mitochondrial biogenesis. Therefore, the effects of ROS on fatigue may be dependent on the concentration of ROS produced, the acute or chronic nature of induction and the presence of ROS scavengers within the muscle fiber.

## **1.2. INTRODUCTION TO SIRT1**

Sirt1 (Silent mating type information regulator 2 homolog 1) protein has received considerable attention for its potential role in longevity. It has been described as a metabolic protein that can sense and communicate the energy status of a cell to key mechanisms of mitochondrial regulation and energy production. These mechanisms include the biogenesis of mitochondria, the clearance of damaged organelles, and the physiological rhythmicity of gene expression. Elucidation of the pathways involved in Sirt1-mediated mitochondrial turnover ultimately allow for the design of pharmaceuticals for the treatment of degenerative processes that are associated with metabolic and mitochondrial health.

As a metabolic sensing protein, Sirt1 has gained considerable attention as part of an essential signalling rheostat coordinating the energy state of the cell to mitochondrial biogenesis.

### **1.2.1. SIRT1 AND MITOCHONDRIAL TURNOVER**

In eukaryotic cells, the ability to adapt to changes in nutrient availability is a highly conserved mechanism that is dependent on mitochondrial function. From single cell organisms to mammals, mitochondria regulate energy homeostasis by providing the machinery necessary for cells to switch from sugars to fatty acids as a source of energy. In skeletal muscle, changes in mitochondrial content and function occur as a result of

an imbalance in energy homeostasis or chronic insults of cellular stress. Cellular stress induced by caloric restriction (CR) or exercise has been shown to have dramatic effects on skeletal muscle bioenergetics through the alteration of cellular substrate use and/or mitochondrial biogenesis (16; 63; 76; 85).

Like all organelles, proteins and metabolites, mitochondria undergo a process of turnover. Mitochondrial turnover minimizes the deleterious effects of ROS and other reactive molecules on mtDNA, proteins and other mitochondrial macromolecules by selectively degrading damaged and less efficient mitochondria (61). The mitochondrial ETC is one of the main generators of ROS, which, as a result of proximity, can induce mitochondrial damage under situations of disease or stress. Unlike genomic DNA, mtDNA lacks protective histones and is thereby vulnerable to nearby oxidative attack. Additionally, mitochondria that are functionally compromised have been shown to produce even more ROS, leading to the acceleration of degenerative processes, such as aging. To fully understand the role of mitochondria in cellular longevity and health, it is important to comprehend the essential balance between mitochondrial biogenesis and autophagy, the process which degrades damaged mitochondria, thus maintaining a proper rate of mitochondrial turnover. Another important consideration in the turnover of mitochondria involves the circadian rhythm of the cell, or molecular clock, which can regulate many of the proteins and enzymes necessary for these processes on a diurnal rhythm, entrained by the cellular environment (40).

During exercise and CR, three proteins have recently emerged as important for regulating and coordinating skeletal muscle bioenergetics. These include the NAD<sup>+</sup>-dependent deacetylase SirT1, AMP-activated protein kinase (AMPK) and Nicotinamide phosphoribosyltransferase (Nampt) (45; 53). Evidence summarized in this review of literature helps to demonstrate how the Nampt-SirT1-AMPK metabolic-sensing pathway plays a dominant role in mitochondrial turnover by influencing mitochondrial biogenesis, autophagy and circadian rhythm.

### **1.2.2. SIRT1**

In mammals there are seven sirtuin proteins (SirT1-7) that share a common catalytic core domain that possesses NAD<sup>+</sup>-dependent deacetylase activity. In contrast to this core domain, each sirtuin protein possesses distinct N- and C-terminal extensions that define both its subcellular function and activity. The SirT1 gene spans approximately 34kb and includes 9 exons. This encodes for a 747 amino acid protein that contains a sirtuin homology domain, the conserved catalytic domain for deacetylation, in the middle of the protein (aa 261-447). SirT1 also contains two functional nuclear localization sequences (NLS) and two nuclear export sequences (NES) that are responsible for the nucleo-cytoplasmic shuttling of the protein (180). The nuclear-cytoplasmic distribution of SirT1 can be altered by cellular events such as differentiation, and this distribution determines its ability to interact with distinct substrates in various subcellular

compartments (79). For example, SirT1 is nuclear in proliferating C2C12 myoblasts, while it is cytoplasmic in differentiated cells. However, recent studies demonstrate that SirT1 nuclear localization in proliferating C2C12 cells can be inhibited by blocking the PI3K/AKT signalling pathway. Although not typically activated downstream of PI3K, JNK appears to be involved in this process since it can enhance SirT1 nuclear localization and enzymatic activity through the phosphorylation of SirT1 at Ser27, Ser47, and Thr530 (137).

#### *1.2.2.1. SIRT1 AND LONGEVITY*

Sirtuin proteins have been implicated in the regulation of cellular processes associated with longevity that range from, but are not limited to, DNA repair (30; 127), transcriptional silencing (1; 12) and apoptosis (133) to nutrient sensing (163), fatty acid oxidation (58) and protein synthesis (59). SirT1 is a mammalian orthologue of the yeast protein silent information regulator 2 (Sir2) and has been associated with longevity in worms and yeast (67; 94; 182). However, studies by Burnett et al. (33) found that since the genetic backgrounds of both the yeast and worms in these studies were not controlled for, these findings appeared to be a result of insufficient backcrossing as opposed to Sir2 expression. Nonetheless, recent evidence still suggests that Sir2 is involved in metabolic health and longevity (64; 161; 188). In mammals, survival and metabolic health benefits have been associated with the SirT1 deacetylation of proteins, such as PGC-1 $\alpha$  (138), p53

(121; 186), Ku70 (90), forkhead transcription factors (FoxO) (191), and histones (25), thus promoting mitochondrial biogenesis, cell survival and attenuating apoptosis.

#### *1.2.2.2. SIRT1 INDUCTION THROUGH CALORIC RESTRICTION*

In yeast, worms and flies, Sir2 has been described as a link between CR and longevity (117; 164; 182). Each of these organisms exhibited increased Sir2 activity and/or expression during CR. CR is the sole intervention that extends lifespan in mammals and improves survival in non human primates (43; 110; 166). In addition, transgenic mice that overexpress SirT1 exhibit similar effects as those treated by CR. This includes an increase in whole-body metabolic efficiency via mitochondrial biogenesis and a reduction of high fat diet-induced metabolic damage (19; 148). More recently, it was also shown that moderate overexpression of SirT1 in mice resulted in decreased expression of the ageing-associated protein p16 (Ink4a), lower levels of DNA damage, and fewer carcinomas and sarcomas (77). CR has also been proposed to induce mitochondrial biogenesis in human muscle as evidenced by increases in mitochondrial regulatory proteins SirT1, PGC-1 $\alpha$  and TFAM, along with an elevation in mtDNA content (42). The induction of mitochondrial biogenesis has also been demonstrated in HeLa cells and rat hepatocytes that were treated with serum from CR rats (120). This resulted in an increase in PGC-1 $\alpha$  protein, along with other mitochondrial regulatory proteins, in addition to markers of mitochondrial mass and content. These CR serum-

treated cells also exhibited reductions in membrane potential and ROS generation, thereby diminishing the damage of mtDNA. In addition, Nisoli et al. (2005) demonstrated that CR resulted in an endothelial nitric oxide synthase (eNOS)-dependent increase in SirT1 and mitochondrial biogenesis in various tissues of mice (139). Anderson et al. (9) confirmed the increase in SirT1 and PGC-1 $\alpha$  within white adipose tissue of 10 month old mice subjected to 40% CR from 8 weeks of age. Similarly, they showed increases in PGC-1 $\alpha$  and SirT1 in skeletal tissue following an oxidative stress treatment. In opposition, Hancock et al. (2010) examined a wide range of mitochondrial proteins in rats following a 14 week period of 30% CR. They did not demonstrate the induction of mitochondrial biogenesis as found by other groups in heart, brain, liver, adipose tissue or skeletal muscle. Perhaps the divergent findings in these studies are a result of the magnitude and/or the duration of the CR. Several studies which employed 40-50% reductions in caloric intake have found evidence of mitochondrial biogenesis in rats (17; 111). Lee et al. (1998) showed that a 50% CR reduction in rats produced fewer mitochondrial abnormalities and deleted mitochondrial genomes with age than when a 35% CR was used. There may also be divergent thresholds for adaptation to CR in mice, compared to rats. In any event, the bulk of the evidence appears to indicate a potential role for an increase in SirT1 activity within muscles following CR.

#### **1.2.2.2. SIRT1 ACTIVATION AND TRANSCRIPTION**

This induction of SirT1 (i.e. activity and expression) is important to clarify, because of its role in mediating downstream events related to mitochondrial biogenesis and function. SirT1 contains a deacetylase core that is only active when its own C-terminal domain, a 25 amino acid sequence that is essential for SirT1 activity (ESA), allosterically interacts with it (96). The endogenous SirT1 inhibitor DBC1, which also binds to the deacetylase core, competes with and inhibits the ESA domain (96). Importantly, the process of SirT1 deacetylation requires  $\text{NAD}^+$  as an acceptor molecule for the acetyl group. This SirT1 catalyzed reaction involves the breakdown of one  $\text{NAD}^+$  molecule for each deacetylated acetyl lysine. While SirT1 activity is directly regulated by the  $\text{NAD}^+/\text{NADH}$  ratio, it appears that this ratiometric indicator of cellular redox state is also important for the transcription of SirT1, as shown in primary human fibroblasts (201). An increase in the  $\text{NAD}^+/\text{NADH}$  ratio has been shown to deactivate an inhibitory complex on the SirT1 promoter that contains the redox sensor transcriptional corepressor CtBP (Carboxylterminal Binding Protein) and the transcriptional repressor HIC1 (Hypermethylated in Cancer; (201), leading to enhanced transcription of the SirT1 gene. In addition to  $\text{NAD}^+/\text{NADH}$  regulation of SirT1 expression, it has also been shown that an increase in free fatty acids, can act as a ligand for  $\text{PPAR}\delta$ , which can then activate SirT1 transcription through the enhanced binding of Sp1 to the SirT1 promoter in human hepatocyte-derived cells (141). This activation of SirT1 was shown to be increased by the

addition of GW501516, a selective PPAR $\delta$  agonist, or inhibited by the Sp1 antagonist, mithramycin (141). Therefore, the physiological mobilization of free fatty acids during caloric restriction, or possibly exercise (52), may be an important mechanism for the induction of SirT1 expression in skeletal muscle.

#### *1.2.2.3. EXERCISE AND SIRT1*

Holloszy et al. (80) was the first to demonstrate that endurance exercise in rats increased the ability of trained muscle to produce ATP through oxidative phosphorylation. More recently, there has been an interest in whether SirT1 expression or activity is proportional to mitochondrial oxidative capacity, and whether exercise can provoke an increase in SirT1 levels or activation, in parallel with adaptive increases in oxidative capacity. However, some evidence has shown that SirT1 expression is not proportional to mitochondrial content across various tissues under steady state conditions. For example, soleus muscle exhibits higher SirT1 expression than in the heart, yet the heart contains considerably more mitochondria than soleus (39). Also, following chronic exercise (multiple bouts of prolonged exercise) in rats, Gurd et al. (66) illustrated a negative correlation between SirT1 expression and an important regulator of mitochondrial biogenesis, PGC-1 $\alpha$ , along with COXIV and citrate synthase, two indicators of mitochondrial content. In addition, SirT1-KO mice exhibited normal mitochondrial content in skeletal muscle throughout development, suggesting that SirT1

expression is not important for the maintenance of basal mitochondrial content (27). In contrast, several studies have illustrated an increase in SirT1 expression with exercise in old (145) or adult (177) rat skeletal muscle. Our laboratory has also demonstrated increases in SirT1 activity with chronic electrical stimulation in rat skeletal muscle, however, this effect was not observed with voluntary running-induced mitochondrial biogenesis (39). Pauli et al. (2010) showed that SirT1 expression decreased with age and recovered following a single, acute bout of intense exercise, while, in direct contrast, Koltai et al. (2010) examined the same muscle in Wistar rats and found that there were elevated amounts of SirT1 protein with aging, which were then reduced with chronic exercise training. However, in humans, both an acute bout of sprint exercise (65), or high intensity training for 2 weeks (118) resulted in elevated SirT1 protein content. Thus, it is apparent from this diverse set of results that more clear evidence is required to understand the relationship between SirT1 expression/activity, and exercise-induced mitochondrial biogenesis. Future work could focus on the enzymatic activity of this protein, as reflected by *in situ* protein deacetylation. Commercially available SirT1 deacetylation assays performed under optimal conditions *in vitro* are indicators of SirT1 protein content within the tissue, and cannot be interpreted to indicate the activity of the enzyme within the cell.

### **1.3. NAMPT MODULATION OF NAD<sup>+</sup> AVAILABILITY**

The enzymatic activity of SirT1 can be modulated by several physiological

cofactors and inhibitors.  $\text{NAD}^+$  is required for various processes in the cell that include, acting as a cofactor in redox reactions during glycolysis, Krebs' cycle, and during the catabolism of carbohydrates, fats, proteins and alcohols. It has also been shown to participate in transcription, DNA repair, G-protein coupled signalling and intracellular calcium signalling (26; 56). As a result of these many requirements, the available  $\text{NAD}^+$  for SirT1 activity is limited despite seemingly high intracellular concentrations ranging from 300-400 $\mu\text{M}$  (26; 36; 75; 102; 163). SirT1 requires  $\text{NAD}^+$  as a co-substrate for the deacetylation of proteins, and it can be inhibited by both NADH (116) and nicotinamide (NAM), a by-product of  $\text{NAD}^+$  metabolism (23). The cycling from  $\text{NAD}^+$  to NAM has been termed the  $\text{NAD}^+$  salvage pathway. The rate-limiting enzyme that converts NAM to  $\text{NAD}^+$  is nicotinamide phosphoribosyltransferase (Nampt, or visfatin; Fig 1.1.) (160). Interestingly, the yeast ortholog of mammalian Nampt, PNC1, is essential for SirT1-dependent lifespan extension during CR (10). Thus, Nampt may serve a similar role in the regulation of longevity in mammals. Similar to SirT1, Nampt expression has been shown to increase in cells that are either deprived of serum (199) or glucose (53), and in skeletal muscles of fasted mice (53). Nampt expression also appears to increase in skeletal muscle with aerobic exercise training of both rats and humans (45; 102). Thus, despite controversy over whether SirT1 expression is altered with varying models of exercise, an increase in Nampt expression may produce increased  $\text{NAD}^+$  levels and lead to an overall increase in cellular SirT1 activity.

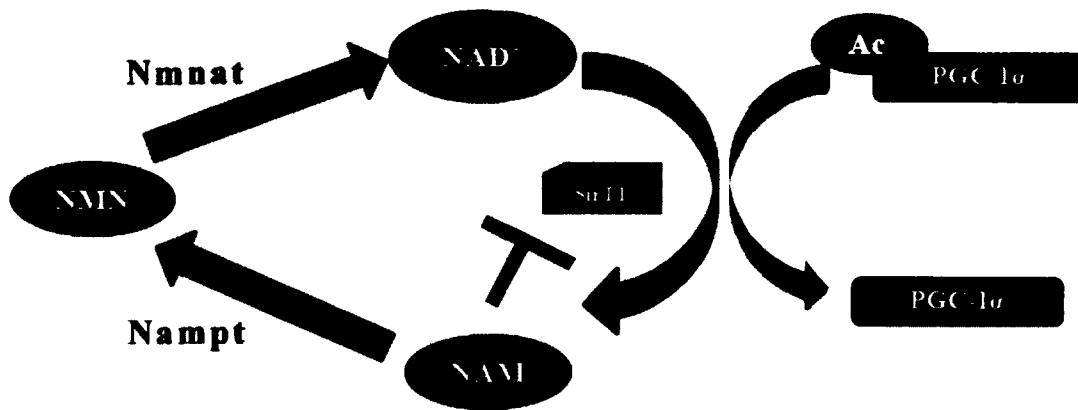


**Figure 1.1.** Schematic of the NAD<sup>+</sup> salvage pathway. NAD<sup>+</sup>, a cofactor for the process of SirT1 deacetylation, is recycled from nicotinamide (NAM) in two steps by Nampt and Nmnat enzymes. SirT1 catalyzes the initial attack of acetyl-lysine on proteins, such as PGC-1 $\alpha$ , along with the cleavage of the nicotinamide ribosyl bond of NAD<sup>+</sup> to form NAM. Nampt is the key regulator and rate-limiting enzyme for this process. Nampt can be induced by fasting and exercise, and its expression cycles every 24 hrs as part of the circadian clock. Nampt, nicotinamide phosphoribosyltransferase; Nmnat, nicotinamide mononucleotide adenylyltransferase.

#### 1.4. AMPK

AMPK is a Ser/Thr kinase that functions as a mediator of cellular metabolism. AMPK can rapidly phosphorylate metabolic enzymes, such as acetyl CoA carboxylase (ACC) for fatty acid oxidation, or it can phosphorylate proteins that regulate gene expression, such as PGC-1 $\alpha$  (88) and FoxO3a (62). AMPK contains a catalytic  $\alpha$  subunit and two regulatory subunits,  $\beta$  and  $\gamma$ . There are two  $\alpha$  ( $\alpha$ 1 and  $\alpha$ 2) and  $\beta$  ( $\beta$ 1 and  $\beta$ 2) subunit isoforms, while there are three forms of the  $\gamma$  ( $\gamma$ 1,  $\gamma$ 2 and  $\gamma$ 3) subunit (71). Of the two  $\alpha$  subunit isoforms,  $\alpha$ 2 is the more readily expressed isoform in skeletal muscle, heart and liver (173). It is localized predominantly within the nuclei of these cells (5). Phosphorylation of the  $\alpha$  subunit by upstream kinases such as liver kinase B1 (LKB1) and calcium calmodulin dependent kinase kinase  $\beta$  (CaMKK $\beta$ ) following processes that consume ATP, such as exercise, results in AMPK activation (174). The  $\beta$  subunit of AMPK is responsible for binding the  $\alpha$  and  $\gamma$  subunits (183), while the  $\gamma$  subunit is responsible for the sensitivity of AMPK to increases in the cellular AMP/ATP ratio (198). When the  $\gamma$  subunit of AMPK interacts with AMP, there is a reduction in the ability of AMPK to act as a substrate for the  $\alpha$  subunit Thr172 phosphatase, which results in an increased likelihood for Thr172 phosphorylation (168). In addition, the resulting conformational change allows for the phosphorylation of a residue within the activation loop on the  $\alpha$ -subunit by upstream kinases LKB1 (171) or CaMKK $\beta$  (74).

LKB1, a Ser/Thr kinase, requires the formation of a heterotrimeric complex with STRAD (Sterile-20-related adaptor) and MO25 (Mouse protein 25) to specifically activate the  $\alpha 2$  subunit (51; 167). However, most evidence would indicate that LKB1 in physiological settings the LKB1/STRAD/MO25 complex is constitutively active (167). This would indicate that the regulation of AMPK is more dependent on changes in phosphatase activity rather than changes in kinase activity. LKB1 has still proven to be the major AMPK kinase (AMPKK) in muscle since muscle-specific LKB1 KO mice display severely impaired AMPK $\alpha 2$  phosphorylation following ex-vivo contraction (167). Other work has shown that CaMKK acts on AMPK independently of changes in AMP (176). CaMKK may therefore be the main AMPKK during the initial phase of mild-tetanic muscle contraction (89). In agreement with this hypothesis, the overexpression of CAMKK $\alpha$  or CAMKK $\beta$  in muscle is enough to increase AMPK phosphorylation (195).

Since AMPK activity is under control of the AMP/ATP ratio, AMPK functions to restore ATP concentrations by activating energy-producing processes such as mitochondrial biogenesis and the oxidation of fatty acids (37; 70). Adenylate kinase transforms two ADP molecules into one ATP and one AMP, thereby creating a sensitive measure of metabolic disturbances (72). These disturbances relate to crisis situations where ATP synthesis is compromised, for example, during low caloric intake, ischemia and hypoxia, or when ATP consumption is accelerated. When ATP levels are disturbed the increase in AMP induces more than a 1000-fold activation of phosphorylated

AMPK (176). Increases in ATP consumption, which occur with muscle contraction, can therefore lead to the compensatory activation of AMPK to initiate processes related to energy production.

Another rapid consequence of AMPK activation in skeletal muscle involves the elevation of glucose uptake via the induction of GLUT4 translocation to the plasma membrane (108). In addition to the resulting influx of glucose, AMPK activation decreases glycogen synthesis rates (38) along with increasing the phosphorylation of 6-phosphofructo-2-kinase (PFK-2) to catalyze the synthesis of fructose 2,6-biphosphate, a strong stimulator of glycolysis (126). AMPK is therefore responsible for the mobilization of glucose into ATP-generating processes while inhibiting glycogen synthesis.

AMPK can also stimulate fatty acid oxidation in order to increase ATP production. This occurs through AMPK phosphorylation and inhibition of ACC 1 and 2 isoforms (73). ACC catalyzes the reaction forming malonyl-CoA from acetyl-CoA, which constitutes the initial step in lipid hydrolysis (73). Malonyl-CoA is an allosteric inhibitor of CPT-1b, the protein responsible for fatty acid intake into mitochondria for  $\beta$ -oxidation. As a result, through the inhibition of ACC, AMPK prevents the inhibition of CPT-1b causing an increase in  $\beta$ -oxidation of fatty acids. The induction of  $\beta$ -oxidation in coordination with an increased glycolytic rate stimulates ATP synthesis to meet cellular energy demands.

## **1.5. METABOLIC SENSING BY THE AMPK-NAMPT-SIRT1 PATHWAY**

AMPK has been shown to have convergent properties with SirT1 by linking energy levels to longevity. For example, an increase in lifespan was observed when the AMPK  $\alpha$  subunit was overexpressed in *C. elegans* (13). In addition, AICAR, a well known activator of AMPK, can increase SirT1 activity. In glucose restricted primary skeletal myoblasts AMPK can also be activated (53) and this leads to the induction of Nampt transcription. The resulting increases in the  $\text{NAD}^+/\text{NADH}$  ratio, serves to activate SirT1 and then provides a clear mechanistic link between the activation of AMPK and an increase in SirT1 activity (53). Once SirT1 is activated it can then bind to, and deacetylate, the myogenic regulatory factor MyoD, inhibiting it from inducing myogenesis (53). Thus, in order to maintain an energy balance when glucose stores are low, the AMPK-Nampt-SirT1 signalling pathway has been shown to delay the energy consumption involved in muscle growth. It also acts to promote energy production in skeletal muscle via the induction of mitochondrial biogenesis through the coactivation of PGC-1 $\alpha$  (36). To illicit further energy savings in muscle, SirT1 acts as a major repressor of the mitochondrial uncoupling protein UCP3, a protein that is known to dissipate energy in the mitochondria (8). In contrast, when nutrients are readily available, AMPK is not active, and UCP3 is upregulated to protect the cell from an overload of fatty acids and the resulting production of reactive oxygen species. These data suggest a model for an AMPK-Nampt-SirT1 pathway that can regulate the metabolic state, thus deciding

between the transition between catabolism and anabolism. This pathway can act as a master switch that can stop energy demanding processes during times of reduced nutrient availability, while increasing energy savings and production through sources that include mitochondrial biogenesis.

## **1.6. SIRT1-REGULATED MITOCHONDRIAL TURNOVER: BIOGENESIS, AUTOPHAGY AND CIRCADIAN RHYTHM**

### **1.6.1. MITOCHONDRIAL BIOGENESIS**

The abundance of mitochondria within cells is proportional to the energy requirements of the tissue. Chronic changes in the energy balance of a cell therefore often produce predictable changes in mitochondrial abundance. As metabolic sensors for energy stores, AMPK and SirT1 modify mitochondrial content via regulation of the important transcriptional coactivator PGC-1 $\alpha$  (Fig. 1.2.). There are approximately 1500 proteins that are nuclear-encoded and imported into the mitochondria during mitochondrial biogenesis. There are also 13 protein subunits encoded by mtDNA that are essential components of the mitochondrial ETC. As a master regulator, activated PGC-1 $\alpha$  induces the expression of nuclear respiratory factors (NRF-1 and NRF-2) and transcription factor A of the mitochondria (TFAM), which coordinate the transcription of

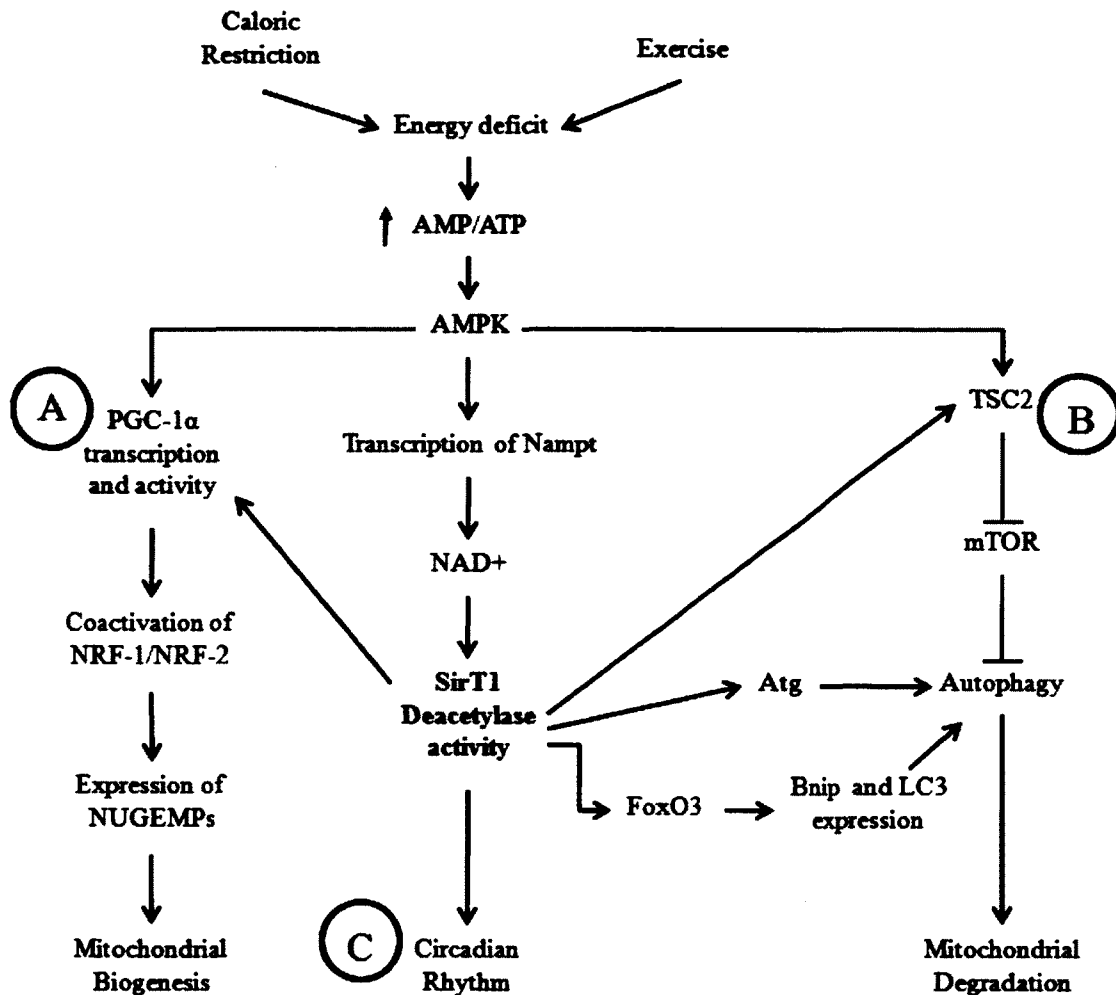


**Figure 1.2.** Mitochondrial turnover can be manipulated by the SirT1 regulation of mitochondrial biogenesis (A), degradation (B) and circadian gene transcription (C). Energy deficits induced by caloric restriction or exercise can activate AMPK and the production of NAD<sup>+</sup>, a cofactor for SirT1 deacetylase activity. A: SirT1 can manipulate mitochondrial biogenesis by deacetylating PGC-1 $\alpha$ , resulting in its activation and transcription. Once activated and upregulated, PGC-1 $\alpha$  can coactivate NRF-1 or NRF-2 to induce the transcription of nuclear genes encoding mitochondrial proteins (NUGEMPS). B: SirT1 deacetylase activity can also induce the clearance of older damaged mitochondria through the activation of TSC2 to arrest the inhibition of mTOR on autophagy or mitochondrial degradation (See Fig. 1.3.). C: SirT1 also has a regulatory role in the periodicity and amplitude of the circadian rhythm. In turn, SirT1 activity can also be manipulated by the circadian transcription of genes such as Nampt (See Fig. 1.4.).

the nuclear and mitochondrial genomes, respectively (197). PGC-1 $\alpha$  is a key regulator of energy metabolism and through the induction of mitochondrial biogenesis can increase the oxidation of fatty acids. In addition, PGC-1 $\alpha$  coactivates pyruvate dehydrogenase kinase 4 (PDK4), a negative regulator of glucose oxidation (192). In fact, many of the proteins and enzymes involved in mtDNA replication, transcription and translation for mitochondrial biogenesis are encoded by nuclear genes that are regulated by PGC-1 $\alpha$ . The expression and activity of PGC-1 $\alpha$  can be altered by cold exposure, physical activity, or fasting (16; 36; 86; 149; 155). PGC-1 $\alpha$  protein can be reversibly activated through phosphorylation (88), methylation (181) or deacetylation (58). In skeletal muscle, activated AMPK has been found to increase mitochondrial biogenesis in a PGC-1 $\alpha$ - and NRF-1-dependent manner (21; 204). Consistent with this, when AICAR is given to mice orally there is an induction of metabolic genes in muscle, including PGC1- $\alpha$ , and a substantial improvement in running endurance (136). Although the mechanism for this effect has not yet been clearly defined, Jager et al. (2007) demonstrated that PGC-1 $\alpha$  phosphorylation in muscle by AMPK is required for the induction of GLUT4, mitochondrial genes, and of PGC-1 $\alpha$  itself. In addition, we have previously shown that AMPK activation led to increased PGC-1 $\alpha$  promoter activity, with a concomitant increase in PGC-1 $\alpha$  mRNA expression in skeletal muscle cells (87). In conjunction with the activation of AMPK, SirT1 is required for the deacetylation and synchronized activation of PGC-1 $\alpha$  following exercise in skeletal muscle (58). To balance the deacetylase activity of SirT1, the transcriptional and biological functions of PGC-1 $\alpha$

can be inhibited by the acetyltransferase GCN5 (114). GCN5 expression in skeletal muscle is positively controlled by the transcriptional coactivator SRC-3 (44). SRC-3 knock-out mice display increased mitochondrial function, and are protected against obesity (44). Indeed, treatment of mice with SirT1 agonists, such as SRT1720 (129) and RSV (109), results in increased skeletal muscle mitochondrial function via the deacetylation and activation of PGC-1 $\alpha$ . In diet-induced-obese mice, these treatments improved insulin resistance (129). It is therefore becoming evident that a concerted metabolic response, via the AMPK-Nampt-SirT1 pathway, controls the induction and progression of mitochondrial biogenesis through the activation of PGC-1 $\alpha$ .

#### **1.6.2. AMPK-NAMPT-SIRT1 PATHWAY INDUCED MITOCHONDRIAL BIOGENESIS**

As alluded to above, the activation of AMPK and SirT1 is strongly connected to the induction of PGC-1 $\alpha$ , and thus, mitochondrial biogenesis. AMPK activation of PGC-1 $\alpha$  was shown to be SirT1-dependent when activated by RSV, metformin, dinitrophenol or A-769662 (35; 36). These effects are a result of the ability of AMPK to increase the cellular levels of the SirT1 cofactor NAD<sup>+</sup>, leading to SirT1 activation and allowing for the deacetylation of PGC-1 $\alpha$  and other downstream targets in mouse skeletal muscle (35). The genetic ablation of the AMP-sensitive AMPK $\gamma$ 3 subunit in muscle impaired the

elevation in  $\text{NAD}^+$  (36). The activation of the PGC-1 $\alpha$  pathway is therefore reliant on the action of AMPK to activate SirT1 via an AMP-sensitive increase in  $\text{NAD}^+$ .

Once SirT1 has been activated by AMPK, SirT1 not only deacetylates and activates PGC-1 $\alpha$ , but also positively regulates PGC-1 $\alpha$  gene expression. It does this in conjunction with MyoD by forming a SirT1-MyoD-PGC-1 $\alpha$  complex on the promoter of PGC-1 $\alpha$  in muscle tissue, creating a positive auto-regulatory loop for PGC-1 $\alpha$  expression (7; 69). This finding was unanticipated, since SirT1 is known to represses the action of MyoD on target genes, as it does with the expression of myogenin during the inhibition of differentiation (54). However, this discovery not only helps to describe a key link between the coordinated regulation of muscle-specific adaptive changes in gene expression and metabolism, but also the regulation of PGC-1 $\alpha$  downstream of AMPK and SirT1. The activation of transcription mediated by the binding of the SirT1-MyoD-PGC-1 $\alpha$  complex to DNA would be terminated by either a decrease in the  $\text{NAD}^+/\text{NADH}$  ratio, or by the acetylation of PGC-1 $\alpha$  via GNC5, thereby releasing SirT1 and MyoD (114; 162). This would allow PGC-1 $\alpha$  to co-localize with its transcriptional repressor, RIP140 (114; 162). This describes a dynamic interaction between SirT1 and PGC-1 $\alpha$  that can modulate both the expression and activity of the coactivator.

Similar to CR, the natural polyphenolic compound resveratrol (RSV) has been shown to increase SirT1 activity and expression, and in turn longevity, in lower organisms and in short-lived vertebrates and mice (20; 83; 109; 185; 196). RSV was first shown to increase lifespan in yeast by activating the SirT1 orthologue Sir2 (83).

Initially, RSV was thought to directly activate SirT1 as was shown with the *in vitro* activation of recombinant SirT1 (83). Despite these initial observations, a number of more recent studies have emerged that demonstrate that AMPK is necessary for the RSV-induced SirT1 activation (28; 93; 184). For example, it has recently been shown that RSV requires intact AMPK activity for the induction of SirT1 in skeletal muscle (36). With prolonged RSV treatment (110 weeks), increases in AMPK were accompanied by PGC-1 $\alpha$  activation in mice, causing an increase in mitochondrial biogenesis and a greater survival rate of animals on a high fat diet with insulin resistance (20). In fact, the metabolic effects of RSV may result from competitive inhibition of cAMP-degrading phosphodiesterases, leading to elevated cAMP levels and the activation of Epac1, an effector protein, thus increasing intracellular Ca<sup>2+</sup> and the activation of the CamKK $\beta$ -AMPK pathway (142). This increase in Ca<sup>2+</sup> was the result of Epac1-activated phospholipase C and the downstream activation of the ryanodine receptor Ca<sup>2+</sup>-release channel. Thus, the pharmacological effects of RSV on metabolic diseases such as type 2 diabetes and obesity appear to be beneficial, and have resulted in a considerable number of clinical trials on similar analogues or small SirT1 activators (34).

### **1.6.3. SIRT1 IN AUTOPHAGY**

Despite the strong influence of the AMPK-Nampt-SirT1 pathway on PGC-1 $\alpha$ -induced mitochondrial biogenesis, it is important to note that the balance of

mitochondrial turnover also depends on the degradation of damaged mitochondria. Thus, for a cell to maintain proper control over mitochondrial turnover it must have synchronous regulation of both mitochondrial biogenesis, and autophagy. Autophagy is a critical process by which a cell can expunge damaged components, such as mitochondria, in order to maintain cellular bioenergetic requirements. This process includes the sequestering of cytoplasm and organelles in double membrane autophagic vacuoles or autophagosomes (Fig. 1.3.; 115). In the absence of autophagy, there is a corresponding increase in damaged organelles as has been shown in HeLa cells (24; 169). The disruption of autophagy has been linked to cancer, liver disease, neurodegenerative disorders and lifespan determination (132). Within mouse embryo fibroblasts, SirT1 appears to play a regulatory role in autophagy, since it can form a complex with, and deacetylate, autophagy genes Atg5, Atg7 and Atg8 in an NAD<sup>+</sup>-dependent fashion (112). The deacetylation of these Atg components is necessary for the activation of autophagy.

Evidence for the requirement of SirT1 in autophagy includes observations made of SirT1 *-/-* mice which exhibit similar pathologies as those found in Atg5 *-/-* mice, such as the accumulation of damaged organelles, disruption of energy homeostasis and perinatal mortality (112). The formation of an autophagosome in mammals is dependent on the subcellular distribution of LC3, the mammalian homolog of the yeast Atg8 gene. The proteolytic conversion of LC3-I to LC3-II has been shown to be a hallmark of mammalian autophagy (131). This conversion is reduced when cells are transfected with a deacetylase-inactive SirT1 DNA construct. The absence of SirT1 also results in an

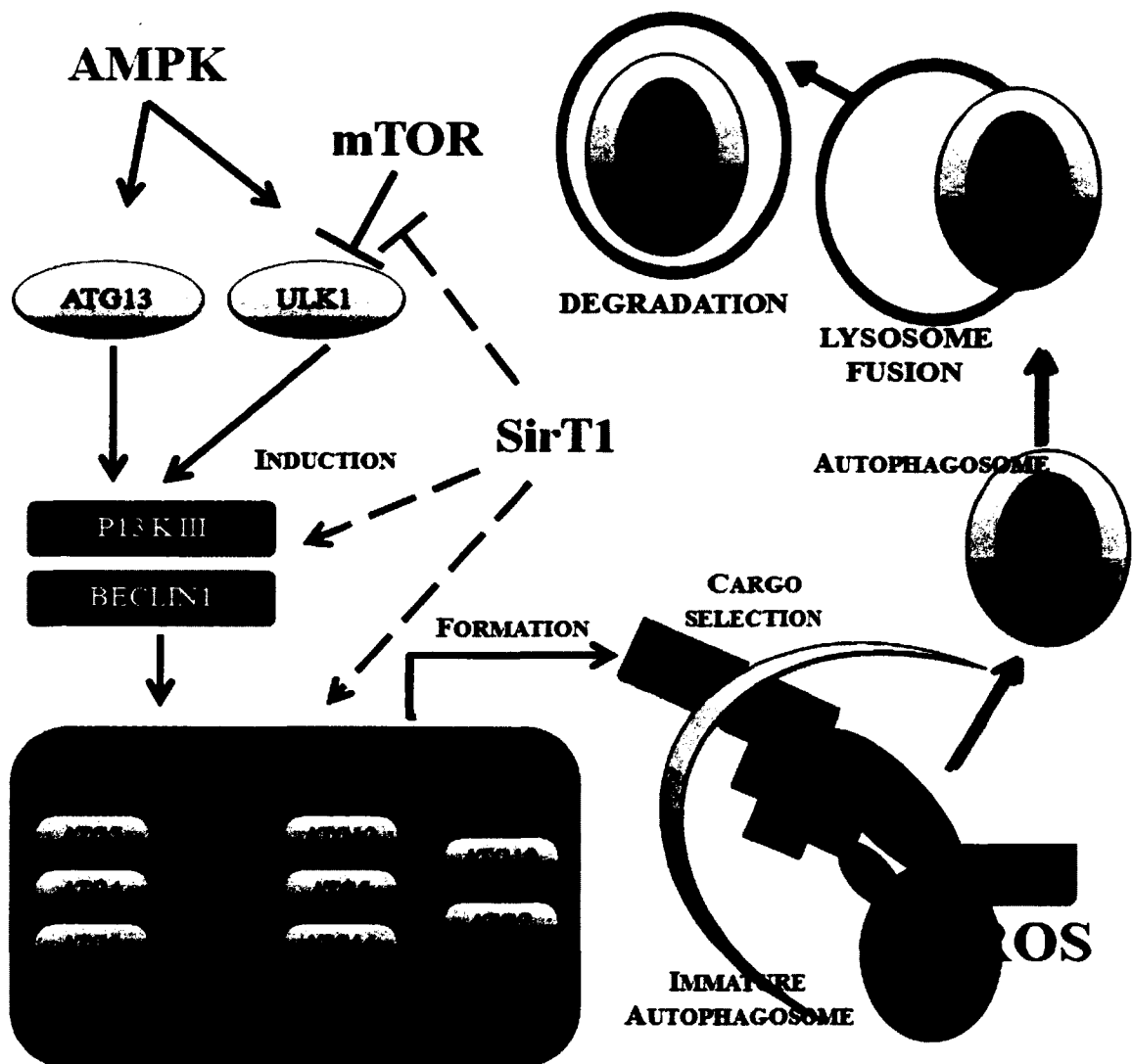


**Figure 1.3.** Schematic describing the influence of SirT1 on the energy saving process of autophagy. Nutrient deprivation has been shown to induce autophagy via both AMPK and SirT1 as metabolic sensors. In addition, nutrient abundance activates the mTOR pathway which inhibits autophagy while increasing protein synthesis within the cell. The mTOR pathway can be inhibited via the activation of TSC2 by SirT1. Bcl-2 also plays an important role in the inhibition of autophagy via its interaction with Beclin-1. The interaction between Bcl-2 and Beclin-1 can be disrupted by a SirT1-mediated increase in Bnip3. The release of Beclin-1 allows for the induction of autophagy via the conversion of LC3I to LC3II by ATG proteins. The deacetylation of ATG proteins by SirT1 is required for this process. In the progression of mitophagy (autophagy of mitochondria) PINK1 binds to damaged ROS-producing mitochondria in the process of cargo selection. PINK1 recruits PARKIN, which ubiquitinates outermitochondrial membrane proteins. These ubiquitinated proteins are then bound by p62. p62 can then bind to LC3II, which is located on immature autophagosomes. Following cargo selection, the autophagosome is then formed and engulfs the cargo. The autophagosome then fuses with a lysosome forming an autophagolysosome and its content is digested by lysosomal enzymes.

accumulation of the autophagy marker p62 (112), which has been described as an *in vivo* indicator of impaired autophagy (131).

In contrast, the overexpression of SirT1 leads to an increase in the formation of GFP-LC3 punctae, consistent with autophagosome formation (112). SirT1 can deacetylate and induce a FoxO3-mediated enhancement of both LC3 and Bnip3 expression (107; 123) during both oxidative stress and CR (31). Bnip3 induces autophagy by disrupting the interactions between Beclin-1, a conserved protein required for the initiation of autophagy, and Bcl2 or Bcl-X<sub>L</sub> (122). In addition, when FoxO3a is overexpressed in C2C12 myotubes, it not only binds to the LC3 promoter, but also to the promoters of other autophagy-related genes such as Gabarapl1 and Atg12 (202). These findings point to SirT1, FoxO3a and Bnip3 as potential therapeutic targets for skeletal muscle autophagy and other degenerative and neoplastic diseases in which autophagy is involved.

Since the activation of SirT1 is important for autophagy, it appears likely that the availability of NAD<sup>+</sup>, which controls SirT1 activity, may also be vital for the process. Hsu et al. examined the role of Nampt activity, the enzyme that controls NAD<sup>+</sup> synthesis, on autophagy (84). They demonstrated that the downregulation of Nampt in cardiac myocytes mimics the effect that SirT1 inhibition has on autophagy (84). This is consistent Nampt enhancing autophagic flux through the activation of SirT1 by controlling NAD<sup>+</sup> synthesis.

The mammalian target of rapamycin (mTOR) is a serine/threonine protein kinase that plays a key role in cellular growth and homeostasis. TOR stimulates protein synthesis in yeast and mammals by modulating components of the translation machinery, such as S6K and 4E-BP (178). Under CR, the TOR pathway is downregulated which has been shown to contribute to longevity in yeast, worms and flies (95; 97; 187). The discovery that autophagy is negatively regulated by mTOR, and that SirT1 has been reported to activate autophagy (144), suggests an inverse relationship between the SirT1 and mTOR signalling pathways. Consistent with this, in both human and mouse cells SirT1 was shown to interact with TSC2, an mTOR inhibitory-complex, which may be linked to a SirT1 inhibition of mTOR complex 1 (59). However, in the nucleus of muscle cells, mTOR has also been shown to control the function of a transcriptional complex involving PGC-1 $\alpha$  and YY1 (ying-yang 1) for the induction of mitochondrial genes (47). The regulatory control of mTOR over this complex would appear to be in juxtaposition to the ability of SirT1 to inhibit mTOR, while also inducing mitochondrial biogenesis. However, SirT1 inhibits mTOR via the activation of TSC2 in the cytoplasm (59), and therefore may not directly affect the role of mTOR within the nucleus. Thus, SirT1 inhibition of mTOR may be a treatment model for some autophagy-associated neurological disorders, such as Huntington's disease (158).

In summary, SirT1 has been shown to regulate the autophagic clearance of old or damaged mitochondria through the deacetylation of Atg genes, the FoxO3-mediated induction of LC3 and Bnip3 expression, and inhibition of the negative regulation of

mTOR on autophagy. SirT1 can therefore be described as a gatekeeper that can regulate the flux of mitochondria by pathways that influence both mitochondrial biogenesis, as well as autophagy.

#### **1.6.4. SIRT1 IN CIRCADIAN RHYTHM**

An additional layer of control over mitochondrial turnover involves the integration of circadian regulation and synchronization of mitochondrial gene expression. The suprachiasmatic nucleus (SCN) of the hypothalamus is also known as the master neural clock in mammals. The SCN controls physiological and behavioural circadian rhythms, and it synchronizes clocks in peripheral organs through hormonal and neural signals. The SCN clock is entrained by light through the retinohypothalamic tract, and it orients the animal to the geophysical time (159). The molecular machinery that governs circadian rhythms in the SCN is also found in most of the cells of the body (100), and SirT1 activity appears to play a major role in regulating this mechanism via its deacetylation of involved transcription factors.

The molecular clock is comprised of the transcription factors CLOCK and BMAL1 (32; 57; 98) which heterodimerize for the regulation of gene transcription. The CLOCK-BMAL1 complex regulates transcription by binding to the E-box motifs within the promoters of the Nampt (156) and MyoD (11) genes. The auto-regulatory feedback mechanisms that regulate the molecular clock result in the oscillation of gene

transcription with a periodicity of approximately 24hrs. In many tissues, this rhythm can be further tuned by various time cues or zeitgebers, such as light, feeding or exercise (130). McCarthy et al. (2007) described approximately 200 skeletal muscle transcripts that possess a circadian pattern of expression. In relation to mitochondrial biogenesis, SirT1, PGC-1 $\alpha$  and MyoD expression all display diurnal rhythms in skeletal muscle, which adds another dimension to this regulatory mechanism that is integrated to the circadian clock (11; 15; 119). The regulation of circadian rhythm begins with the CLOCK-mediated acetylation of histone H3 and BMAL1 to induce circadian controlled gene expression (78). The acetylation of BMAL1 recruits components of the negative feedback arm of the molecular clock, Period (PER1, PER2, and PER3) and cryptochrome (CRY1 and CRY2) (106; 203). CRY and PER proteins are important regulatory proteins that can complex with CLOCK-BMAL1 to act in a retrograde manner to inhibit the transcription of circadian controlled genes, including their own gene loci, as demonstrated in mouse liver (Fig. 1.4.; 153). In fact, the inhibitory interaction between the CRY-PER and CLOCK-BMAL1 complexes in liver is facilitated by the acetylation of BMAL1 by CLOCK, thereby recruiting the CRY1 protein to the CLOCK-BMAL1 heterodimer (78). This auto-regulatory feedback loop is also dependent on the development of a critical concentration of PER and CRY proteins, which is then followed by the translocation of these proteins to the nucleus to inhibit the CLOCK-BMAL1 complex (128). In relation to the 24 hour light and dark period on earth, called a nycthemeron, the transcriptional activity of the CLOCK-BMAL1 complex is elevated

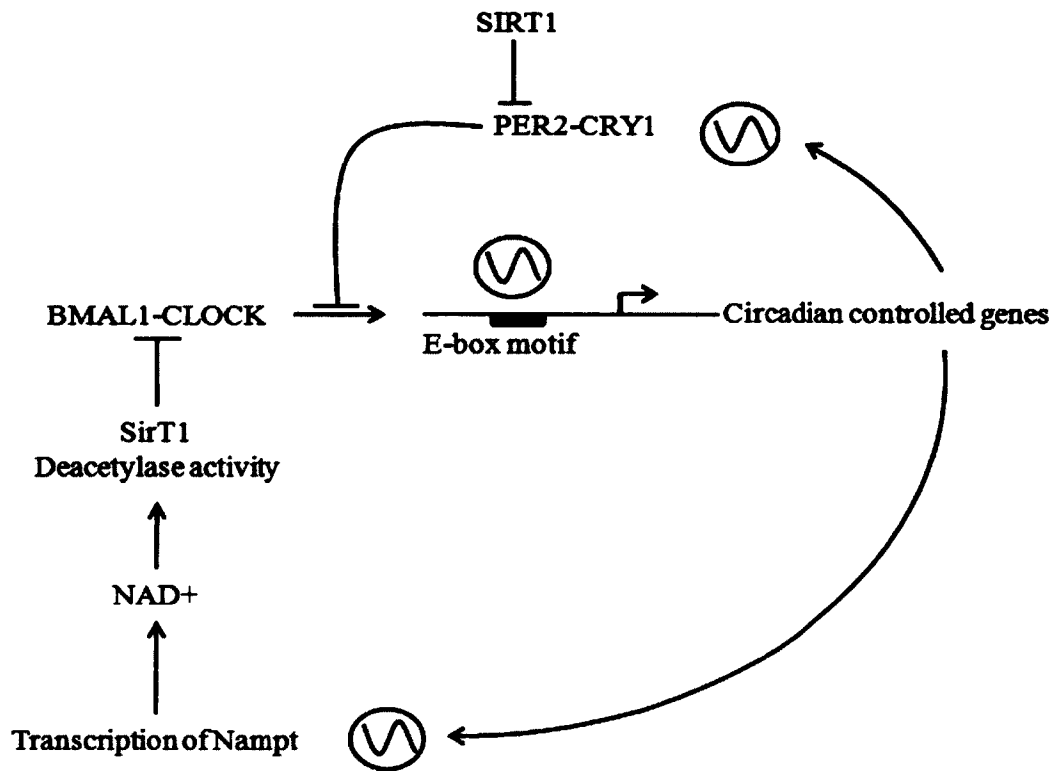


**Figure 1.4.** Circadian transcription factors, BMAL1 and CLOCK, direct E-box motif transcription of circadian controlled genes, which act as activators and repressors of the circadian system. For example, the BMAL1-CLOCK complex controls the rhythmic transcription of Nampt which will increase NAD<sup>+</sup> levels and thereby activate SirT1. SirT1 deacetylase activity inhibits the BMAL1-CLOCK complex, through the deacetylation of BMAL1, thus manipulating circadian rhythm and the activation of gene transcription in a negative feedback loop. PER and CRY are also circadian-controlled genes which can act in a negative feedback loop to repress the activity of BMAL1-CLOCK activation. In addition, SirT1 can also inhibit the influence of the PER2-CRY1 complex on circadian rhythm via the deacetylation of PER2. The sigmoidal curved symbol represents a circadian rhythmic event.

during the light period, while the PER-CRY heterodimer is higher during the dark period, thus helping to maintain a daily circadian oscillation (175). CLOCK and BMAL1 have been shown to cause major reductions in mitochondrial content, along with profound mitochondrial pathologies in skeletal muscle when either of these proteins is mutated (11). The positive arm of circadian rhythm is controlled by SirT1, which opposes the inhibitory actions of both CLOCK and the PER-CRY complex through deacetylation of H3 and H4, BMAL1 and PER2. In SirT1 liver-specific knockout mice BMAL1 acetylation was significantly increased, leading to disturbances in the circadian cycle (134). Nonetheless, SirT1-KO mouse embryonic fibroblasts still demonstrate PER and CRY circadian expression, however, the magnitude is significantly reduced (15). Normally when PER2 is deacetylated it is subsequently degraded, thereby arresting the inhibition of CLOCK-BMAL1-regulated transcription by the PER-CRY complex. Likewise, when SirT1 is inhibited pharmacologically, there is a loss in the stringency and magnitude of circadian gene expression (134).

Since SirT1 activity is responsive to NAD<sup>+</sup> availability, it is likely that the regulation of BMAL1 activity through deacetylation is linked to metabolism. However, as was demonstrated in mouse embryo fibroblasts, SirT1 can inhibit the CLOCK-BMAL1 complex induced transcription of *Nampt* (135). Likewise, *Nampt* inhibition promotes oscillation of the clock gene *PER2* by releasing CLOCK-BMAL1 from suppression by SirT1 (135). In turn, this describes a feedback mechanism, where the

resulting decline in Nampt protein will then diminish the enzymatic production of NAD<sup>+</sup>, leading to reduced SirT1 deacetylase activity and the activation of CLOCK-BMAL1 transcriptional targets (156). Since the NAD<sup>+</sup>/NADH redox equilibrium depends on the metabolic state of the cell, the value of this ratio during exercise or feeding results in the phase-shifting of cyclic gene expression. Nampt protein has been shown to increase in human skeletal muscle following exercise (45), demonstrating that there may be a concomitant tuning of the molecular clock within tissues through SirT1 activation. Also, when bound to CLOCK-BMAL1, SirT1 can inhibit the negative arm of the circadian rhythm by reducing PER2 transcription (156). Therefore, SirT1 expression and activity are important factors that determine the integration of the mammalian clock to the modulation of NAD<sup>+</sup> availability, and as a result, energy metabolism. The influence of exercise on Nampt expression or NAD<sup>+</sup> concentrations would most likely alter the periodicity and magnitude of many circadian-controlled genes within skeletal muscle. Additionally, obesity and high-fat diets have been shown to affect circadian clock genes in mice, which would indicate that metabolism and circadian rhythms at the molecular level are interconnected (101). Taken together, it appears that SirT1 has the ability to mediate information concerning both nutrient availability and exercise to the molecular clock, thereby transducing signals originating from cellular metabolites to the circadian machinery.

### **1.6.5. CONCLUSION**

Mitochondrial biogenesis and turnover are required to maintain an active and healthy cellular state that synchronizes energy status to changes in metabolism. The processes involved in maintaining mitochondrial health have become increasingly complex. It is apparent that the tight regulation and coordination of AMPK, Nampt, SirT1 and PGC-1 $\alpha$  create a balance of mitochondrial biogenesis, autophagy and circadian rhythm which are synchronized and coordinated. Pharmacological or alternative therapies (i.e. exercise) offer promising approaches that can modulate the activity of this integrated system, leading to the maintenance of mitochondrial content and function, and ultimately skeletal muscle health.

### **1.7. DISSERTATION PURPOSES**

Previous studies have shown that SirT1 can induce mitochondrial biogenesis in tissues ranging from fat to pancreatic tissue, thus demonstrating the potential beneficial effects of SirT1 on metabolic diseases ranging from obesity to diabetes. It is less known whether SirT1 is responsible for mediating the basal mitochondrial biogenesis that occurs in skeletal muscle or that which is induced following exercise. In addition, many of the studies that examine the role of SirT1 on longevity, metabolic sensing, apoptosis, mitochondrial biogenesis or autophagy have used RSV as a SirT1 agonist. These studies are therefore dependent on the assumption that RSV directly activates SirT1 and has

limited secondary effects on other pathways associated with each of these cellular events. We have therefore designed a series of projects: 1) to further examine the role of RSV treatment in skeletal muscle mitochondrial biogenesis using cell culture and *in vitro* models; 2) to compare the overall level of mitochondrial biogenesis induction following RSV-treatment to those induced by either chronic contractile activity in cultured mouse skeletal muscle myotubes, or by voluntary exercise in mice; 3) to determine the role of SirT1 on basal mitochondrial biogenesis by generating, and comparing, skeletal muscle-specific SirT1-KO mice to wildtype (WT) mice; 4) to explore the SirT1-dependent and -independent effects of RSV and voluntary running on mitochondrial biogenesis using muscle-specific SirT1-KO and WT mice; 5) to investigate the potential for an additive or synergistic effect between RSV-treatment and chronic contractile activity (in cell culture) or exercise (*in vivo*) and whether this effect is dependent on SirT1.

## 1.8. REFERENCES

1. **Abdelmohsen K, Pullmann R, Jr., Lal A, Kim HH, Galban S, Yang X, Blethrow JD, Walker M, Shubert J, Gillespie DA, Furneaux H and Gorospe M.** Phosphorylation of HuR by Chk2 regulates SIRT1 expression. *Mol Cell* 25: 543-557, 2007.
2. **Adams GR, Fisher MJ and Meyer RA.** Hypercapnic acidosis and increased H. *Am J Physiol* 260: C805-C812, 1991.
3. **Adhihetty PJ, Ljubicic V and Hood DA.** Effect of chronic contractile activity on SS and IMF mitochondrial apoptotic susceptibility in skeletal muscle. *Am J Physiol Endocrinol Metab* 292: E748-E755, 2007.
4. **Adhihetty PJ, Ljubicic V, Menzies KJ and Hood DA.** Differential susceptibility of subsarcolemmal and intermyofibrillar mitochondria to apoptotic stimuli. *Am J Physiol Cell Physiol* 289: C994-C1001, 2005.
5. **Ai H, Ihlemann J, Hellsten Y, Lauritzen HP, Hardie DG, Galbo H and Ploug T.** Effect of fiber type and nutritional state on A. *Am J Physiol Endocrinol Metab* 282: E1291-E1300, 2002.
6. **Allen DG, Lamb GD and Westerblad H.** Skeletal muscle fatigue: cellular mechanisms. *Physiol Rev* 88: 287-332, 2008.
7. **Amat R, Planavila A, Chen SL, Iglesias R, Giralt M and Villarroya F.** SIRT1 controls the transcription of the peroxisome proliferator-activated receptor-gamma Co-activator-1alpha (PGC-1alpha) gene in skeletal muscle through the

- PGC-1alpha autoregulatory loop and interaction with MyoD. *J Biol Chem* 284: 21872-21880, 2009.
8. **Amat R, Solanes G, Giralt M and Villarroya F.** SIRT1 is involved in glucocorticoid-mediated control of uncoupling protein-3 gene transcription. *J Biol Chem* 282: 34066-34076, 2007.
  9. **Anderson RM, Barger JL, Edwards MG, Braun KH, O'Connor CE, Prolla TA and Weindruch R.** Dynamic regulation of PGC-1alpha localization and turnover implicates mitochondrial adaptation in calorie restriction and the stress response. *Aging Cell* 7: 101-111, 2008.
  10. **Anderson RM, Bitterman KJ, Wood JG, Medvedik O and Sinclair DA.** Nicotinamide and PNC1 govern lifespan extension by calorie restriction in *Saccharomyces cerevisiae*. *Nature* 423: 181-185, 2003.
  11. **Andrews JL, Zhang X, McCarthy JJ, McDearmon EL, Hornberger TA, Russell B, Campbell KS, Arbogast S, Reid MB, Walker JR, Hogenesch JB, Takahashi JS and Esser KA.** CLOCK and BMAL1 regulate MyoD and are necessary for maintenance of skeletal muscle phenotype and function. *Proc Natl Acad Sci U S A* 2010.
  12. **Aparicio OM, Billington BL and Gottschling DE.** Modifiers of position effect are shared between telomeric and silent mating-type loci in *S. cerevisiae*. *Cell* 66: 1279-1287, 1991.

13. **Apfeld J, O'Connor G, McDonagh T, DiStefano PS and Curtis R.** The AMP-activated protein kinase AAK-2 links energy levels and insulin-like signals to lifespan in *C. elegans*. *Genes Dev* 18: 3004-3009, 2004.
14. **Arany Z, He H, Lin J, Hoyer K, Handschin C, Toka O, Ahmad F, Matsui T, Chin S, Wu PH, Rybkin II, Shelton JM, Manieri M, Cinti S, Schoen FJ, Bassel-Duby R, Rosenzweig A, Ingwall JS and Spiegelman BM.** Transcriptional coactivator PGC-1 alpha controls the energy state and contractile function of cardiac muscle. *Cell Metab* 1: 259-271, 2005.
15. **Asher G, Gatfield D, Stratmann M, Reinke H, Dibner C, Kreppel F, Mostoslavsky R, Alt FW and Schibler U.** SIRT1 regulates circadian clock gene expression through PER2 deacetylation. *Cell* 134: 317-328, 2008.
16. **Baar K, Wende AR, Jones TE, Marison M, Nolte LA, Chen M, Kelly DP and Holloszy JO.** Adaptations of skeletal muscle to exercise: rapid increase in the transcriptional coactivator PGC-1. *FASEB J* 16: 1879-1886, 2002.
17. **Baker DJ, Betik AC, Krause DJ and Hepple RT.** No decline in skeletal muscle oxidative capacity with aging in long-term calorically restricted rats: effects are independent of mitochondrial DNA integrity. *J Gerontol A Biol Sci Med Sci* 61: 675-684, 2006.
18. **Baldwin KM, Klinkerfuss GH, Terjung RL, Mole PA and Holloszy JO.** Respiratory capacity of white, red, and intermediate muscle: adaptative response to exercise. *Am J Physiol* 222: 373-378, 1972.

19. **Banks AS, Kon N, Knight C, Matsumoto M, Gutierrez-Juarez R, Rossetti L, Gu W and Accili D.** SirT1 gain of function increases energy efficiency and prevents diabetes in mice. *Cell Metab* 8: 333-341, 2008.
20. **Baur JA, Pearson KJ, Price NL, Jamieson HA, Lerin C, Kalra A, Prabhu VV, Allard JS, Lopez-Lluch G, Lewis K, Pistell PJ, Poosala S, Becker KG, Boss O, Gwinn D, Wang M, Ramaswamy S, Fishbein KW, Spencer RG, Lakatta EG, Le CD, Shaw RJ, Navas P, Puigserver P, Ingram DK, de CR and Sinclair DA.** Resveratrol improves health and survival of mice on a high-calorie diet. *Nature* 444: 337-342, 2006.
21. **Bergeron R, Ren JM, Cadman KS, Moore IK, Perret P, Pypaert M, Young LH, Semenkovich CF and Shulman GI.** Chronic activation of AMP kinase results in NRF-1 activation and mitochondrial biogenesis. *Am J Physiol Endocrinol Metab* 281: E1340-E1346, 2001.
22. **Bessman SP and Carpenter CL.** The creatine-creatine phosphate energy shuttle. *Annu Rev Biochem* 54: 831-862, 1985.
23. **Bitterman KJ, Anderson RM, Cohen HY, Latorre-Esteves M and Sinclair DA.** Inhibition of silencing and accelerated aging by nicotinamide, a putative negative regulator of yeast sir2 and human SIRT1. *J Biol Chem* 277: 45099-45107, 2002.
24. **Bjorkoy G, Lamark T, Brech A, Outzen H, Perander M, Overvatn A, Stenmark H and Johansen T.** p62/SQSTM1 forms protein aggregates

- degraded by autophagy and has a protective effect on huntingtin-induced cell death. *J Cell Biol* 171: 603-614, 2005.
25. **Blander G and Guarente L.** The Sir2 family of protein deacetylases. *Annu Rev Biochem* 73: 417-435, 2004.
  26. **Bogan KL and Brenner C.** Nicotinic acid, nicotinamide, and nicotinamide riboside: a molecular evaluation of NAD<sup>+</sup> precursor vitamins in human nutrition. *Annu Rev Nutr* 28: 115-130, 2008.
  27. **Boily G, Seifert EL, Bevilacqua L, He XH, Sabourin G, Estey C, Moffat C, Crawford S, Saliba S, Jardine K, Xuan J, Evans M, Harper ME and McBurney MW.** SirT1 regulates energy metabolism and response to caloric restriction in mice. *PLoS ONE* 3: e1759, 2008.
  28. **Borra MT, Smith BC and Denu JM.** Mechanism of human SIRT1 activation by resveratrol. *J Biol Chem* 280: 17187-17195, 2005.
  29. **Bottinelli R and Reggiani C.** Human skeletal muscle fibres: molecular and functional diversity. *Prog Biophys Mol Biol* 73: 195-262, 2000.
  30. **Boulton SJ and Jackson SP.** Components of the Ku-dependent non-homologous end-joining pathway are involved in telomeric length maintenance and telomeric silencing. *EMBO J* 17: 1819-1828, 1998.
  31. **Brunet A, Sweeney LB, Sturgill JF, Chua KF, Greer PL, Lin Y, Tran H, Ross SE, Mostoslavsky R, Cohen HY, Hu LS, Cheng HL, Jedrychowski MP, Gygi SP, Sinclair DA, Alt FW and Greenberg ME.** Stress-dependent

- regulation of FOXO transcription factors by the SIRT1 deacetylase. *Science* 303: 2011-2015, 2004.
32. **Bunger MK, Wilsbacher LD, Moran SM, Clendenin C, Radcliffe LA, Hogenesch JB, Simon MC, Takahashi JS and Bradfield CA.** Mop3 is an essential component of the master circadian pacemaker in mammals. *Cell* 103: 1009-1017, 2000.
  33. **Burnett C, Valentini S, Cabreiro F, Goss M, Somogyvari M, Piper MD, Hoddinott M, Sutphin GL, Leko V, McElwee JJ, Vazquez-Manrique RP, Orfila AM, Ackerman D, Au C, Vinti G, Riesen M, Howard K, Neri C, Bedalov A, Kaeberlein M, Soti C, Partridge L and Gems D.** Absence of effects of Sir2 overexpression on lifespan in *C. elegans* and *Drosophila*. *Nature* 477: 482-485, 2011.
  34. **Camins A, Sureda FX, Junyent F, Verdaguer E, Folch J, Pelegri C, Vilaplana J, Beas-Zarate C and Pallas M.** Sirtuin activators: Designing molecules to extend life span. *Biochim Biophys Acta* 2010.
  35. **Canto C, Gerhart-Hines Z, Feige JN, Lagouge M, Noriega L, Milne JC, Elliott PJ, Puigserver P and Auwerx J.** AMPK regulates energy expenditure by modulating NAD<sup>+</sup> metabolism and SIRT1 activity. *Nature* 458: 1056-1060, 2009.
  36. **Canto C, Jiang LQ, Deshmukh AS, Matakai C, Coste A, Lagouge M, Zierath JR and Auwerx J.** Interdependence of AMPK and SIRT1 for metabolic

- adaptation to fasting and exercise in skeletal muscle. *Cell Metab* 11: 213-219, 2010.
37. **Carling D.** The AMP-activated protein kinase cascade--a unifying system for energy control. *Trends Biochem Sci* 29: 18-24, 2004.
  38. **Carling D and Hardie DG.** The substrate and sequence specificity of the AMP-activated protein kinase. Phosphorylation of glycogen synthase and phosphorylase kinase. *Biochim Biophys Acta* 1012: 81-86, 1989.
  39. **Chabi B, Adhietty PJ, O'Leary MF, Menzies KJ and Hood DA.** Relationship between Sirt1 expression and mitochondrial proteins during conditions of chronic muscle use and disuse. *J Appl Physiol* 107: 1730-1735, 2009.
  40. **Challet E, Caldelas I, Graff C and Pevet P.** Synchronization of the molecular clockwork by light- and food-related cues in mammals. *Biol Chem* 384: 711-719, 2003.
  41. **Chan DC.** Mitochondria: dynamic organelles in disease, aging, and development. *Cell* 125: 1241-1252, 2006.
  42. **Civitarese AE, Carling S, Heilbronn LK, Hulver MH, Ukropcova B, Deutsch WA, Smith SR and Ravussin E.** Calorie restriction increases muscle mitochondrial biogenesis in healthy humans. *PLoS Med* 4: e76, 2007.
  43. **Colman RJ, Anderson RM, Johnson SC, Kastman EK, Kosmatka KJ, Beasley TM, Allison DB, Cruzen C, Simmons HA, Kemnitz JW and**

- Weindruch R.** Caloric restriction delays disease onset and mortality in rhesus monkeys. *Science* 325: 201-204, 2009.
44. **Coste A, Louet JF, Lagouge M, Lerin C, Antal MC, Meziane H, Schoonjans K, Puigserver P, O'Malley BW and Auwerx J.** The genetic ablation of SRC-3 protects against obesity and improves insulin sensitivity by reducing the acetylation of PGC-1{alpha}. *Proc Natl Acad Sci U S A* 105: 17187-17192, 2008.
45. **Costford SR, Bajpeyi S, Pasarica M, Albarado DC, Thomas SC, Xie H, Church TS, Jubrias SA, Conley KE and Smith SR.** Skeletal muscle NAMPT is induced by exercise in humans. *Am J Physiol Endocrinol Metab* 298: E117-E126, 2010.
46. **Coupland ME, Puchert E and Ranatunga KW.** Temperature dependence of active tension in mammalian (rabbit psoas) muscle fibres: effect of inorganic phosphate. *J Physiol* 536: 879-891, 2001.
47. **Cunningham JT, Rodgers JT, Arlow DH, Vazquez F, Mootha VK and Puigserver P.** mTOR controls mitochondrial oxidative function through a YY1-PGC-1alpha transcriptional complex. *Nature* 450: 736-740, 2007.
48. **Dahlstedt AJ, Katz A, Tavi P and Westerblad H.** Creatine kinase injection restores contractile function in creatine-kinase-deficient mouse skeletal muscle fibres. *J Physiol* 547: 395-403, 2003.
49. **Dudley GA, Abraham WM and Terjung RL.** Influence of exercise intensity

- and duration on biochemical adaptations in skeletal muscle. *J Appl Physiol* 53: 844-850, 1982.
50. **Ferreira R, Vitorino R, Alves RM, Appell HJ, Powers SK, Duarte JA and Amado F.** Subsarcolemmal and intermyofibrillar mitochondria proteome differences disclose functional specializations in skeletal muscle. *Proteomics* 10: 3142-3154, 2010.
  51. **Fisslthaler B and Fleming I.** Activation and signaling by the AMP-activated protein kinase in endothelial cells. *Circ Res* 105: 114-127, 2009.
  52. **Frayn KN.** Fat as a fuel: emerging understanding of the adipose tissue-skeletal muscle axis. *Acta Physiol (Oxf)* 199: 509-518, 2010.
  53. **Fulco M, Cen Y, Zhao P, Hoffman EP, McBurney MW, Sauve AA and Sartorelli V.** Glucose restriction inhibits skeletal myoblast differentiation by activating SIRT1 through AMPK-mediated regulation of Nampt. *Dev Cell* 14: 661-673, 2008.
  54. **Fulco M, Schiltz RL, Iezzi S, King MT, Zhao P, Kashiwaya Y, Hoffman E, Veech RL and Sartorelli V.** Sir2 regulates skeletal muscle differentiation as a potential sensor of the redox state. *Mol Cell* 12: 51-62, 2003.
  55. **Gandevia SC.** Spinal and supraspinal factors in human muscle fatigue. *Physiol Rev* 81: 1725-1789, 2001.
  56. **Garten A, Petzold S, Korner A, Imai S and Kiess W.** Nampt: linking NAD biology, metabolism and cancer. *Trends Endocrinol Metab* 20: 130-138, 2009.

57. **Gekakis N, Staknis D, Nguyen HB, Davis FC, Wilsbacher LD, King DP, Takahashi JS and Weitz CJ.** Role of the CLOCK protein in the mammalian circadian mechanism. *Science* 280: 1564-1569, 1998.
58. **Gerhart-Hines Z, Rodgers JT, Bare O, Lerin C, Kim SH, Mostoslavsky R, Alt FW, Wu Z and Puigserver P.** Metabolic control of muscle mitochondrial function and fatty acid oxidation through SIRT1/PGC-1alpha. *EMBO J* 26: 1913-1923, 2007.
59. **Ghosh HS, McBurney M and Robbins PD.** SIRT1 negatively regulates the mammalian target of rapamycin. *PLoS ONE* 5: e9199, 2010.
60. **Gladden LB.** Lactate metabolism: a new paradigm for the third millennium. *J Physiol* 558: 5-30, 2004.
61. **Gottlieb RA and Carreira RS.** Autophagy in health and disease. 5. Mitophagy as a way of life. *Am J Physiol Cell Physiol* 299: C203-C210, 2010.
62. **Greer EL, Oskoui PR, Banko MR, Maniar JM, Gygi MP, Gygi SP and Brunet A.** The energy sensor AMP-activated protein kinase directly regulates the mammalian FOXO3 transcription factor. *J Biol Chem* 282: 30107-30119, 2007.
63. **Guarente L.** Mitochondria--a nexus for aging, calorie restriction, and sirtuins? *Cell* 132: 171-176, 2008.
64. **Guarente L. Franklin H.** Epstein Lecture: Sirtuins, aging, and medicine. *N Engl J Med* 364: 2235-2244, 2011.

65. **Guerra B, Guadalupe-Grau A, Fuentes T, Ponce-Gonzalez JG, Morales-Alamo D, Olmedillas H, Guillen-Salgado J, Santana A and Calbet JA.** SIRT1, AMP-activated protein kinase phosphorylation and downstream kinases in response to a single bout of sprint exercise: influence of glucose ingestion. *Eur J Appl Physiol* 109: 731-743, 2010.
66. **Gurd BJ, Yoshida Y, Lally J, Holloway GP and Bonen A.** The deacetylase enzyme SIRT1 is not associated with oxidative capacity in rat heart and skeletal muscle and its overexpression reduces mitochondrial biogenesis. *J Physiol* 587: 1817-1828, 2009.
67. **Haigis MC and Guarente LP.** Mammalian sirtuins--emerging roles in physiology, aging, and calorie restriction. *Genes Dev* 20: 2913-2921, 2006.
68. **Handschin C, Chin S, Li P, Liu F, Maratos-Flier E, Lebrasseur NK, Yan Z and Spiegelman BM.** Skeletal muscle fiber-type switching, exercise intolerance, and myopathy in PGC-1alpha muscle-specific knock-out animals. *J Biol Chem* 282: 30014-30021, 2007.
69. **Handschin C, Rhee J, Lin J, Tarr PT and Spiegelman BM.** An autoregulatory loop controls peroxisome proliferator-activated receptor gamma coactivator 1alpha expression in muscle. *Proc Natl Acad Sci U S A* 100: 7111-7116, 2003.
70. **Hardie DG.** The AMP-activated protein kinase pathway--new players upstream and downstream. *J Cell Sci* 117: 5479-5487, 2004.

71. **Hardie DG.** AMP-activated/SNF1 protein kinases: conserved guardians of cellular energy. *Nat Rev Mol Cell Biol* 8: 774-785, 2007.
72. **Hardie DG and Hawley SA.** AMP-activated protein kinase: the energy charge hypothesis revisited. *Bioessays* 23: 1112-1119, 2001.
73. **Hardie DG and Pan DA.** Regulation of fatty acid synthesis and oxidation by the AMP-activated protein kinase. *Biochem Soc Trans* 30: 1064-1070, 2002.
74. **Hawley SA, Pan DA, Mustard KJ, Ross L, Bain J, Edelman AM, Frenguelli BG and Hardie DG.** Calmodulin-dependent protein kinase kinase-beta is an alternative upstream kinase for AMP-activated protein kinase. *Cell Metab* 2: 9-19, 2005.
75. **Hayashida S, Arimoto A, Kuramoto Y, Kozako T, Honda S, Shimeno H and Soeda S.** Fasting promotes the expression of SIRT1, an NAD<sup>+</sup> -dependent protein deacetylase, via activation of PPARalpha in mice. *Mol Cell Biochem* 339: 285-292, 2010.
76. **Hepple RT.** Why eating less keeps mitochondria working in aged skeletal muscle. *Exerc Sport Sci Rev* 37: 23-28, 2009.
77. **Herranz D, Munoz-Martin M, Canamero M, Mulero F, Martinez-Pastor B, Fernandez-Capetillo O and Serrano M.** Sirt1 improves healthy ageing and protects from metabolic syndrome-associated cancer. *Nat Commun* 1: 1-8, 2010.
78. **Hirayama J, Sahar S, Grimaldi B, Tamaru T, Takamatsu K, Nakahata Y**

- and Sassone-Corsi P.** CLOCK-mediated acetylation of BMAL1 controls circadian function. *Nature* 450: 1086-1090, 2007.
79. **Hisahara S, Chiba S, Matsumoto H, Tanno M, Yagi H, Shimohama S, Sato M and Horio Y.** Histone deacetylase SIRT1 modulates neuronal differentiation by its nuclear translocation. *Proc Natl Acad Sci U S A* 105: 15599-15604, 2008.
80. **Holloszy JO.** Biochemical adaptations in muscle. Effects of exercise on mitochondrial oxygen uptake and respiratory enzyme activity in skeletal muscle. *J Biol Chem* 242: 2278-2282, 1967.
81. **Hoppeler H.** Exercise-induced ultrastructural changes in skeletal muscle. *Int J Sports Med* 7: 187-204, 1986.
82. **Howald H, Hoppeler H, Claassen H, Mathieu O and Straub R.** Influences of endurance training on the ultrastructural composition of the different muscle fiber types in humans. *Pflugers Arch* 403: 369-376, 1985.
83. **Howitz KT, Bitterman KJ, Cohen HY, Lamming DW, Lavu S, Wood JG, Zipkin RE, Chung P, Kisielewski A, Zhang LL, Scherer B and Sinclair DA.** Small molecule activators of sirtuins extend *Saccharomyces cerevisiae* lifespan. *Nature* 425: 191-196, 2003.
84. **Hsu CP, Oka S, Shao D, Hariharan N and Sadoshima J.** Nicotinamide phosphoribosyltransferase regulates cell survival through NAD<sup>+</sup> synthesis in cardiac myocytes. *Circ Res* 105: 481-491, 2009.

85. **Irrcher I, Adhihetty PJ, Joseph AM, Ljubicic V and Hood DA.** Regulation of mitochondrial biogenesis in muscle by endurance exercise. *Sports Med* 33: 783-793, 2003.
86. **Irrcher I, Adhihetty PJ, Sheehan T, Joseph AM and Hood DA.** PPARgamma coactivator-1alpha expression during thyroid hormone- and contractile activity-induced mitochondrial adaptations. *Am J Physiol Cell Physiol* 284: C1669-C1677, 2003.
87. **Irrcher I, Ljubicic V, Kirwan AF and Hood DA.** AMP-activated protein kinase-regulated activation of the PGC-1alpha promoter in skeletal muscle cells. *PLoS ONE* 3: e3614, 2008.
88. **Jager S, Handschin C, St-Pierre J and Spiegelman BM.** AMP-activated protein kinase (AMPK) action in skeletal muscle via direct phosphorylation of PGC-1alpha. *Proc Natl Acad Sci U S A* 104: 12017-12022, 2007.
89. **Jensen TE, Rose AJ, Jorgensen SB, Brandt N, Schjerling P, Wojtaszewski JF and Richter EA.** Possible CaMKK-dependent regulation of AMPK phosphorylation and glucose uptake at the onset of mild tetanic skeletal muscle contraction. *Am J Physiol Endocrinol Metab* 292: E1308-E1317, 2007.
90. **Jeong J, Juhn K, Lee H, Kim SH, Min BH, Lee KM, Cho MH, Park GH and Lee KH.** SIRT1 promotes DNA repair activity and deacetylation of Ku70. *Exp Mol Med* 39: 8-13, 2007.

91. **Jones DA, de Ruiter CJ and de HA.** Change in contractile properties of human muscle in relationship to the loss of power and slowing of relaxation seen with fatigue. *J Physiol* 576: 913-922, 2006.
92. **Joseph AM, Joannisse DR, Baillot RG and Hood DA.** Mitochondrial dysregulation in the pathogenesis of diabetes: potential for mitochondrial biogenesis-mediated interventions. *Exp Diabetes Res* 2012: 642038, 2012.
93. **Kaeberlein M and Kennedy BK.** Does resveratrol activate yeast Sir2 in vivo? *Aging Cell* 6: 415-416, 2007.
94. **Kaeberlein M, McVey M and Guarente L.** The SIR2/3/4 complex and SIR2 alone promote longevity in *Saccharomyces cerevisiae* by two different mechanisms. *Genes Dev* 13: 2570-2580, 1999.
95. **Kaeberlein M, Powers RW, III, Steffen KK, Westman EA, Hu D, Dang N, Kerr EO, Kirkland KT, Fields S and Kennedy BK.** Regulation of yeast replicative life span by TOR and Sch9 in response to nutrients. *Science* 310: 1193-1196, 2005.
96. **Kang H, Suh JY, Jung YS, Jung JW, Kim MK and Chung JH.** Peptide switch is essential for Sirt1 deacetylase activity. *Mol Cell* 44: 203-213, 2011.
97. **Kapahi P, Zid BM, Harper T, Koslover D, Sapin V and Benzer S.** Regulation of lifespan in *Drosophila* by modulation of genes in the TOR signaling pathway. *Curr Biol* 14: 885-890, 2004.

98. **King DP, Zhao Y, Sangoram AM, Wilsbacher LD, Tanaka M, Antoch MP, Steeves TD, Vitaterna MH, Kornhauser JM, Lowrey PL, Turek FW and Takahashi JS.** Positional cloning of the mouse circadian clock gene. *Cell* 89: 641-653, 1997.
99. **Kirkwood SP, Munn EA and Brooks GA.** Mitochondrial reticulum in limb skeletal muscle. *Am J Physiol* 251: C395-C402, 1986.
100. **Kohsaka A and Bass J.** A sense of time: how molecular clocks organize metabolism. *Trends Endocrinol Metab* 18: 4-11, 2007.
101. **Kohsaka A, Laposky AD, Ramsey KM, Estrada C, Joshu C, Kobayashi Y, Turek FW and Bass J.** High-fat diet disrupts behavioral and molecular circadian rhythms in mice. *Cell Metab* 6: 414-421, 2007.
102. **Koltai E, Szabo Z, Atalay M, Boldogh I, Naito H, Goto S, Nyakas C and Radak Z.** Exercise alters SIRT1, SIRT6, NAD and NAMPT levels in skeletal muscle of aged rats. *Mech Ageing Dev* 131: 21-28, 2010.
103. **Kornberg H.** Krebs and his trinity of cycles. *Nat Rev Mol Cell Biol* 1: 225-228, 2000.
104. **Krebs HA.** The history of the tricarboxylic acid cycle. *Perspect Biol Med* 14: 154-170, 1970.
105. **Krieger DA, Tate CA, Millin-Wood J and Booth FW.** Populations of rat skeletal muscle mitochondria after exercise and immobilization. *J Appl Physiol* 48: 23-28, 1980.

106. **Kume K, Zylka MJ, Sriram S, Shearman LP, Weaver DR, Jin X, Maywood ES, Hastings MH and Reppert SM.** mCRY1 and mCRY2 are essential components of the negative limb of the circadian clock feedback loop. *Cell* 98: 193-205, 1999.
107. **Kume S, Uzu T, Horiike K, Chin-Kanasaki M, Isshiki K, Araki S, Sugimoto T, Haneda M, Kashiwagi A and Koya D.** Calorie restriction enhances cell adaptation to hypoxia through Sirt1-dependent mitochondrial autophagy in mouse aged kidney. *J Clin Invest* 120: 1043-1055, 2010.
108. **Kurth-Kraczek EJ, Hirshman MF, Goodyear LJ and Winder WW.** 5' AMP-activated protein kinase activation causes GLUT4 translocation in skeletal muscle. *Diabetes* 48: 1667-1671, 1999.
109. **Lagouge M, Argmann C, Gerhart-Hines Z, Meziane H, Lerin C, Daussin F, Messadeq N, Milne J, Lambert P, Elliott P, Geny B, Laakso M, Puigserver P and Auwerx J.** Resveratrol improves mitochondrial function and protects against metabolic disease by activating SIRT1 and PGC-1alpha. *Cell* 127: 1109-1122, 2006.
110. **Lane MA, Black A, Handy A, Tilmont EM, Ingram DK and Roth GS.** Caloric restriction in primates. *Ann N Y Acad Sci* 928: 287-295, 2001.
111. **Lee CM, Aspnes LE, Chung SS, Weindruch R and Aiken JM.** Influences of caloric restriction on age-associated skeletal muscle fiber characteristics and mitochondrial changes in rats and mice. *Ann N Y Acad Sci* 854: 182-191, 1998.

112. **Lee IH, Cao L, Mostoslavsky R, Lombard DB, Liu J, Bruns NE, Tsokos M, Alt FW and Finkel T.** A role for the NAD-dependent deacetylase Sirt1 in the regulation of autophagy. *Proc Natl Acad Sci U S A* 105: 3374-3379, 2008.
113. **Leeuwenburgh C and Heinecke JW.** Oxidative stress and antioxidants in exercise. *Curr Med Chem* 8: 829-838, 2001.
114. **Lerin C, Rodgers JT, Kalume DE, Kim SH, Pandey A and Puigserver P.** GCN5 acetyltransferase complex controls glucose metabolism through transcriptional repression of PGC-1alpha. *Cell Metab* 3: 429-438, 2006.
115. **Levine B and Klionsky DJ.** Development by self-digestion: molecular mechanisms and biological functions of autophagy. *Dev Cell* 6: 463-477, 2004.
116. **Lin SJ, Ford E, Haigis M, Liszt G and Guarente L.** Calorie restriction extends yeast life span by lowering the level of NADH. *Genes Dev* 18: 12-16, 2004.
117. **Lin SJ, Kaeberlein M, Andalis AA, Sturtz LA, Defossez PA, Culotta VC, Fink GR and Guarente L.** Calorie restriction extends *Saccharomyces cerevisiae* lifespan by increasing respiration. *Nature* 418: 344-348, 2002.
118. **Little JP, Safdar A, Wilkin GP, Tarnopolsky MA and Gibala MJ.** A practical model of low-volume high-intensity interval training induces mitochondrial biogenesis in human skeletal muscle: potential mechanisms. *J Physiol* 588: 1011-1022, 2010.
119. **Liu C, Li S, Liu T, Borjigin J and Lin JD.** Transcriptional coactivator PGC-

- 1alpha integrates the mammalian clock and energy metabolism. *Nature* 447: 477-481, 2007.
120. **Lopez-Lluch G, Hunt N, Jones B, Zhu M, Jamieson H, Hilmer S, Cascajo MV, Allard J, Ingram DK, Navas P and de CR.** Calorie restriction induces mitochondrial biogenesis and bioenergetic efficiency. *Proc Natl Acad Sci U S A* 103: 1768-1773, 2006.
121. **Luo J, Nikolaev AY, Imai S, Chen D, Su F, Shiloh A, Guarente L and Gu W.** Negative control of p53 by Sir2alpha promotes cell survival under stress. *Cell* 107: 137-148, 2001.
122. **Maiuri MC, Le TG, Criollo A, Rain JC, Gautier F, Juin P, Tasdemir E, Pierron G, Troulinaki K, Tavernarakis N, Hickman JA, Geneste O and Kroemer G.** Functional and physical interaction between Bcl-X(L) and a BH3-like domain in Beclin-1. *EMBO J* 26: 2527-2539, 2007.
123. **Mammucari C, Milan G, Romanello V, Masiero E, Rudolf R, Del PP, Burden SJ, Di LR, Sandri C, Zhao J, Goldberg AL, Schiaffino S and Sandri M.** FoxO3 controls autophagy in skeletal muscle in vivo. *Cell Metab* 6: 458-471, 2007.
124. **Margulis L and Bermudes D.** Symbiosis as a mechanism of evolution: status of cell symbiosis theory. *Symbiosis* 1: 101-124, 1985.
125. **Margulis L and Stolz JF.** Cell symbiosis [correction of symbiosis] theory: status and implications for the fossil record. *Adv Space Res* 4: 195-201, 1984.

126. **Marsin AS, Bertrand L, Rider MH, Deprez J, Beauloye C, Vincent MF, Vandenberg BG, Carling D and Hue L.** Phosphorylation and activation of heart PFK-2 by AMPK has a role in the stimulation of glycolysis during ischaemia. *Curr Biol* 10: 1247-1255, 2000.
127. **Martin SG, Laroche T, Suka N, Grunstein M and Gasser SM.** Relocalization of telomeric Ku and SIR proteins in response to DNA strand breaks in yeast. *Cell* 97: 621-633, 1999.
128. **Maury E, Ramsey KM and Bass J.** Circadian rhythms and metabolic syndrome: from experimental genetics to human disease. *Circ Res* 106: 447-462, 2010.
129. **Milne JC, Lambert PD, Schenk S, Carney DP, Smith JJ, Gagne DJ, Jin L, Boss O, Perni RB, Vu CB, Bemis JE, Xie R, Disch JS, Ng PY, Nunes JJ, Lynch AV, Yang H, Galonek H, Israelian K, Choy W, Iffland A, Lavu S, Medvedik O, Sinclair DA, Olefsky JM, Jirousek MR, Elliott PJ and Westphal CH.** Small molecule activators of SIRT1 as therapeutics for the treatment of type 2 diabetes. *Nature* 450: 712-716, 2007.
130. **Mistlberger RE and Skene DJ.** Nonphotic entrainment in humans? *J Biol Rhythms* 20: 339-352, 2005.
131. **Mizushima N, Yamamoto A, Matsui M, Yoshimori T and Ohsumi Y.** In vivo analysis of autophagy in response to nutrient starvation using transgenic mice expressing a fluorescent autophagosome marker. *Mol Biol Cell* 15: 1101-1111, 2004.

132. **Morselli E, Galluzzi L, Kepp O, Criollo A, Maiuri MC, Tavernarakis N, Madeo F and Kroemer G.** Autophagy mediates pharmacological lifespan extension by spermidine and resveratrol. *Aging (Albany NY)* 1: 961-970, 2009.
133. **Motta MC, Divecha N, Lemieux M, Kamel C, Chen D, Gu W, Bultsma Y, McBurney M and Guarente L.** Mammalian SIRT1 represses forkhead transcription factors. *Cell* 116: 551-563, 2004.
134. **Nakahata Y, Kaluzova M, Grimaldi B, Sahar S, Hirayama J, Chen D, Guarente LP and Sassone-Corsi P.** The NAD<sup>+</sup>-dependent deacetylase SIRT1 modulates CLOCK-mediated chromatin remodeling and circadian control. *Cell* 134: 329-340, 2008.
135. **Nakahata Y, Sahar S, Astarita G, Kaluzova M and Sassone-Corsi P.** Circadian control of the NAD<sup>+</sup> salvage pathway by CLOCK-SIRT1. *Science* 324: 654-657, 2009.
136. **Narkar VA, Downes M, Yu RT, Embler E, Wang YX, Banayo E, Mihaylova MM, Nelson MC, Zou Y, Juguilon H, Kang H, Shaw RJ and Evans RM.** AMPK and PPARdelta agonists are exercise mimetics. *Cell* 134: 405-415, 2008.
137. **Nasrin N, Kaushik VK, Fortier E, Wall D, Pearson KJ, de CR and Bordone L.** JNK1 phosphorylates SIRT1 and promotes its enzymatic activity. *PLoS ONE* 4: e8414, 2009.
138. **Nemoto S, Fergusson MM and Finkel T.** SIRT1 functionally interacts with the

- metabolic regulator and transcriptional coactivator PGC-1{alpha}. *J Biol Chem* 280: 16456-16460, 2005.
139. **Nisoli E, Tonello C, Cardile A, Cozzi V, Bracale R, Tedesco L, Falcone S, Valerio A, Cantoni O, Clementi E, Moncada S and Carruba MO.** Calorie restriction promotes mitochondrial biogenesis by inducing the expression of eNOS. *Science* 310: 314-317, 2005.
140. **O'Leary MF and Hood DA.** Effect of prior chronic contractile activity on mitochondrial function and apoptotic protein expression in denervated muscle. *J Appl Physiol* 105: 114-120, 2008.
141. **Okazaki M, Iwasaki Y, Nishiyama M, Taguchi T, Tsugita M, Nakayama S, Kambayashi M, Hashimoto K and Terada Y.** PPARbeta/delta regulates the human SIRT1 gene transcription via Sp1. *Endocr J* 57: 403-413, 2010.
142. **Park SJ, Ahmad F, Philp A, Baar K, Williams T, Luo H, Ke H, Rehmann H, Taussig R, Brown AL, Kim MK, Beaven MA, Burgin AB, Manganiello V and Chung JH.** Resveratrol ameliorates aging-related metabolic phenotypes by inhibiting cAMP phosphodiesterases. *Cell* 148: 421-433, 2012.
143. **Patti ME, Butte AJ, Crunkhorn S, Cusi K, Berria R, Kashyap S, Miyazaki Y, Kohane I, Costello M, Saccone R, Landaker EJ, Goldfine AB, Mun E, DeFronzo R, Finlayson J, Kahn CR and Mandarino LJ.** Coordinated reduction of genes of oxidative metabolism in humans with insulin resistance and

- diabetes: Potential role of PGC1 and NRF1. *Proc Natl Acad Sci U S A* 100: 8466-8471, 2003.
144. **Pattingre S, Espert L, Biard-Piechaczyk M and Codogno P.** Regulation of macroautophagy by mTOR and Beclin 1 complexes. *Biochimie* 90: 313-323, 2008.
145. **Pauli JR, Ropelle ER, Cintra DE, De Souza CT, da Silva AS, Moraes JC, Prada PO, de Almeida Leme JA, Luciano E, Velloso LA, Carvalheira JB and Saad MJ.** Acute exercise reverses aged-induced impairments in insulin signaling in rodent skeletal muscle. *Mech Ageing Dev* 131: 323-329, 2010.
146. **Periasamy M and Kalyanasundaram A.** SERCA pump isoforms: their role in calcium transport and disease. *Muscle Nerve* 35: 430-442, 2007.
147. **Pette D and Staron RS.** Cellular and molecular diversities of mammalian skeletal muscle fibers. *Rev Physiol Biochem Pharmacol* 116: 1-76, 1990.
148. **Pfluger PT, Herranz D, Velasco-Miguel S, Serrano M and Tschop MH.** Sirt1 protects against high-fat diet-induced metabolic damage. *Proc Natl Acad Sci U S A* 105: 9793-9798, 2008.
149. **Pilegaard H, Saltin B and Neufer PD.** Exercise induces transient transcriptional activation of the PGC-1alpha gene in human skeletal muscle. *J Physiol* 546: 851-858, 2003.
150. **Place N, Bruton JD and Westerblad H.** Mechanisms of fatigue induced by

isometric contractions in exercising humans and in mouse isolated single muscle fibres. *Clin Exp Pharmacol Physiol* 36: 334-339, 2009.

151. **Posterino GS, Dutka TL and Lamb GD.** L(+)-lactate does not affect twitch and tetanic responses in mechanically skinned mammalian muscle fibres. *Pflugers Arch* 442: 197-203, 2001.
152. **Powers SK and Jackson MJ.** Exercise-induced oxidative stress: cellular mechanisms and impact on muscle force production. *Physiol Rev* 88: 1243-1276, 2008.
153. **Preitner N, Damiola F, Lopez-Molina L, Zakany J, Duboule D, Albrecht U and Schibler U.** The orphan nuclear receptor REV-ERB $\alpha$  controls circadian transcription within the positive limb of the mammalian circadian oscillator. *Cell* 110: 251-260, 2002.
154. **Puigserver P and Spiegelman BM.** Peroxisome proliferator-activated receptor-gamma coactivator 1 alpha (PGC-1 alpha): transcriptional coactivator and metabolic regulator. *Endocr Rev* 24: 78-90, 2003.
155. **Puigserver P, Wu Z, Park CW, Graves R, Wright M and Spiegelman BM.** A cold-inducible coactivator of nuclear receptors linked to adaptive thermogenesis. *Cell* 92: 829-839, 1998.
156. **Ramsey KM, Yoshino J, Brace CS, Abrassart D, Kobayashi Y, Marcheva B, Hong HK, Chong JL, Buhr ED, Lee C, Takahashi JS, Imai S and Bass J.**

- Circadian clock feedback cycle through NAMPT-mediated NAD<sup>+</sup> biosynthesis. *Science* 324: 651-654, 2009.
157. **Rasbach KA, Gupta RK, Ruas JL, Wu J, Naseri E, Estall JL and Spiegelman BM.** PGC-1alpha regulates a HIF2alpha-dependent switch in skeletal muscle fiber types. *Proc Natl Acad Sci U S A* 107: 21866-21871, 2010.
158. **Ravikumar B, Vacher C, Berger Z, Davies JE, Luo S, Oroz LG, Scaravilli F, Easton DF, Duden R, O'Kane CJ and Rubinsztein DC.** Inhibition of mTOR induces autophagy and reduces toxicity of polyglutamine expansions in fly and mouse models of Huntington disease. *Nat Genet* 36: 585-595, 2004.
159. **Reppert SM and Weaver DR.** Coordination of circadian timing in mammals. *Nature* 418: 935-941, 2002.
160. **Revollo JR, Grimm AA and Imai S.** The NAD biosynthesis pathway mediated by nicotinamide phosphoribosyltransferase regulates Sir2 activity in mammalian cells. *J Biol Chem* 279: 50754-50763, 2004.
161. **Rizki G, Iwata TN, Li J, Riedel CG, Picard CL, Jan M, Murphy CT and Lee SS.** The evolutionarily conserved longevity determinants HCF-1 and SIR-2.1/SIRT1 collaborate to regulate DAF-16/FOXO. *PLoS Genet* 7: e1002235, 2011.
162. **Rodgers JT, Lerin C, Gerhart-Hines Z and Puigserver P.** Metabolic adaptations through the PGC-1 alpha and SIRT1 pathways. *FEBS Lett* 582: 46-53, 2008.

163. **Rodgers JT, Lerin C, Haas W, Gygi SP, Spiegelman BM and Puigserver P.** Nutrient control of glucose homeostasis through a complex of PGC-1alpha and SIRT1. *Nature* 434: 113-118, 2005.
164. **Rogina B and Helfand SL.** Sir2 mediates longevity in the fly through a pathway related to calorie restriction. *Proc Natl Acad Sci U S A* 101: 15998-16003, 2004.
165. **Rolfe DF and Brown GC.** Cellular energy utilization and molecular origin of standard metabolic rate in mammals. *Physiol Rev* 77: 731-758, 1997.
166. **Roth GS, Ingram DK and Lane MA.** Caloric restriction in primates and relevance to humans. *Ann N Y Acad Sci* 928: 305-315, 2001.
167. **Sakamoto K, Zarrinpashneh E, Budas GR, Pouleur AC, Dutta A, Prescott AR, Vanoverschelde JL, Ashworth A, Jovanovic A, Alessi DR and Bertrand L.** Deficiency of LKB1 in heart prevents ischemia-mediated activation of AMPKalpha2 but not AMPKalpha1. *Am J Physiol Endocrinol Metab* 290: E780-E788, 2006.
168. **Sanders MJ, Grondin PO, Hegarty BD, Snowden MA and Carling D.** Investigating the mechanism for AMP activation of the AMP-activated protein kinase cascade. *Biochem J* 403: 139-148, 2007.
169. **Sano M, Tokudome S, Shimizu N, Yoshikawa N, Ogawa C, Shirakawa K, Endo J, Katayama T, Yuasa S, Ieda M, Makino S, Hattori F, Tanaka H and Fukuda K.** Intramolecular control of protein stability, subnuclear compartmentalization, and coactivator function of peroxisome proliferator-

- activated receptor gamma coactivator 1alpha. *J Biol Chem* 282: 25970-25980, 2007.
170. **Schiaffino S and Serrano A.** Calcineurin signaling and neural control of skeletal muscle fiber type and size. *Trends Pharmacol Sci* 23: 569-575, 2002.
171. **Shaw RJ, Kosmatka M, Bardeesy N, Hurley RL, Witters LA, DePinho RA and Cantley LC.** The tumor suppressor LKB1 kinase directly activates AMP-activated kinase and regulates apoptosis in response to energy stress. *Proc Natl Acad Sci U S A* 101: 3329-3335, 2004.
172. **Spangenburg EE and Booth FW.** Molecular regulation of individual skeletal muscle fibre types. *Acta Physiol Scand* 178: 413-424, 2003.
173. **Stapleton D, Mitchelhill KI, Gao G, Widmer J, Michell BJ, Teh T, House CM, Fernandez CS, Cox T, Witters LA and Kemp BE.** Mammalian AMP-activated protein kinase subfamily. *J Biol Chem* 271: 611-614, 1996.
174. **Steinberg GR, O'Neill HM, Dzamko NL, Galic S, Naim T, Koopman R, Jorgensen SB, Honeyman J, Hewitt K, Chen ZP, Schertzer JD, Scott J, Koentgen F, Lynch GS, Watt MJ, Vandenderen BJ, Campbell DJ and Kemp BE.** Whole-body deletion of AMPK  $\beta$ 2 reduces muscle AMPK and exercise capacity. *J Biol Chem* 2010.
175. **Sukumaran S, Almon RR, DuBois DC and Jusko WJ.** Circadian rhythms in gene expression: Relationship to physiology, disease, drug disposition and drug action. *Adv Drug Deliv Rev* 62: 904-917, 2010.

176. **Suter M, Riek U, Tuerk R, Schlattner U, Wallimann T and Neumann D.** Dissecting the role of 5'-AMP for allosteric stimulation, activation, and deactivation of AMP-activated protein kinase. *J Biol Chem* 281: 32207-32216, 2006.
177. **Suwa M, Nakano H, Radak Z and Kumagai S.** Endurance exercise increases the SIRT1 and peroxisome proliferator-activated receptor gamma coactivator-1alpha protein expressions in rat skeletal muscle. *Metabolism* 57: 986-998, 2008.
178. **Syntichaki P, Troulinaki K and Tavernarakis N.** eIF4E function in somatic cells modulates ageing in *Caenorhabditis elegans*. *Nature* 445: 922-926, 2007.
179. **Takahashi M and Hood DA.** Protein import into subsarcolemmal and intermyofibrillar skeletal muscle mitochondria. Differential import regulation in distinct subcellular regions. *J Biol Chem* 271: 27285-27291, 1996.
180. **Tanno M, Sakamoto J, Miura T, Shimamoto K and Horio Y.** Nucleocytoplasmic shuttling of the NAD<sup>+</sup>-dependent histone deacetylase SIRT1. *J Biol Chem* 282: 6823-6832, 2007.
181. **Teyssier C, Ma H, Emter R, Kralli A and Stallcup MR.** Activation of nuclear receptor coactivator PGC-1alpha by arginine methylation. *Genes Dev* 19: 1466-1473, 2005.
182. **Tissenbaum HA and Guarente L.** Increased dosage of a sir-2 gene extends lifespan in *Caenorhabditis elegans*. *Nature* 410: 227-230, 2001.

183. **Townley R and Shapiro L.** Crystal structures of the adenylate sensor from fission yeast AMP-activated protein kinase. *Science* 315: 1726-1729, 2007.
184. **Um JH, Park SJ, Kang H, Yang S, Foretz M, McBurney MW, Kim MK, Viollet B and Chung JH.** AMP-activated protein kinase-deficient mice are resistant to the metabolic effects of resveratrol. *Diabetes* 59: 554-563, 2010.
185. **Valenzano DR, Terzibasi E, Genade T, Cattaneo A, Domenici L and Cellarino A.** Resveratrol prolongs lifespan and retards the onset of age-related markers in a short-lived vertebrate. *Curr Biol* 16: 296-300, 2006.
186. **Vaziri H, Dessain SK, Ng EE, Imai SI, Frye RA, Pandita TK, Guarente L and Weinberg RA.** hSIR2(SIRT1) functions as an NAD-dependent p53 deacetylase. *Cell* 107: 149-159, 2001.
187. **Vellai T, Takacs-Vellai K, Zhang Y, Kovacs AL, Orosz L and Muller F.** Genetics: influence of TOR kinase on lifespan in *C. elegans*. *Nature* 426: 620, 2003.
188. **Viswanathan M and Guarente L.** Regulation of *Caenorhabditis elegans* lifespan by sir-2.1 transgenes. *Nature* 477: E1-E2, 2011.
189. **Wallace DC.** Mitochondrial DNA mutations in disease and aging. *Environ Mol Mutagen* 51: 440-450, 2010.
190. **Wallace DC.** Mitochondrial genetics: a paradigm for aging and degenerative diseases? *Science* 256: 628-632, 1992.

191. **Wang F, Nguyen M, Qin FX and Tong Q.** SIRT2 deacetylates FOXO3a in response to oxidative stress and caloric restriction. *Aging Cell* 6: 505-514, 2007.
192. **Wende AR, Huss JM, Schaeffer PJ, Giguere V and Kelly DP.** PGC-1alpha coactivates PDK4 gene expression via the orphan nuclear receptor ERRalpha: a mechanism for transcriptional control of muscle glucose metabolism. *Mol Cell Biol* 25: 10684-10694, 2005.
193. **Westerblad H, Allen DG and Lannergren J.** Muscle fatigue: lactic acid or inorganic phosphate the major cause? *News Physiol Sci* 17: 17-21, 2002.
194. **Westerblad H, Lannergren J and Allen DG.** Slowed relaxation in fatigued skeletal muscle fibers of *Xenopus* and Mouse. Contribution of  $[Ca^{2+}]_i$  and cross-bridges. *J Gen Physiol* 109: 385-399, 1997.
195. **Witczak CA, Fujii N, Hirshman MF and Goodyear LJ.**  $Ca^{2+}$ /calmodulin-dependent protein kinase kinase-alpha regulates skeletal muscle glucose uptake independent of AMP-activated protein kinase and Akt activation. *Diabetes* 56: 1403-1409, 2007.
196. **Wood JG, Rogina B, Lavu S, Howitz K, Helfand SL, Tatar M and Sinclair D.** Sirtuin activators mimic caloric restriction and delay ageing in metazoans. *Nature* 430: 686-689, 2004.
197. **Wu Z, Puigserver P, Andersson U, Zhang C, Adelmant G, Mootha V, Troy A, Cinti S, Lowell B, Scarpulla RC and Spiegelman BM.** Mechanisms

controlling mitochondrial biogenesis and respiration through the thermogenic coactivator PGC-1. *Cell* 98: 115-124, 1999.

198. **Xiao B, Heath R, Saiu P, Leiper FC, Leone P, Jing C, Walker PA, Haire L, Eccleston JF, Davis CT, Martin SR, Carling D and Gamblin SJ.** Structural basis for AMP binding to mammalian AMP-activated protein kinase. *Nature* 449: 496-500, 2007.
199. **Yang H, Yang T, Baur JA, Perez E, Matsui T, Carmona JJ, Lamming DW, Souza-Pinto NC, Bohr VA, Rosenzweig A, de CR, Sauve AA and Sinclair DA.** Nutrient-sensitive mitochondrial NAD<sup>+</sup> levels dictate cell survival. *Cell* 130: 1095-1107, 2007.
200. **Zechner C, Lai L, Zechner JF, Geng T, Yan Z, Rumsey JW, Colliia D, Chen Z, Wozniak DF, Leone TC and Kelly DP.** Total skeletal muscle PGC-1 deficiency uncouples mitochondrial derangements from fiber type determination and insulin sensitivity. *Cell Metab* 12: 633-642, 2010.
201. **Zhang Q, Wang SY, Fleuriel C, Leprince D, Rocheleau JV, Piston DW and Goodman RH.** Metabolic regulation of SIRT1 transcription via a HIC1:CtBP corepressor complex. *Proc Natl Acad Sci U S A* 104: 829-833, 2007.
202. **Zhao J, Brault JJ, Schild A, Cao P, Sandri M, Schiaffino S, Lecker SH and Goldberg AL.** FoxO3 coordinately activates protein degradation by the autophagic/lysosomal and proteasomal pathways in atrophying muscle cells. *Cell Metab* 6: 472-483, 2007.

203. **Zheng B, Albrecht U, Kaasik K, Sage M, Lu W, Vaishnav S, Li Q, Sun ZS, Eichele G, Bradley A and Lee CC.** Nonredundant roles of the mPer1 and mPer2 genes in the mammalian circadian clock. *Cell* 105: 683-694, 2001.
204. **Zong H, Ren JM, Young LH, Pypaert M, Mu J, Birnbaum MJ and Shulman GI.** AMP kinase is required for mitochondrial biogenesis in skeletal muscle in response to chronic energy deprivation. *Proc Natl Acad Sci U S A* 99: 15983-15987, 2002.

**CHAPTER 2: CONTRACTILE ACTIVITY AND RESVERATROL EXERT  
A SYNERGISTIC EFFECT ON MITOCHONDRIAL CONTENT**

## **Rationale for Chapter 2**

Resveratrol (RSV) is a natural polyphenolic compound mainly found in the skin of grapes, and is well known for its phytoestrogenic and antioxidant properties. Similar to exercise, RSV treatment induces a higher aerobic capacity in mice, along with increased oxygen consumption in muscle fibers. These RSV-mediated effects are due to enhancements in mitochondrial function and metabolic homeostasis, which are postulated to occur through the modulation of SirT1. SirT1 has been shown to regulate the tissue-dependent deacetylation and activation of PGC-1 $\alpha$ , an important protein for mitochondrial biogenesis, via thermogenesis or in response to caloric restriction. The increase in SirT1 deacetylase activity with RSV is proposed to occur through the activation of the AMPK pathway, which results in an increase in the SirT1 cofactor NAD<sup>+</sup> and therefore an increase in SirT1 activity. Since exercise is also known to activate the AMPK pathway, in Chapter 2 we compared the ability of RSV to a cell culture model of exercise to induce SirT1-mediated mitochondrial biogenesis. To do this we compared the effects of electrical stimulation of C2C12 mouse myotubes, also known as chronic contractile activity (CCA), to that of an RSV treatment. With each treatment we examined the activity and expression of known mediators (p38 and AMPK) for the induction of mitochondrial biogenesis, in addition to the expression and subcellular localization of SirT1 and PGC-1 $\alpha$  protein. We hypothesized that CCA would activate more pathways (p38, AMPK, CamKK $\beta$ ) that lead to the induction of mitochondrial

biogenesis when compared to RSV, therefore resulting in a more robust effect than RSV. In addition, we hypothesized that RSV may produce a SirT1-mediated additive effect on mitochondrial biogenesis when combined with CCA in C2C12 myotubes.

#### **Author contributions**

Conceived and designed the experiments: KJM and DAH. Performed the experiments: KJM. Analyzed the data: KJM and DAH. Wrote the paper: KJM and DAH.

# **Contractile activity and resveratrol exert a synergistic effect on mitochondrial content**

Keir J. Menzies<sup>2,3</sup> and David A. Hood<sup>1,2,3</sup>

School of Kinesiology and Health Science<sup>1</sup>, Department of Biology<sup>2</sup>, and the Muscle Health Research Centre<sup>3</sup>, York University, Toronto M3J 1P3

**To whom correspondence should be addressed:** Dr. David A. Hood  
School of Kinesiology and Health Science,  
Farquharson Life Science Bldg.,  
Room 302,  
York University, Toronto, Ontario  
M3J 1P3, Canada  
Tel: (416) 736-2100 ext. 66640  
Fax: (416) 736-5698  
E-mail: dhood@yorku.ca

Running head: Resveratrol and contractile activity on mitochondria

Key words: Mitochondrial biogenesis, AMP Kinase, SirT1, PGC-1 $\alpha$ , cytochrome c oxidase

To be submitted to *Am J Physiol Cell Physiol*.

## **Abstract**

Exercise has dramatic effects on skeletal muscle mitochondrial bioenergetics and substrate utilization. Similarly, resveratrol (RSV) can induce an increase in mitochondrial content and function in various tissues. In this study we utilized an excitable C2C12 myotube cell culture model to compare the individual and combined effects of RSV treatment and chronic contractile activity (CCA) on mitochondrial biogenesis. Differentiated C2C12 myotubes were treated with CCA for 3 hrs per day for up to 4 days with, or without, the addition of RSV. PGC-1 $\alpha$  protein content was elevated 1.6-fold with CCA but did not increase with RSV treatment. Alternatively, RSV treatment, but not CCA, induced a 2-fold increase in SirT1 levels. Cytochrome c oxidase (COX) activity, an indicator of mitochondrial content, increased by 1.6- and 3.1-fold with RSV treatment and CCA, respectively. The combined treatments of RSV and CCA that resulted in elevations of both SirT1 and PGC-1 $\alpha$  induced a synergistic 6.1-fold increase in COX activity and mitochondrial mass, along with an enhanced translocation of cytosolic PGC-1 $\alpha$  and SirT1 to the nucleus. This synergistic effect was blocked by the SirT1 inhibitor nicotinamide (NAM). These results indicate that RSV treatment can produce a modest increase in mitochondrial content in muscle cells, which is less robust than the effect of CCA. However, the combination of treatments can lead to a potentiation of the contractile activity effect, in a manner which is SirT1-dependent.

## **Introduction**

Resveratrol (RSV) is a naturally occurring polyphenol mainly found in the skin of grapes and in the root of *Polygonum cuspidatum*, a root used in traditional folk medicine for the treatment of atherosclerosis and other diseases (10). The reported effects of RSV include cardioprotective, anti-diabetic and anti-obesity properties along with evidence of lifespan extension (24; 35; 36). Many of these are a result of improvements in mitochondrial function and metabolic homeostasis that occur in part through the modulation of SirT1 (5). As a class III NAD-dependent histone deacetylase, SirT1 has been implicated in various cellular processes, such as adipogenesis (38), DNA repair (6; 31), genomic stability (16; 27) and transcriptional silencing (2; 41). Importantly, SirT1 has been shown to be a promising target for improving mitochondrial biogenesis in various tissues including skeletal muscle (4; 9; 15; 25).

Skeletal muscle health is an important determinant of metabolic diseases (37; 40). Recent studies have demonstrated that resveratrol has many beneficial effects on muscle health. For example, RSV was shown to reduce the functional decrements and the oxidative stress that occurs with skeletal muscle disuse in rats and in mdx mice, a model of Duchenne muscular dystrophy (17; 23). In C2C12 mouse skeletal muscle cells, RSV has been shown to stimulate glucose uptake and improve insulin sensitivity by activating AMPK (35). AMPK is essential for the phosphorylation and activation of the master regulator of mitochondrial biogenesis PGC-1 $\alpha$  (24). In addition, RSV was demonstrated

to increase SirT1 activity and expression in skeletal muscle, which has been shown to be important in PGC-1 $\alpha$  deacetylation and the subsequent induction of mitochondrial biogenesis (3; 29; 42). The exact mechanism of RSV effects is elusive, yet it has been suggested that RSV may not be working through SirT1 directly, as has been previously debated, but may induce an elevation in the NAD-to-NADH ratio in an AMPK-dependent manner (8; 48). In agreement with this theory, RSV increased the phosphorylation status of AMPK $\alpha$  in skeletal muscle of high fat-fed diet-induced obese mice (28). Besides the activation of SirT1, RSV has been shown to induce a cytoplasmic-to-nuclear shuttling of SirT1 in skeletal muscle myotubes (13). Since the dependence of RSV effectiveness on SirT1 activation is controversial, we have examined the role of SirT1 from the viewpoint that this protein may be required, in part, during skeletal muscle mitochondrial biogenesis, and that this effect may also depend on the metabolic status of the tissue.

Chronic electrical stimulation of C2C12 mouse skeletal muscle myotubes has been used previously to examine the molecular events induced by contractile activity which lead to mitochondrial biogenesis (11; 46). In the present study, we used this model to examine the differences in mitochondrial biogenesis when induced by chronic stimulation, RSV or the combination of these treatments. Our study demonstrates that CCA has a more robust effect on the induction of mitochondrial biogenesis compared to RSV treatment in C2C12 myotubes. However, we found that resveratrol can be used as an ergogenic aid to induce a strong synergistic increase in markers of mitochondrial

biogenesis when combined with contractile activity. These results indicate that RSV can facilitate mitochondrial adaptations in skeletal muscle tissue when the tissue is experiencing an altered metabolic state, as seen with contractile activity.

## **Methods**

***Cell culture and CCA.*** Embryonic murine skeletal muscle C2C12 myoblasts (ATCC) were maintained at 37°C in 5% CO<sub>2</sub> on 30-mm gelatin-coated plastic 6-well plates containing Dulbecco's modified Eagle's medium (DMEM) supplemented with 10% fetal bovine serum and 1% penicillin/streptomycin. At a confluence of 90%, C2C12 cells were induced to differentiate in DMEM supplemented with 5% heat-inactivated horse serum (HS) and antibiotic. Cells were differentiated for 4 days until myotubes were formed before treating with chronic contractile activity (CCA). CCA was performed using either 1 or 4 successive 3-h bouts (1- and 4-day protocols) of electrical stimulation (5 Hz, 7 V) with an intervening 21-h recovery period following each 3-h bout. The design of the electrical stimulation protocol was derived by modifying existing methods (20). Myotubes were treated separately with CCA, or in combination with 100 μM RSV, 50 μM Quercetin, or the SirT1 inhibitor nicotinamide (NAM).

***Immunoblotting.*** Protein extracts of C2C12 myotubes were separated via electrophoresis through SDS-polyacrylamide gels and were then transferred to nitrocellulose membranes (Amersham Biosciences). Membranes were incubated

overnight with antibodies against,  $\alpha$ -tubulin (1:8000; Calbiochem, CP06), COX-IV (1:500; Invitrogen, A21348), phospho-AMP-activated protein kinase (pAMPK; Thr172; 1:200; Cell Signaling, 25315), total-AMPK $\alpha$  (1:1,000; Cell Signaling, 2532), phospho-p38 (Thr180/Thr182; 1:200; Cell Signaling, 9211S), total p38 (1:1,000; Cell Signaling, 9212), PGC-1 $\alpha$  (1:500; Millipore, AB3242), Acetyl-p53 (lys379; 1:500; Cell Signaling, 2570S), and SirT1 (1:4000; Upstate, 05-707). This was followed by a 2-h incubation at room temperature with the appropriate secondary antibodies. Western blot signals are semi-quantitative and obtained within the linear range of the film.

***Cytochrome c oxidase (COX) assay.*** Cells were washed and scraped with ice-cold Dulbecco's phosphate buffered saline following each of the treatments. After centrifugation, pellets were resuspended in 100 mM Na<sub>2</sub>HPO<sub>4</sub> /K<sub>2</sub>HPO<sub>4</sub> / 2 mM EDTA (pH 7.2), sonicated on ice (3 x 3s), frozen in liquid N<sub>2</sub> and then thawed. Samples were then centrifuged again and supernatants were mixed with a test solution (10 mM K<sub>2</sub>HPO<sub>4</sub>) containing reduced cytochrome c (Sigma-Aldrich, St. Louis, MO). Enzyme activity was determined by measuring the maximal rate of oxidation of reduced cytochrome c using the change in absorbance at 550 nm on a Bio-Tek Synergy HT microplate reader.

***Mitochondrial mass and ROS (Reactive Oxygen Species).*** Mitochondrial mass was examined using MitoTracker Green FM (MTGFM; Invitrogen). Cells were stained with 20 nM MTGFM for 45 min at 37°C in differentiation media. ROS were monitored

using 2',7'-dichlorodihydrofluorescein diacetate (H<sub>2</sub>DCFDA, Sigma-Aldrich, St. Louis, MO). Cells were preincubated with 5  $\mu$ M of H<sub>2</sub>DCFDA for 45 min at 37°C in differentiation media. Staining for both of these fluorescent probes was performed in 6-well cell culture plates then quantified using a Bio-Tek Synergy HT microplate reader. Each well was then scraped for protein and quantified using a Bradford assay. All fluorescent values were expressed per  $\mu$ g of protein.

***Immunofluorescence.*** Cells were grown in a 6-well cell culture dish and fixed with 4% paraformaldehyde in PBS for 7 min at room temperature and permeabilized with a 0.1% solution of triton x-100 in PBS for 15 min at 4°C. Cells were then incubated overnight at 4°C with SirT1 and PGC-1 $\alpha$  antibodies. Alexa Fluor 488 and Alexa fluor 594 secondary antibodies (Invitrogen) were co-incubated for 1hr at room temperature. To visualize the nuclei within the myotubes, DAPI was included with the 1hr secondary antibody incubation at a dilution of 0.5  $\mu$ g/ml. Images were taken using a Nikon Eclipse fluorescent microscope.

***Statistics.*** Comparisons between control and CCA treated cells were evaluated using 2-way analyses of variance for each of the treatment conditions (DMSO, RSV, Quercetin, and NAM). Bonferroni post-tests were performed when applicable and error bars represent standard error of the mean. Additionally, the interaction term of a two factor ANOVA was used to test for synergism when examining a combined treatment of RSV and CA, as described previously (43), with significance defined as  $p < 0.05$ .

## **Results**

***Effectiveness of RSV.*** To document the effectiveness of RSV to induce SirT1 activity we examined several early phosphorylation and acetylation events which are downstream of SirT1 activity (35; 47) in differentiated muscle cells. Following a 1 hr RSV treatment, AMPK phosphorylation increased by 1.7-fold ( $p < 0.05$ ), while there was no effect on p38 (Fig. 1A, B). We also examined the deacetylation of p53, a known SirT1 target (Fig. 1C). Our results indicate that p53 was deacetylated by 15% after a 1 hr treatment with RSV compared to the vehicle control ( $p < 0.05$ ). This effect was inhibited when RSV was combined with the SirT1 inhibitor NAM. These results indicate that RSV treatment was effective in triggering several early signaling pathways in C2C12 myotubes.

***p38 protein phosphorylation - acute treatment.*** To examine the persistence of the RSV effect in combination with contractile activity, we electrically stimulated C2C12 myotubes for 3 hrs followed by 21 hrs of recovery in the presence or absence of RSV. The phosphorylation levels of p38 increased 6-fold with RSV treatment alone, 8-fold with stimulation alone and 9.5-fold with the combined treatment of RSV and stimulation compared to vehicle treated myotubes ( $p < 0.05$ ; Fig. 1D). However, the effects of RSV and stimulation on p38 phosphorylation were SirT1-independent, as NAM did not attenuate the RSV, or the stimulation-induced responses. p38 can disrupt the negative regulation of p160 myb binding protein on PGC-1 $\alpha$  via a phosphorylation event (14).

***SirT1 and PGC-1 $\alpha$  protein - chronic treatment.*** To investigate the effect of chronic treatment of RSV and CCA on SirT1, we treated C2C12 myotubes over a 4-day period and examined SirT1 expression. RSV treatment induced a 2-fold increase in SirT1 protein expression ( $p < 0.05$ ; Fig. 2A, B). However, CCA had no effect on SirT1 expression during this time. Alternatively, RSV did not alter PGC-1 $\alpha$  protein levels, but PGC-1 $\alpha$  expression increased 1.6-fold following 4 days of CCA ( $p < 0.05$ ; Fig. 2A, C). The combination of both RSV and CCA had no additional effects on either SirT1 or PGC-1 $\alpha$  protein expression.

***Indicators of mitochondrial biogenesis.*** COX activity and COX subunit IV (COXIV) expression are well known biochemical indicators of mitochondrial biogenesis (30). Contractile activity for 4 days resulted in a 1.4-fold increase in COXIV protein in the absence of RSV ( $p < 0.05$ ; Fig. 3A). RSV treatment of the cells also increased COXIV protein levels by 1.5-fold ( $p < 0.05$ ). When RSV and CCA were combined an additive effect was observed, since COXIV protein increased by 2.2-fold relative to vehicle-treated control cells. The RSV/CCA treatment also resulted in 1.4- and 1.6-fold more COXIV protein than the RSV, or CCA vehicle-treated myotubes, respectively, indicating the specific effect of RSV to increase COXIV expression when combined with stimulation ( $p < 0.05$ ).

COX activity was 3.1-fold higher following CCA ( $p < 0.05$ ; Fig. 3B). RSV treatment alone produced a smaller, but significant 1.6-fold increase in COX activity in

comparison to vehicle-treated myotubes. The combination of RSV and CCA treatment induced a synergistic 6.1-fold increase over the vehicle-treated myotubes ( $p < 0.05$ ). Treatment with NAM attenuated this increase, indicating that this synergistic effect occurred in a SirT1-dependent manner. Interestingly, treatment of the cells with Quercetin, another polyphenolic compound, did not increase COX activity in the presence or absence of CCA, indicating that RSV is a more potent inducer of mitochondrial biogenesis.

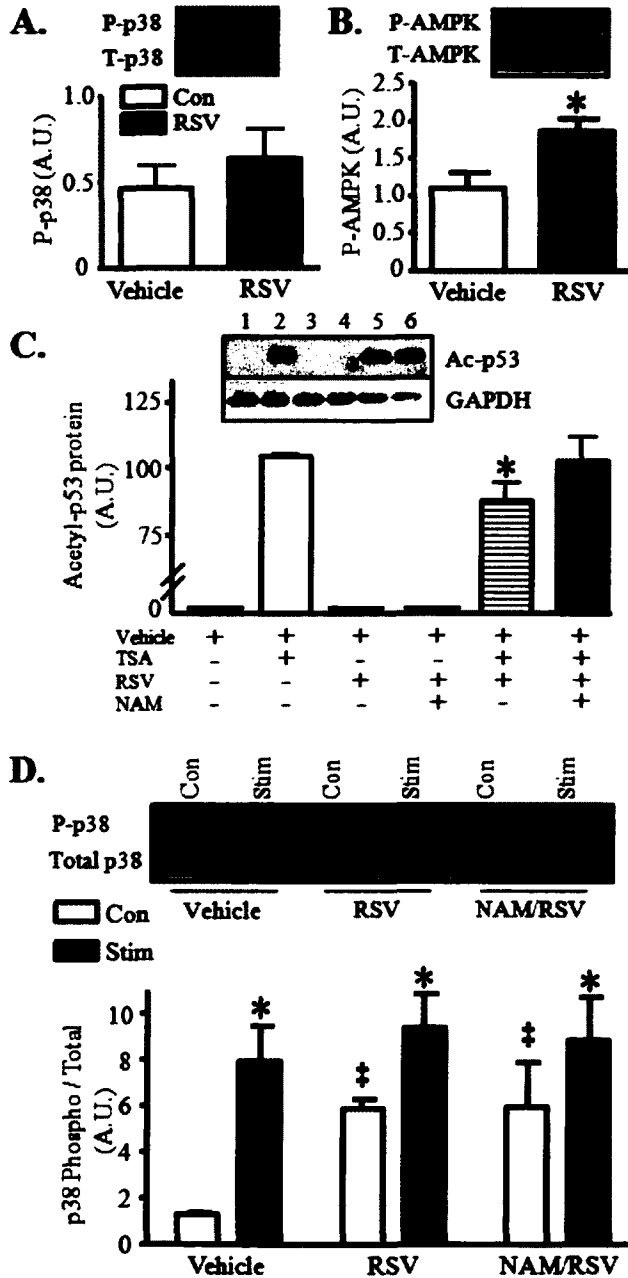
Myotubes treated for 4 days were also stained with MTGFM to confirm the biochemical changes in mitochondrial mass as indicated by COX activity. Myotube fluorescence intensity was quantified using a microplate reader and corrected for protein content (Fig. 3C). Fluorescent images of myotubes stained with MTGFM are shown in figure 3D. These images largely support the effects of RSV and CCA, and their combination, on mitochondrial content within the myotubes (Figs. 3B, C).

***ROS production and MnSOD expression.*** In parallel to mitochondrial mass and COX activity, ROS generation was increased by both CCA and RSV. CCA and RSV treatments produced 1.6- and 1.2-fold increases in ROS above the vehicle-treated myotubes ( $p < 0.05$ ; Fig. 4A). The combined treatments of RSV or Quercetin with CCA resulted in 2.6- and 2.3-fold changes in ROS production, respectively, compared to the vehicle-treated control cells ( $p < 0.05$ ). The effect of the RSV/CCA combination treatment on ROS generation appeared to be dependent on SirT1 activity, as indicated by the

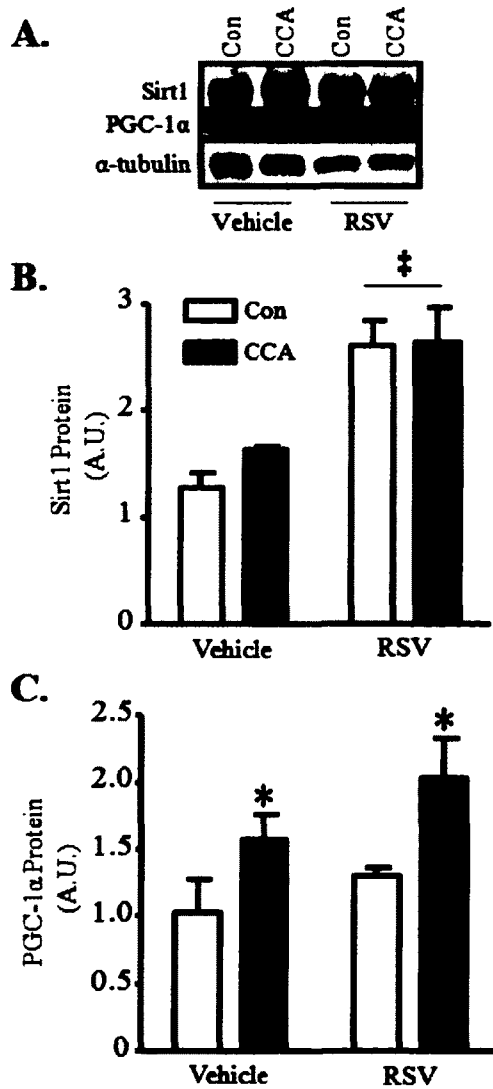
reduced ROS production when combined with NAM treatment ( $p < 0.05$ ).

Antioxidant capacities were assessed by measuring MnSOD expression. A 1.6-fold increase in MnSOD protein was observed with CCA treatment ( $p < 0.05$ ; Fig. 4B). RSV also induced MnSOD expression by 1.3-fold ( $p < 0.05$ ). The combined CCA/RSV treatment produced a 1.8-fold increase in MnSOD expression compared to the vehicle-treated cells that was not significantly different from the CCA treated cells. NAM did not reduce MnSOD expression in the CCA/RSV-treated myotubes indicating a SirT1-independent effect ( $p < 0.05$ ).

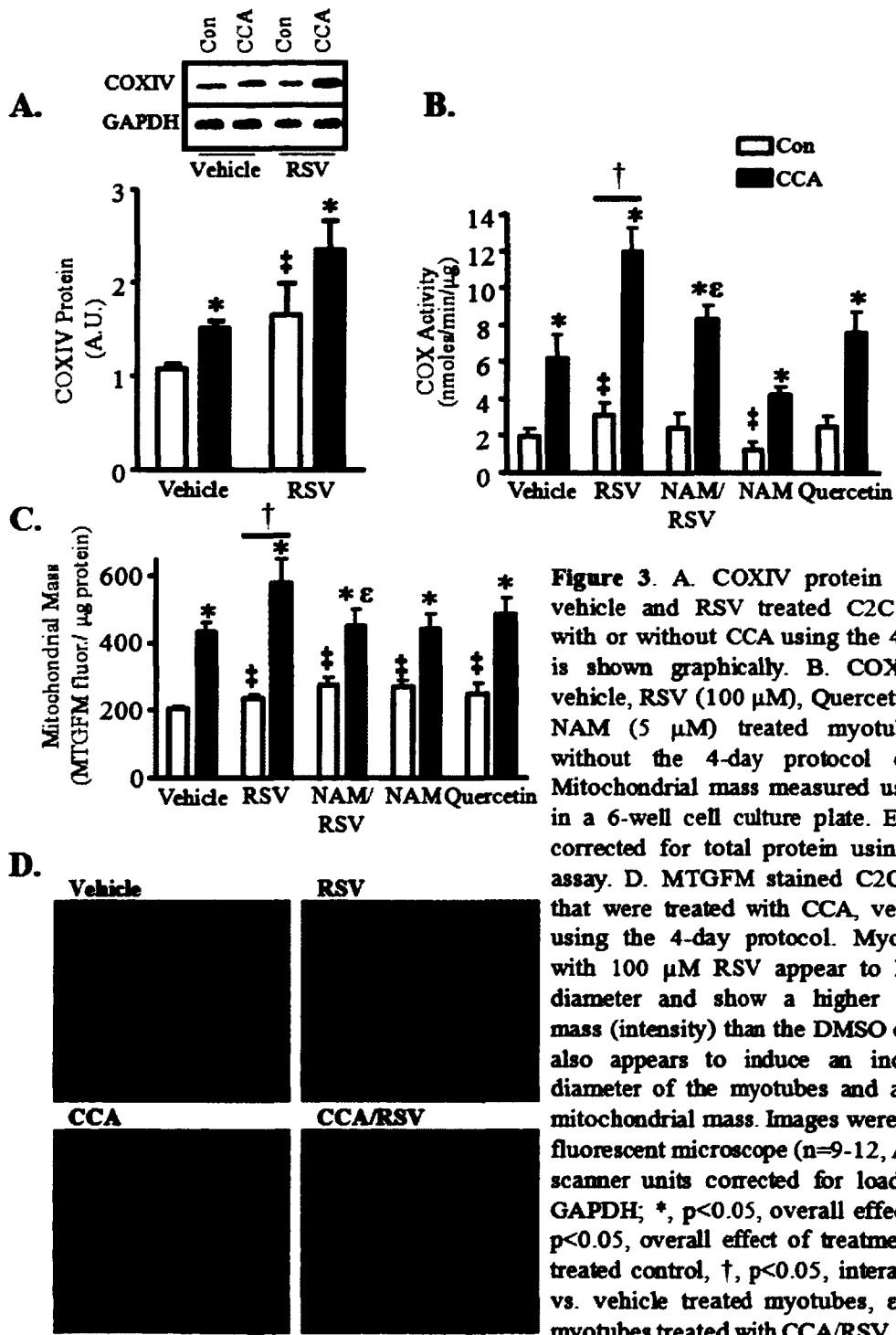
***SirT1 and PGC-1 $\alpha$  translocation and co-localization.*** Immunofluorescence measures were made to provide a preliminary view of the subcellular location of PGC-1 $\alpha$  and SirT1 in response to the RSV and CCA treatments. In vehicle-treated myotubes, both SirT1 and PGC-1 $\alpha$  were found to be dispersed evenly throughout the cell (Fig. 5). SirT1 and PGC-1 $\alpha$  appeared to translocate and co-localize in the nucleus with CCA. This was not evident with RSV treatment. However, the combined treatment of RSV and CCA appeared to result in the most prominent translocation and co-localization of SirT1 and PGC-1 $\alpha$  to the nucleus.



**Figure 1.** A and B. P-p38 and P-AMPK protein expression treated with vehicle and 100  $\mu$ M RSV for 1hr. Total-p38 and Total-AMPK did not change with treatment. C. Acetyl-p53 (lys379) expression in cells treated with TSA for 1hr in combination with vehicle, RSV (100  $\mu$ M) or NAM (5  $\mu$ M). D. p38 (phospho/total) was measured following 24hrs of vehicle, RSV, or NAM/RSV treated myotubes in combination with CA (n=9, A.U., arbitrary scanner units corrected for loading using GAPDH; \*, p<0.05, vs. vehicle (B) or vehicle and TSA for Acetyl-p53 measurements (C) or overall effect of CA (D) ‡, p<0.05, effect of treatment with no CA vs. vehicle).



**Figure 2.** A. SirT1 and PGC-1 $\alpha$  protein expression in vehicle and RSV (100  $\mu$ M) treated C2C12 myotubes, with or without CCA using the 4-day protocol were measured using western techniques. B. and C. SirT1 and PGC-1 $\alpha$  protein expression is shown graphically ( $n=9$ , A.U., arbitrary scanner units corrected for loading using  $\alpha$ -tubulin; \*,  $p<0.05$ , overall effect of CCA, ‡,  $p<0.05$ , overall effect of RSV).



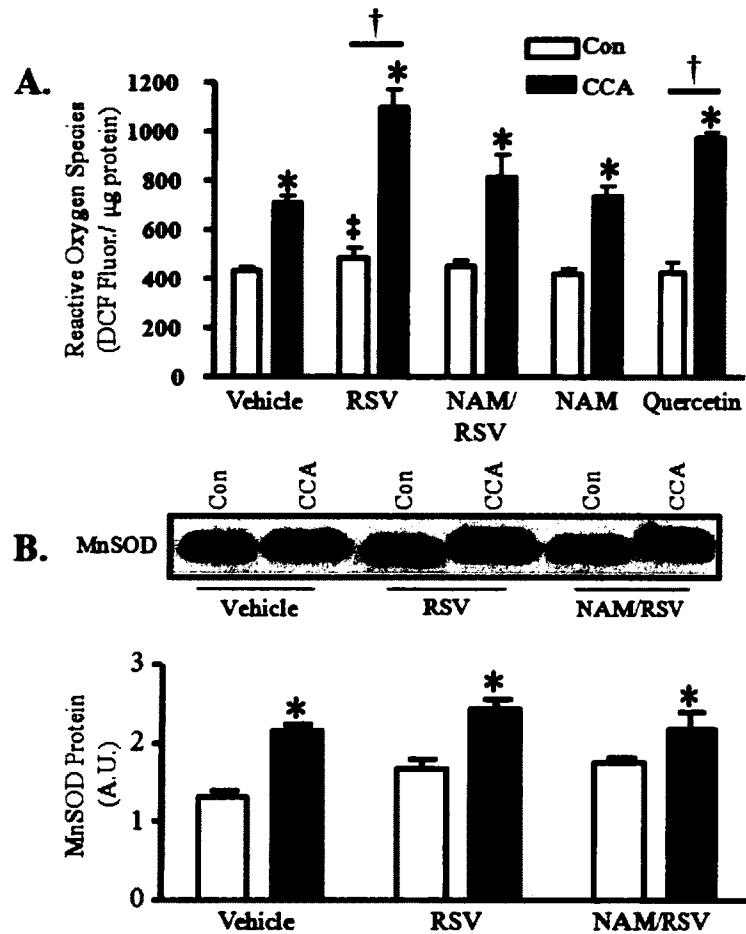


**Figure 4.** A. ROS production measured using DCF fluorescence with and without CCA and treated with vehicle, RSV or Quercetin using the 4-day protocol. All measurements were made in a 6-well cell culture plate using a Bio-Tek Synergy HT microplate reader. Each well was corrected for total protein using a Bradford assay. B. MnSOD measured using western techniques (n=9-12, A.U., arbitrary scanner units corrected for loading using  $\alpha$ -tubulin; \*, p<0.05, overall effect of CCA vs. control, ‡, p<0.05, overall effect of treatment vs. control, †, p<0.05, interaction vs. vehicle treated myotubes).

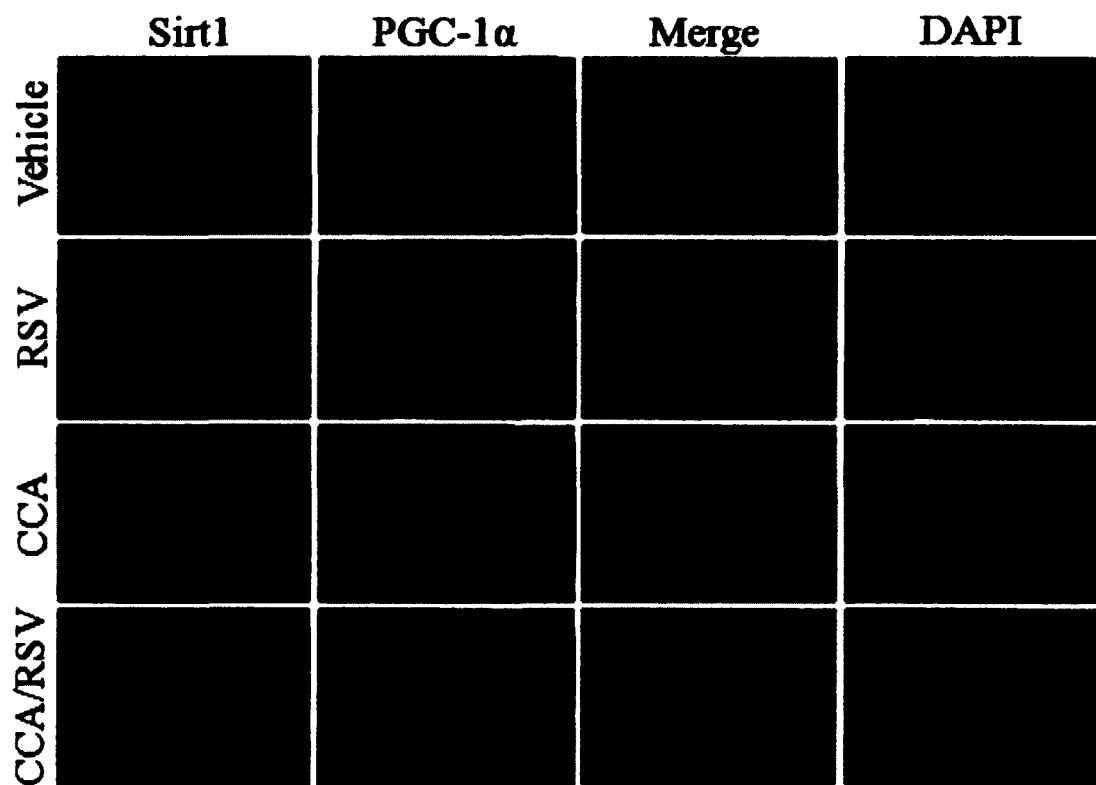


**Figure 5.** Immunofluorescence of SirT1 (red) and PGC-1 $\alpha$  (green) with DAPI (blue) stained nuclei. Images examine SirT1 and PGC-1 $\alpha$  nuclear localization in C212 myotubes treated with vehicle or RSV, with and without CCA using the 4-day protocol. Higher levels of SirT1 and PGC-1 $\alpha$  nuclear localization are seen with CCA and in the combined treatment of RSV and CCA (n=6).

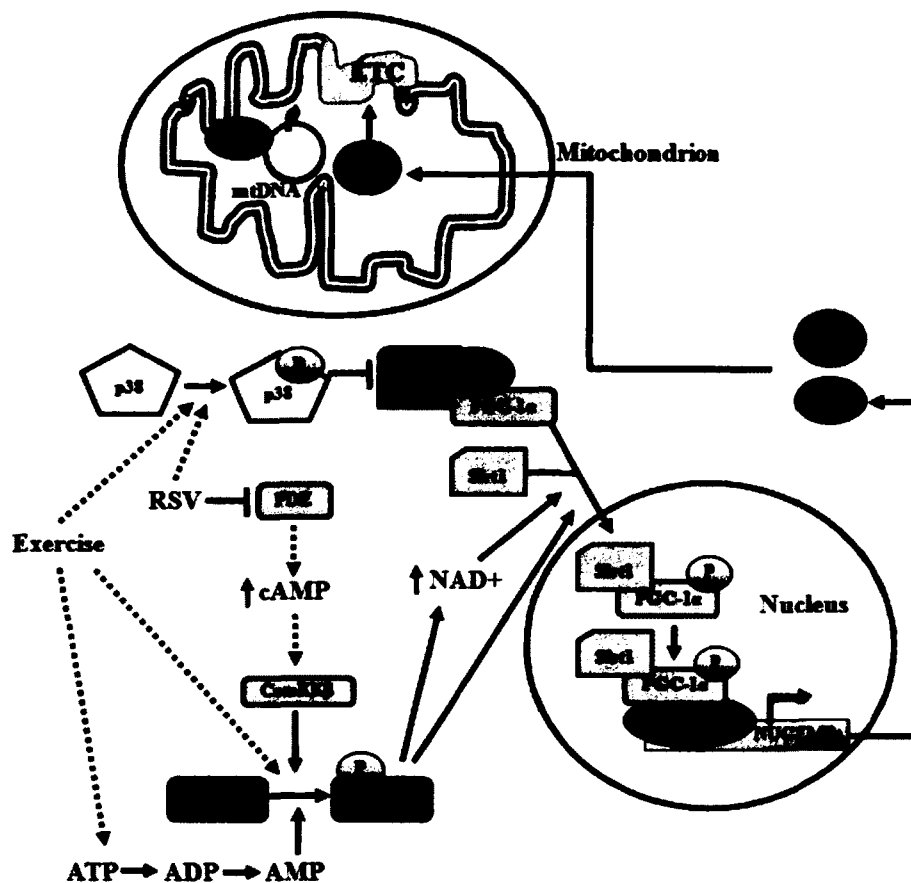


**Figure 6.** Schematic representation of RSV and CCA induced mitochondrial biogenesis through the activation of PGC-1 $\alpha$ . Exercise activates AMPK and p38 resulting in the phosphorylation of PGC-1 $\alpha$ , and the release of inhibition by the binding protein p160, respectively. The differential activation of AMPK via exercise and RSV elevates NAD<sup>+</sup>, a necessary substrate for the deacetylation of PGC-1 $\alpha$  by SirT1. When PGC-1 $\alpha$  is deacetylated it coactivates the transcription of nuclear gene-encoded mitochondrial proteins (NUGEMPs) through Nuclear Respiratory Factor 1 (NRF-1). These proteins are then shuttled to the mitochondria and are either incorporated into the electron transport chain (ie. COXIV) or help to initiate mtDNA replication and transcription (Tfam). We hypothesize that RSV acts in a similar manner to chronic contractile activity (CCA) when inducing mitochondrial biogenesis. However, unlike with RSV, contractile activity increases AMP/ATP ratio. AMP can then allosterically activate AMPK. This may account for the larger effect of CCA over RSV treatment for the PGC-1 $\alpha$ -dependent increase in mitochondrial biogenesis. Similarly, both exercise and RSV induce the phosphorylation of AMPK. Our data suggest that the synergistic response relies on RSV as a direct or indirect activator of SirT1, in combination with the change in energy status, (i.e. increases in AMP/ATP and NAD<sup>+</sup>/NADH), which occur with CCA. The synergistic activation of AMPK helps to elevate NAD<sup>+</sup>-directed SirT1 deacetylation activity. Thus, the separate and mutual effects of RSV and CCA may be combined to produce a more robust increase in mitochondrial content than either treatment alone. The synergistic response is SirT1-dependent, since it was absent when SirT1 was inhibited.

## **Discussion**

We have previously shown in mature myotubes that chronic contractile activity induces adaptations in the expression of genes that encode mitochondrial proteins (11; 46). Likewise, it has also been shown that RSV can induce the expression of genes encoding mitochondrial proteins, which increase both mitochondrial function and metabolic homeostasis (29). The goal of this study was to examine the similarities and differences between CCA and RSV treatment on the activation of mitochondrial biogenesis in muscle cells. By examining these two treatments in the context of mitochondrial biogenesis, we can determine the possibility of RSV to act as an exercise mimetic. In addition, our aim was to determine if RSV could enhance the ability of CCA to induce mitochondrial biogenesis. The induction of mitochondrial biogenesis by RSV may not only have consequences for exercise performance, but also for the treatment of individuals who are unable to exercise, those with mitochondrial myopathies, and during the aging process in which mitochondrial content and function may be reduced. Thus, we set out to compare the biochemical responses to CCA and RSV, while examining the possible additive or synergistic outcomes of their combined treatments.

C2C12 myotubes treated with 4 days of CCA responded with an elevation in PGC-1 $\alpha$  protein and mRNA levels (46) as well as an increase in the nuclear-encoded mitochondrial protein COXIV. The basis for this increase in PGC-1 $\alpha$  expression may be related to the transient increases in p38 phosphorylation evident with each bout of

contractile activity. It has been previously shown that p38 $\gamma$  is required to illicit an increase in PGC-1 $\alpha$  expression for the induction of endurance exercise-induced mitochondrial biogenesis in mouse skeletal muscle (39). Despite the robust increase in PGC-1 $\alpha$  protein, SirT1 protein levels were not altered following CCA. However, it is possible that changes in SirT1 activity could have occurred, as has been shown in skeletal muscle following a supramaximal bout of exercise in rodents, due to an increase in the cellular NAD<sup>+</sup>/NADH ratio (8). In addition, we observed an increase in SirT1 nuclear localization with CCA, suggesting a mechanism for SirT1 to directly influence PGC-1 $\alpha$  co-transcriptional activity. This may be mediated by ROS, a signalling molecule elevated during exercise, which promotes JNK-induced phosphorylation of SirT1 to increase both nuclear localization, and enzymatic activity (33; 45). The involvement of SirT1 in CCA-induced mitochondrial biogenesis is substantiated by the attenuated increase in COX activity found when myotubes treated with CCA are exposed to the SirT1 inhibitor NAM. The induction of mitochondrial biogenesis with CCA was confirmed by the coincident increases in COX activity and mitochondrial mass, along with concurrent elevations in ROS production and oxidative protection provided by elevated MnSOD protein levels.

In contrast to CCA, RSV treatment increased the levels of SirT1 protein but did not change the expression of PGC-1 $\alpha$ . Since SirT1 has been shown to deacetylate and activate PGC-1 $\alpha$  it is probable that the elevated SirT1 levels contributed to the deacetylation and enhancement of PGC-1 $\alpha$  transcriptional coactivator activity (34). In addition, RSV was able to activate both AMPK and p38 in temporally distinct stages,

contributing to PGC-1 $\alpha$  phosphorylation (24), and expression (1; 22), along with the release of PGC-1 $\alpha$  from an inhibitory complex with p160 myb-binding protein (14). An increase in PGC-1 $\alpha$  activity via the RSV-induced increase in SirT1 protein and activity is a likely event, since the modest increase in COX activity with RSV alone was attenuated with the addition of NAM, a SirT1 inhibitor. However, in comparison to CCA, the RSV-induced mitochondrial biogenesis was far less robust than that observed following CCA, as evident from the changes in mitochondrial mass, COX activity, ROS production and MnSOD expression data. This may be a result of the reduced PGC-1 $\alpha$  shuttling to the nucleus in response to RSV. In addition, Irrcher et al. (21) revealed that ROS is an important signalling molecule for the induction PGC-1 $\alpha$  transcription and the resulting increase in mitochondrial biogenesis. CCA treatment elicits much higher ROS production in comparison to RSV treatment, and this may be important in contributing to the induction of PGC-1 $\alpha$ , and the subsequent triggering of mitochondrial biogenesis. Overall, both CCA and RSV treatment affect mitochondrial content in muscle cells via distinct signalling and protein induction pathways.

With the complimentary, yet asymmetrical, effects of RSV and CCA on mitochondrial biogenesis, we hypothesised that there may be the potential for an additive, or synergistic effect with a combined treatment. The combination of CCA and RSV treatment did produce greater increases in both PGC-1 $\alpha$  and SirT1 protein levels. In addition, there was an increase in nuclear localization of PGC-1 $\alpha$  and SirT1. As a result, the combination of these treatments induced an additive effect on COXIV protein

levels, and a distinctly synergistic effect on both COX activity and mitochondrial mass as indicated by statistical interactions. We can attribute this potentiation to the interaction between the elevations in the protein levels of PGC-1 $\alpha$  via CCA, and SirT1 via RSV treatment. With increases in both of these proteins, along with nuclear localization, there is a greater potential for PGC-1 $\alpha$  to be deacetylated and to coactivate the transcription of nuclear genes encoding mitochondrial proteins. To add to this effect on expression levels, it has also been shown that RSV treatment can increase SirT1 activity, in either a direct (5; 26; 32) or indirect (7; 12; 18; 36) manner, to further deacetylate and activate PGC-1 $\alpha$ . In addition, repeated bouts of contractile activity are known to elevate levels of the AMP, the allosteric activator of AMPK. This distinction may be important since AMP has been found to modulate the activity of phosphorylated AMPK by 1000-fold (44). Both CCA and RSV treatments may also differentially induce the phosphorylation of AMPK through LKB1- or CamKK $\beta$ -induced pathways, thus influencing the total AMPK activation. Recently, RSV was shown to increase the phosphorylation of AMPK via CamKK $\beta$  (36). Thus, these mutually exclusive and overlapping effects of RSV and CCA produce a more robust increase in mitochondrial content than either treatment alone (Fig. 6). Since NAM attenuated the synergistic response of the combined treatment on COX activity and mitochondrial mass and therefore demonstrates that this synergy was reliant, at least in part, on SirT1 activity. These results emphasize the concept that both CCA and RSV treatment can induce molecular pathways that are exclusive, yet mutually beneficial. This appears to be consistent with other observations that indicate that RSV

treatment, combined with a metabolic stress (i.e. high calorie diet), can induce a protective effect on lifespan that is above that of RSV treatment alone (3).

The combined effect of CCA and RSV on mitochondrial content is likely to have a more substantial impact on muscle function than either treatment alone, since mitochondrial content is highly correlated to endurance performance (19). Our data also suggest that the potential of RSV, or other modulators of SirT1 activity, to be used as ergogenic aids for skeletal muscle mitochondrial biogenesis is limited to cellular environments in which there is a shift in the energy balance of the cell, thus creating synergistic metabolic signalling events.

## **Acknowledgements**

This work was supported by Canadian Institutes of Health Research (CIHR) grants to D. A. Hood. K. J. Menzies was a recipient of a CIHR Doctoral Award. D.A. Hood is the holder of a Canadian Research Chair in Cell Physiology.

## References

1. **Akimoto T, Pohnert SC, Li P, Zhang M, Gumbs C, Rosenberg PB, Williams RS and Yan Z.** Exercise stimulates Pgc-1alpha transcription in skeletal muscle through activation of the p38 MAPK pathway. *J Biol Chem* 280: 19587-19593, 2005.
2. **Aparicio OM, Billington BL and Gottschling DE.** Modifiers of position effect are shared between telomeric and silent mating-type loci in *S. cerevisiae*. *Cell* 66: 1279-1287, 1991.
3. **Baur JA, Pearson KJ, Price NL, Jamieson HA, Lerin C, Kalra A, Prabhu VV, Allard JS, Lopez-Lluch G, Lewis K, Pistell PJ, Poosala S, Becker KG, Boss O, Gwinn D, Wang M, Ramaswamy S, Fishbein KW, Spencer RG, Lakatta EG, Le CD, Shaw RJ, Navas P, Puigserver P, Ingram DK, de CR and Sinclair DA.** Resveratrol improves health and survival of mice on a high-calorie diet. *Nature* 444: 337-342, 2006.
4. **Boily G, Seifert EL, Bevilacqua L, He XH, Sabourin G, Estey C, Moffat C, Crawford S, Saliba S, Jardine K, Xuan J, Evans M, Harper ME and McBurney MW.** SirT1 regulates energy metabolism and response to caloric restriction in mice. *PLoS ONE* 3: e1759, 2008.
5. **Borra MT, Smith BC and Denu JM.** Mechanism of human SIRT1 activation by resveratrol. *J Biol Chem* 280: 17187-17195, 2005.

6. **Boulton SJ and Jackson SP.** Components of the Ku-dependent non-homologous end-joining pathway are involved in telomeric length maintenance and telomeric silencing. *EMBO J* 17: 1819-1828, 1998.
7. **Breen DM, Sanli T, Giacca A and Tsiani E.** Stimulation of muscle cell glucose uptake by resveratrol through sirtuins and AMPK. *Biochem Biophys Res Commun* 374: 117-122, 2008.
8. **Canto C, Gerhart-Hines Z, Feige JN, Lagouge M, Noriega L, Milne JC, Elliott PJ, Puigserver P and Auwerx J.** AMPK regulates energy expenditure by modulating NAD<sup>+</sup> metabolism and SIRT1 activity. *Nature* 458: 1056-1060, 2009.
9. **Canto C, Jiang LQ, Deshmukh AS, Matakai C, Coste A, Lagouge M, Zierath JR and Auwerx J.** Interdependence of AMPK and SIRT1 for metabolic adaptation to fasting and exercise in skeletal muscle. *Cell Metab* 11: 213-219, 2010.
10. **Chen L, Han Y, Yang F and Zhang T.** High-speed counter-current chromatography separation and purification of resveratrol and piceid from *Polygonum cuspidatum*. *J Chromatogr A* 907: 343-346, 2001.
11. **Connor MK, Irrcher I and Hood DA.** Contractile activity-induced transcriptional activation of cytochrome C involves Sp1 and is proportional to mitochondrial ATP synthesis in C2C12 muscle cells. *J Biol Chem* 276: 15898-15904, 2001.

12. **Dasgupta B and Milbrandt J.** Resveratrol stimulates AMP kinase activity in neurons. *Proc Natl Acad Sci U S A* 104: 7217-7222, 2007.
13. **Deng JY, Hsieh PS, Huang JP, Lu LS and Hung LM.** Activation of estrogen receptor is crucial for resveratrol-stimulating muscular glucose uptake via both insulin-dependent and -independent pathways. *Diabetes* 57: 1814-1823, 2008.
14. **Fan M, Rhee J, St-Pierre J, Handschin C, Puigserver P, Lin J, Jaeger S, Erdjument-Bromage H, Tempst P and Spiegelman BM.** Suppression of mitochondrial respiration through recruitment of p160 myb binding protein to PGC-1alpha: modulation by p38 MAPK. *Genes Dev* 18: 278-289, 2004.
15. **Gerhart-Hines Z, Rodgers JT, Bare O, Lerin C, Kim SH, Mostoslavsky R, Alt FW, Wu Z and Puigserver P.** Metabolic control of muscle mitochondrial function and fatty acid oxidation through SIRT1/PGC-1alpha. *EMBO J* 26: 1913-1923, 2007.
16. **Gottlieb S and Esposito RE.** A new role for a yeast transcriptional silencer gene, SIR2, in regulation of recombination in ribosomal DNA. *Cell* 56: 771-776, 1989.
17. **Hori YS, Kuno A, Hosoda R, Tanno M, Miura T, Shimamoto K and Horio Y.** Resveratrol ameliorates muscular pathology in the dystrophic mdx mouse, a model for Duchenne muscular dystrophy. *J Pharmacol Exp Ther* 338: 784-794, 2011.
18. **Hou X, Xu S, Maitland-Toolan KA, Sato K, Jiang B, Ido Y, Lan F, Walsh K, Wierzbicki M, Verbeuren TJ, Cohen RA and Zang M.** SIRT1 regulates

- hepatocyte lipid metabolism through activating AMP-activated protein kinase. *J Biol Chem* 283: 20015-20026, 2008.
19. **Irrcher I, Adhietty PJ, Joseph AM, Ljubicic V and Hood DA.** Regulation of mitochondrial biogenesis in muscle by endurance exercise. *Sports Med* 33: 783-793, 2003.
  20. **Irrcher I and Hood DA.** Regulation of Egr-1, SRF, and Sp1 mRNA expression in contracting skeletal muscle cells. *J Appl Physiol* 97: 2207-2213, 2004.
  21. **Irrcher I, Ljubicic V and Hood DA.** Interactions between ROS and AMP kinase activity in the regulation of PGC-1alpha transcription in skeletal muscle cells. *Am J Physiol Cell Physiol* 296: C116-C123, 2009.
  22. **Irrcher I, Ljubicic V, Kirwan AF and Hood DA.** AMP-activated protein kinase-regulated activation of the PGC-1alpha promoter in skeletal muscle cells. *PLoS ONE* 3: e3614, 2008.
  23. **Jackson JR, Ryan MJ, Hao Y and Alway SE.** Mediation of endogenous antioxidant enzymes and apoptotic signaling by resveratrol following muscle disuse in the gastrocnemius muscles of young and old rats. *Am J Physiol Regul Integr Comp Physiol* 299: R1572-R1581, 2010.
  24. **Jager S, Handschin C, St-Pierre J and Spiegelman BM.** AMP-activated protein kinase (AMPK) action in skeletal muscle via direct phosphorylation of PGC-1alpha. *Proc Natl Acad Sci U S A* 104: 12017-12022, 2007.

25. **Jian B, Yang S, Chaudry IH and Raju R.** Resveratrol improves cardiac contractility following trauma-hemorrhage by modulating Sirt1. *Mol Med* 2011.
26. **Kaeberlein M, McDonagh T, Heltweg B, Hixon J, Westman EA, Caldwell SD, Napper A, Curtis R, DiStefano PS, Fields S, Bedalov A and Kennedy BK.** Substrate-specific activation of sirtuins by resveratrol. *J Biol Chem* 280: 17038-17045, 2005.
27. **Kaeberlein M, McVey M and Guarente L.** The SIR2/3/4 complex and SIR2 alone promote longevity in *Saccharomyces cerevisiae* by two different mechanisms. *Genes Dev* 13: 2570-2580, 1999.
28. **Kang W, Hong HJ, Guan J, Kim DG, Yang EJ, Koh G, Park D, Han CH, Lee YJ and Lee DH.** Resveratrol improves insulin signaling in a tissue-specific manner under insulin-resistant conditions only: in vitro and in vivo experiments in rodents. *Metabolism* 2011.
29. **Lagouge M, Argmann C, Gerhart-Hines Z, Meziane H, Lerin C, Daussin F, Messadeq N, Milne J, Lambert P, Elliott P, Geny B, Laakso M, Puigserver P and Auwerx J.** Resveratrol improves mitochondrial function and protects against metabolic disease by activating SIRT1 and PGC-1alpha. *Cell* 127: 1109-1122, 2006.
30. **Li Y, Park JS, Deng JH and Bai Y.** Cytochrome c oxidase subunit IV is essential for assembly and respiratory function of the enzyme complex. *J Bioenerg Biomembr* 38: 283-291, 2006.

31. **Martin SG, Laroche T, Suka N, Grunstein M and Gasser SM.** Relocalization of telomeric Ku and SIR proteins in response to DNA strand breaks in yeast. *Cell* 97: 621-633, 1999.
32. **Milne JC, Lambert PD, Schenk S, Carney DP, Smith JJ, Gagne DJ, Jin L, Boss O, Perni RB, Vu CB, Bemis JE, Xie R, Disch JS, Ng PY, Nunes JJ, Lynch AV, Yang H, Galonek H, Israelian K, Choy W, Iffland A, Lavu S, Medvedik O, Sinclair DA, Olefsky JM, Jirousek MR, Elliott PJ and Westphal CH.** Small molecule activators of SIRT1 as therapeutics for the treatment of type 2 diabetes. *Nature* 450: 712-716, 2007.
33. **Nasrin N, Kaushik VK, Fortier E, Wall D, Pearson KJ, de CR and Bordone L.** JNK1 phosphorylates SIRT1 and promotes its enzymatic activity. *PLoS ONE* 4: e8414, 2009.
34. **Nemoto S, Fergusson MM and Finkel T.** SIRT1 functionally interacts with the metabolic regulator and transcriptional coactivator PGC-1 {alpha}. *J Biol Chem* 280: 16456-16460, 2005.
35. **Park CE, Kim MJ, Lee JH, Min BI, Bae H, Choe W, Kim SS and Ha J.** Resveratrol stimulates glucose transport in C2C12 myotubes by activating AMP-activated protein kinase. *Exp Mol Med* 39: 222-229, 2007.
36. **Park SJ, Ahmad F, Philp A, Baar K, Williams T, Luo H, Ke H, Rehmann H, Taussig R, Brown AL, Kim MK, Beaven MA, Burgin AB, Manganiello V and**

- Chung JH.** Resveratrol ameliorates aging-related metabolic phenotypes by inhibiting cAMP phosphodiesterases. *Cell* 148: 421-433, 2012.
37. **Petersen KF, Dufour S, Savage DB, Bilz S, Solomon G, Yonemitsu S, Cline GW, Befroy D, Zeman L, Kahn BB, Papademetris X, Rothman DL and Shulman GI.** The role of skeletal muscle insulin resistance in the pathogenesis of the metabolic syndrome. *Proc Natl Acad Sci U S A* 104: 12587-12594, 2007.
38. **Picard F, Kurtev M, Chung N, Topark-Ngarm A, Senawong T, Hado De OR, Leid M, McBurney MW and Guarente L.** Sirt1 promotes fat mobilization in white adipocytes by repressing PPAR-gamma. *Nature* 429: 771-776, 2004.
39. **Pogozelski AR, Geng T, Li P, Yin X, Lira VA, Zhang M, Chi JT and Yan Z.** p38gamma mitogen-activated protein kinase is a key regulator in skeletal muscle metabolic adaptation in mice. *PLoS ONE* 4: e7934, 2009.
40. **Rabøl R, Petersen KF, Dufour S, Flannery C and Shulman GI.** Reversal of muscle insulin resistance with exercise reduces postprandial hepatic de novo lipogenesis in insulin resistant individuals. *Proc Natl Acad Sci U S A* 108: 13705-13709, 2011.
41. **Rine J and Herskowitz I.** Four genes responsible for a position effect on expression from HML and HMR in *Saccharomyces cerevisiae*. *Genetics* 116: 9-22, 1987.
42. **Rodgers JT, Lerin C, Haas W, Gygi SP, Spiegelman BM and Puigserver P.**

- Nutrient control of glucose homeostasis through a complex of PGC-1alpha and SIRT1. *Nature* 434: 113-118, 2005.
43. **Slinker BK.** The statistics of synergism. *J Mol Cell Cardiol* 30: 723-731, 1998.
44. **Suter M, Riek U, Tuerk R, Schlattner U, Wallimann T and Neumann D.**  
Dissecting the role of 5'-AMP for allosteric stimulation, activation, and deactivation of AMP-activated protein kinase. *J Biol Chem* 281: 32207-32216, 2006.
45. **Tanno M, Sakamoto J, Miura T, Shimamoto K and Horio Y.**  
Nucleocytoplasmic shuttling of the NAD<sup>+</sup>-dependent histone deacetylase SIRT1. *J Biol Chem* 282: 6823-6832, 2007.
46. **Ugucioni G and Hood DA.** The importance of PGC-1alpha in contractile activity-induced mitochondrial adaptations. *Am J Physiol Endocrinol Metab* 300: E361-E371, 2011.
47. **Ulrich S, Loitsch SM, Rau O, von KA, Brune B, Schubert-Zsilavecz M and Stein JM.** Peroxisome proliferator-activated receptor gamma as a molecular target of resveratrol-induced modulation of polyamine metabolism. *Cancer Res* 66: 7348-7354, 2006.
48. **Um JH, Park SJ, Kang H, Yang S, Foretz M, McBurney MW, Kim MK, Viollet B and Chung JH.** AMP-activated protein kinase-deficient mice are resistant to the metabolic effects of resveratrol. *Diabetes* 59: 554-563, 2010.

**CHAPTER 3: SIRT1-MEDIATED EFFECTS OF EXERCISE AND  
RESVERATROL ON MITOCHONDRIAL BIOGENESIS**

### **Rationale for Chapter 3**

The purpose of Chapter 2 was to compare the ability of resveratrol (RSV) and chronic contractile activity (CCA), as a model of exercise, to induce SirT1-mediated mitochondrial biogenesis. Results showed that the effects of CCA were more robust than RSV on the induction of mitochondrial biogenesis. Importantly, RSV and CCA together produced a synergistic increase in mitochondrial biogenesis. This synergistic effect is proposed to be the result of the combined induction of PGC-1 $\alpha$  by chronic stimulation, and activation of SirT1 by RSV. Therefore, the possibility of a SirT1-mediated synergistic effect between RSV and exercise in skeletal muscle mitochondrial function and biogenesis forms the main purpose of Chapter 3. To address this purpose, we generated muscle-specific SirT1-KO mice that were submitted to a voluntary wheel running protocol, while being fed an RSV or control diet. We hypothesized that RSV and voluntary exercise may act in both a SirT1-dependent, and -independent manner to regulate mitochondrial biogenesis and function.

### **Author contributions**

Conceived and designed the experiments: KJM and DAH. Performed the experiments: KJM with technical assistance from Kaustubh Singh. Analyzed the data: KJM and DAH. Wrote the paper: KJM and DAH.

# **SirT1-mediated effects of exercise and resveratrol on mitochondrial biogenesis**

Keir J. Menzies<sup>2,3</sup>, Kaustabh Singh<sup>1,3</sup> and David A. Hood<sup>1,2,3</sup>

School of Kinesiology and Health Science<sup>1</sup>, Department of Biology<sup>2</sup>, and the Muscle Health Research Centre<sup>3</sup>, York University, Toronto M3J 1P3

**To whom correspondence should be addressed:** Dr. David A. Hood  
School of Kinesiology and Health Science,  
Farquharson Life Science Bldg.,  
Room 302,  
York University, Toronto, Ontario  
M3J 1P3, Canada  
Tel: (416) 736-2100 ext. 66640  
Fax: (416) 736-5698  
E-mail: dhood@yorku.ca

Running head: SirT1-KO and mitochondrial biogenesis

Key words: PGC-1 $\alpha$ , Nampt, skeletal muscle, reactive oxygen species, cytochrome c oxidase activity, respiration

To be submitted to Am J Physiol Cell Physiol

## **Abstract**

The purpose of this research was to evaluate the role of SirT1 in exercise- and resveratrol (RSV)-induced skeletal muscle mitochondrial biogenesis. To do this, we produced skeletal-muscle specific SirT1-deficient (KO) mice. Despite the similar expression of PGC-1 $\alpha$ , an important regulator of mitochondrial biogenesis, KO mice exhibited a modest decline in muscle COX activity, and 30% and 47% reductions in state 3 and state 4 mitochondrial respiration, respectively. There were also corresponding 3.5- and 1.5-fold elevations in ROS generation for the KO mice during both state 3 and state 4 mitochondrial respiration. To examine the dependence of exercise- or RSV-induced mitochondrial biogenesis on SirT1, we trained WT and KO mice on voluntary running wheels, or fed them a RSV diet for 9 weeks. Both WT and KO mice ran the same average and total distances, while RSV fed animals from both groups showed elevated levels of volitional running. Voluntary exercise produced 1.4- and 1.8-fold increases in COX activity in both the WT and KO animals, bringing them to the same absolute value of COX activity. In addition, the deficits in state 3 and 4 mitochondrial respiration, along with the elevated ROS levels in KO mice, were rescued to values similar to those of the WT mice. Resveratrol did not alter COX activity or respiration in WT mice mitochondria, but did help restore these values back to WT levels in the KO animals. The combination of exercise with RSV feeding resulted in a synergistic increase in COX activity and mitochondrial respiration that was apparent in the WT, but not in the KO animals. Our data indicate that SirT1 may be partially responsible for the maintenance

of basal mitochondrial content and function. In addition, SirT1 is important for the synergistic effect of RSV on exercise-induced mitochondrial biogenesis. Thus, the magnitude of the effect of RSV on skeletal muscle mitochondrial biogenesis is reliant on SirT1, as well as the cellular environment produce by repeated bouts of exercise.

## **Introduction**

Sirt1 is a NAD<sup>+</sup>-dependent histone deacetylase that can directly affect metabolism through the deacetylation of PGC-1 $\alpha$ , the important regulator of mitochondrial biogenesis (3; 31). Another requirement for the induction of mitochondrial biogenesis via PGC-1 $\alpha$  is its phosphorylation by AMP kinase (AMPK) (24). A necessary communication link between Sirt1 and AMPK occurs via nicotinamide phosphoribosyltransferase (Nampt), which is essential for the proper integration of the metabolic signals leading to mitochondrial biogenesis in skeletal muscle (15; 18). Nampt is the rate-limiting enzyme for NAD<sup>+</sup> biosynthesis (36), a coenzyme which is important for Sirt1 activity (35; 44). Nampt expression has previously been shown to be under the regulation of both AMPK and Sirt1 (18; 29). During exercise and caloric restriction, the integration of these reactions has been shown to coordinate tissue bioenergetics. Canto et al. demonstrated an interdependence between AMPK and Sirt1 for the induction of metabolic adaptations that occur during states of energy deprivation, such as fasting or exercise (12). We suspect that this Nampt-Sirt1-AMPK metabolic-sensing pathway plays a dominant role in mitochondrial turnover by influencing mitochondrial biogenesis, autophagy and circadian rhythm following cellular stress (28). AMPK can be activated through the modulation of the AMP/ATP ratio, while Sirt1 activity is dependent on NAD<sup>+</sup> levels within the cell (18). Therefore, the metabolic changes that occur with exercise or caloric restriction activate these enzyme systems to regulate the

phosphorylation and deacetylation of PGC-1 $\alpha$ , and the subsequent induction of mitochondrial biogenesis.

The natural polyphenolic compound resveratrol (RSV) is found mainly in the skin of grapes, and it is well known for its phytoestrogenic and antioxidant properties (4). RSV became widely researched when indications that this organic compound could increase longevity in lower organisms, and increase the health and survival of mice (5; 22; 25; 41; 42). RSV has also been described as an exercise mimetic through its activation of SirT1 and AMPK (30). Mice treated with RSV demonstrate elevations in AMPK and PGC-1 $\alpha$  activation, along with increases in mitochondrial number in animals fed a high fat diet (5). Once activated, PGC-1 $\alpha$  acts as a transcriptional coactivator for nuclear genes encoding mitochondrial proteins (40). As a result, RSV treatment appears to induce a higher aerobic capacity in mice, as shown by increased running time and consumption of oxygen in muscle fibers (9). Thus, these findings have generated interest in the therapeutic potential of RSV, or of similar analogues, for the treatment of type 2 diabetes and obesity (6; 11; 39). However, there is still some contention as to how RSV activates mitochondrial biogenesis, and the dependency of this effect on SirT1 and AMPK. Various studies have demonstrated that RSV can activate AMPK in a SirT1-dependent manner (5; 10; 25), while others have revealed that this activation is independent of SirT1 (13; 43). These conflicting results may hinge on the types of tissues being examined, the energy status of that tissue. Thus, based on the literature, we predict

that RSV may have both SirT1-dependent and -independent effects on the induction of mitochondrial biogenesis induced by exercise.

To address how SirT1 is involved in skeletal muscle mitochondrial function and biogenesis, we compared WT mice to those that express a deacetylase-deficient SirT1 protein driven by an MLC1f-Cre promoter. These mice were either treated with dietary RSV, or submitted to a voluntary wheel running protocol to induce mitochondrial biogenesis. In addition, we combined these two treatments to examine the potential for an additive or synergistic effect. Thus, the purposes of this study were 1) to examine the dependence of basal muscle mitochondrial biogenesis on SirT1 protein by comparing the SirT1-KO to WT animals, and 2) to determine if exercise- or RSV-induced mitochondrial biogenesis depends on SirT1 protein.

## **Methods**

***Animal models.*** SirT1<sup>loxP/loxP</sup> mice (generated with heterozygous B6;129-SirT1<sup>tm1Ygu/J</sup> mice; JAX Laboratory) have a loxP-flanked neomycin cassette just upstream of exon 4 and another loxP site downstream of exon 4 that was inserted to create this targeted mutant SirT1 allele. These mice were then bred with MLC1f<sup>Cre</sup> recombinase mice to create a Cre/loxP recombination. MLC1f is a splice variant, along with MLC3f, of the MYL1 gene expressed in fast skeletal muscle fibers. The resulting offspring have exon 4 of the SirT1 gene, encoding 51 amino acids of the SirT1 catalytic domain, deleted in cre-

expressing tissues. We describe our data by referring to the Cre<sup>+</sup>-SirT1<sup>loxP/loxP</sup> animals as muscle-specific “SirT1-KO” mice. All experimental mice were paired to the WT Cre negative SirT1<sup>loxP/loxP</sup> littermates of the same age, approximately 2-3 months.

***SirtT1 activity.*** Muscle-specific SirT1-KO quadriceps exhibited 50% lower SirT1 activity than WT mice. Residual SirT1 activity was expected from any non-muscular tissues and muscle fibres not expressing MLCf1. It has been estimated that 45% of the nuclei within skeletal muscle tissue is within muscle cells, while the remaining nuclei are composed of other tissue types such as adipocytes, fibroblasts and Schwann cells (8). SirT1 activity was measured using an *in vitro* SirT1 fluorometric assay (BIOMOL, Plymouth Meeting, PA) as described by the manufacturer. For this assay, 25 µg of total protein from quadriceps was incubated with Fluor de Lys-SirT1 substrate (100 µM) and NAD (100 µM) at 37°C for 30 min. Measurements of total deacetylase activity were made following the addition of developer reagent, and fluorescence was monitored using a Bio-Tek Synergy HT microplate reader for 60 min at 360 nm (excitation) and 460 nm (emission). The difference between total deacetylase activity before and after SirT1-specific inhibition with NAM (50mM) determined the SirT1-specific activity of the sample.

***Acute in situ muscle stimulation.*** The stimulation protocol was performed as described previously (38). Briefly, mice were anesthetized and the Achilles tendon of the gastrocnemius muscle was attached to a force transducer, and adjusted to be at resting

length. Stimulation of the muscle was induced using electrodes that were placed next to the sciatic nerve. Muscle temperature was maintained at 37°C using heat lamps and monitored using a thermistor. The gastrocnemius muscle of the other limb was also exposed, wrapped in plastic and kept moist with saline. The sciatic nerve from the gastrocnemius muscle of one leg was stimulated at 1 tetanic contraction per second (TPS) and 3 TPS for 2 min each, intensities that are sufficient to cause moderate and more severe muscle fatigue, respectively. Following the *in situ* stimulation protocol, the gastrocnemius muscles from the electrically stimulated leg and the non-stimulated contralateral leg of the animal were excised and weighed.

***RSV treatment and voluntary wheel running.*** SirT1-KO and WT mice were treated for 9 weeks with RSV. RSV was reconstituted in mouse chow at a concentration of 1g/kg in a phytoestrogen-free control diet (20; 21). This treatment was performed in conjunction with mice that were placed in cages with voluntary running wheels and trained over a 9 week period. RSV treated mice were compared to untrained or trained mice fed with control diets.

***Muscle isolation and preparation.*** The tibialis anterior (TA), triceps and gastrocnemius muscles from both sides of the animal were quickly harvested, weighed, and placed in ice-cold mitochondrial isolation buffer. The quadriceps muscles were sectioned, freeze-clamped with aluminum tongs pre-cooled in liquid nitrogen, and stored at -70 °C for

subsequent use in cytochrome c oxidase (COX) enzyme activity measurements and western blotting analyses.

***Isolation of mitochondrial and cytosolic fractions.*** The triceps, TA and gastrocnemius muscles were briefly minced, fractionated by mechanical disruption and subjected to differential centrifugation in order to isolate the subsarcolemmal mitochondria, as described previously in detail (2). Mitochondria were then resuspended (100 mM KCl, 10 mM MOPS, 0.2% BSA) and an aliquot of the suspension was taken for measurements of protein content, and the yield was expressed as mg/g muscle wet weight.

***Mitochondrial respiration.*** Samples of isolated mitochondria were incubated with 250  $\mu$ l of VO<sub>2</sub> buffer (250 mM sucrose, 50 mM KCl, 25 mM Tris-HCl, and 10 mM K<sub>2</sub>HPO<sub>4</sub>, pH 7.4) at 30°C in a respiratory chamber with continuous stirring. Respiration rates driven by complex I in the mitochondrial electron transport chain were evaluated in the presence of 10 mM glutamate (state 4 respiration) and glutamate with 0.44 mM ADP (state 3 respiration) using the Mitocell S200 Micro Respirometry System (Strathkelvin Instruments, Motherwell, UK). The addition of NADH during state 3 measurements had no substantial effect on the respiration rate, indicating good inner mitochondrial membrane integrity.

***Mitochondrial ROS production.*** ROS were measured as described previously (1). Briefly, mitochondria from WT and muscle specific SirT1-KO animals were incubated

with VO<sub>2</sub> buffer in a 96-well plate. ROS production was assessed at 37 °C for 30 min during state 4 and state 3 respiration by adding 10 mM glutamate or glutamate with 0.44 mM ADP, respectively, immediately prior to the addition of 50 μM dichlorodihydrofluorescein diacetate. The fluorescence emission between 480-520 nm, measured with a multi-detection micro-plate reader, is directly related to ROS production. ROS production measured in absolute fluorescence units was linear over the entire measurement period. ROS levels were expressed per natom of O<sub>2</sub> consumed, measured during the mitochondrial respiration assay.

***Immunoblotting.*** Protein extraction from frozen quadriceps sections were performed as previously described (27). Proteins extracted from the muscle homogenates were resolved by SDS-PAGE (10-15% polyacrylamide gels). Protein extracts were incubated overnight with antibodies against, aciculin (1:200), cytochrome c (cyt c) (1:1000), PGC1α (1:1000) and Nampt (1:3000). These were followed by incubations at room temperature with the appropriate secondary antibodies.

***Cytochrome c oxidase (COX) assay.*** COX activity of the mixed powdered muscle from control and muscle specific SirT1-KO animals were evaluated as described previously (27). Enzyme activity was determined spectrophotometrically at 30 °C as the maximal rate of oxidation of fully reduced cytochrome c, measured by the change in absorbance at 550 nm.

**Statistics.** Comparison between WT and SirT1-KO animals were evaluated using 2-way analyses of variance on each of the treatment conditions (Control diet, RSV diet, training and RSVdiet with training). Bonferroni post-tests were performed when applicable and all error bars represent standard error of the mean. Additionally, the interaction term of a two factor ANOVA was used to test for synergism when examining a combined treatment of RSV and CA, with significance defined as  $p < 0.05$ .

## **Results**

***SirT1 activity, in situ fatigue and training effects in both WT and SirT1-KO mice.*** To examine the role of SirT1 during the induction of mitochondrial biogenesis in muscle we compared the effects of CA or RSV on SirT1-KO mice to those of WT mice. We set out to investigate the physiological consequences of SirT1-KO mice with respect to muscle fatigue and running performance. *In situ* maximal stimulation of the gastrocnemius muscle exhibited greater fatigability of muscle-specific SirT1-KO animals compared to WT animals (Fig. 1A). However, with sub-maximal voluntary exercise over a 9 week period, both WT and muscle-specific SirT1-KO mice matched each other's performance on a weekly basis (Fig. 1B). The average running distance per week was higher in animals fed with an RSV-supplemented diet.

***Muscle mass, food consumption and body weight of WT and muscle-specific SirT1-KO animals.*** The TA, gastrocnemius and tricep muscles from SirT1-KO mice exhibited a

modest reduced muscle mass, per unit of body weight, compared to control WT mice (Fig. 2A). However, all treatments served to restore this muscle mass in SirT1-KO animals. The WT and SirT1-KO animals consumed the same quantity of food with each treatment condition (Fig. 2B). This quantity increased with RSV treatment and voluntary running. Despite the difference in food consumption, mice from all groups had similar body weights (Fig. 2C) suggesting that there was an elevation in energy expenditure with both training and RSV treatments to match the energy intake. As expected, all animals demonstrated a slight cardiac hypertrophy with training (Fig. 2D).

***PGC-1 $\alpha$  and Nampt protein expression.*** PGC-1 $\alpha$  protein expression was not altered in SirT1-KO animals compared to WT animals (Fig. 3A, B). However, each treatment group increased PGC-1 $\alpha$  expression compared to sedentary, control WT mice. Nampt protein was not influenced by RSV treatment, but increased in both the WT and SirT1-KO animals following training (Fig. 3A, C). In WT animals, a synergistic increase in NAMPT expression was observed that was not seen in the SirT1-KO animals as demonstrated by an interaction effect ( $p < 0.05$ ).

***Mitochondrial content in SirT1-KO and WT animals.*** COX activity was 23% lower in control SirT1-KO mice compared to WT mice indicating that there is less mitochondrial content within muscle of the KO animals (Fig. 4A). SirT1-KO animals fed a RSV diet exhibited improved COX activity that matched that of the WT control fed animal. However, WT animals treated with RSV did not demonstrate a significant change in

COX activity. Voluntary wheel training increased COX activity by 1.4- and 1.8-fold in both the WT and SirT1-KO mice, respectively. The most dramatic treatment response for COX activity (2.1-fold) occurred when WT mice were both trained and fed an RSV supplemented diet. Interestingly, this response was not duplicated for the combined treatment in SirT1-KO mice. This may suggest that a synergistic effect between training and the consumption of dietary RSV is dependent on SirT1 protein expression. Measurements of cytochrome c protein content largely supported the changes seen for each of the treatment groups evaluated (Fig 4.B).

***Respiration and ROS production in isolated mitochondria.*** Glutamate-stimulated state 4 (basal) and 3 (active) mitochondrial oxygen consumption ( $VO_2$ ) through complex I was 47% and 30% lower in the SirT1-KO animals compared to the WT control animals, respectively (Fig. 5A, B). State 4 and 3 respiration rates were not altered for any of the treatments in WT animals. Conversely, in the SirT1-KO animals, state 3 respiration was restored to control levels with an RSV diet, training and/or the combination of these treatments. State 4 respiration was not altered with RSV treatment alone but did recover with training and the combined treatment.

In mitochondria, ROS production is a metabolic by-product of respiration that occurs at complex I and 3 of the electron transport chain (17). ROS production from isolated mitochondria of SirT1-KO mice was 1.5- and 3.1-fold higher than the WT control mice during both state 4 and 3 respiration, respectively (Fig. 5C, D). Following

RSV feeding or training, ROS production was reduced in the SirT1-KO mice to a level that was equal to those of the similarly treated WT mice. WT mice only exhibited a reduction in ROS production in State 4 respiration following training or the combined treatment of training and RSV feeding.

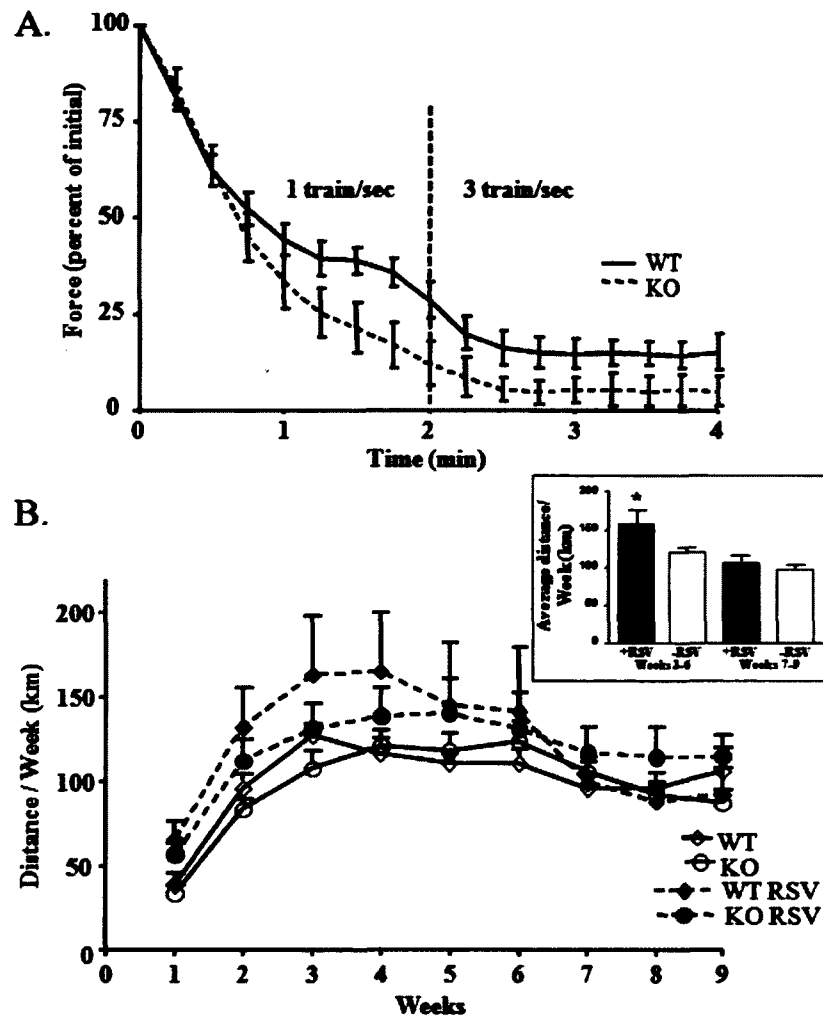


**Figure 1.** (A) Fatigue response from the in situ stimulation of WT or SirT1-KO gastrocnemius muscle as a percent of initial twitch force. (B) Voluntary wheel running distance by mice over 9 weeks fed with control or RSV diets. (B: inset) Total running distance of RSV or control fed mice for weeks 3 to 6 or 7 to 9 of the treatment protocol (n=8-12, \*, p<0.05, effect of RSV vs. control).

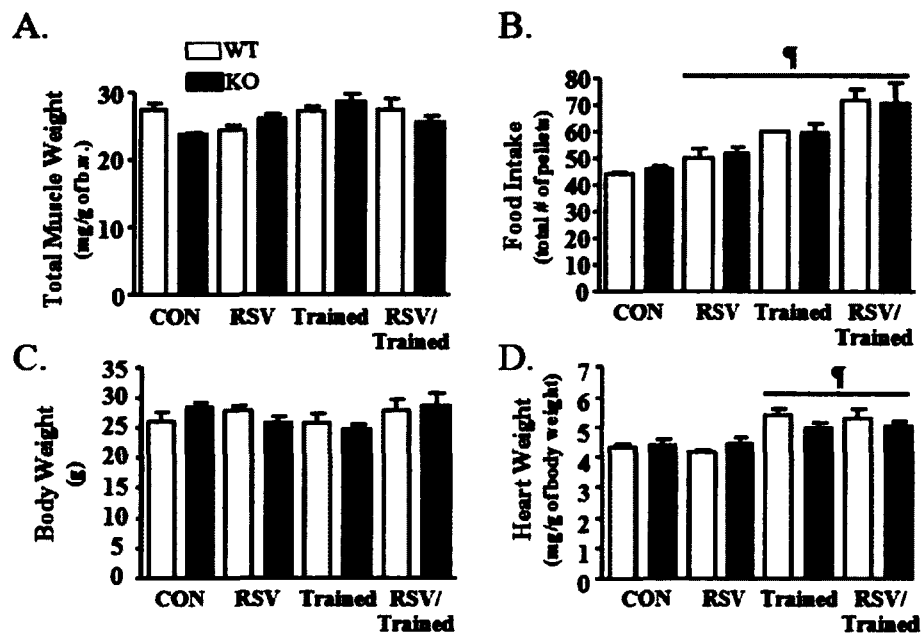


**Figure 2.** (A) Total wet muscle weight (TA, Gastrocnemius and Triceps) per gram of body weight for WT and SirT1-KO animals. (B) Total number of pellets of RSV or control diet consumed throughout the treatment. (C) Body weight of animals. (D) Heart weight per gram of body weight (following 9 weeks of treatment; n=12-7, ¶, p<0.05, overall effect of treatment vs. control).

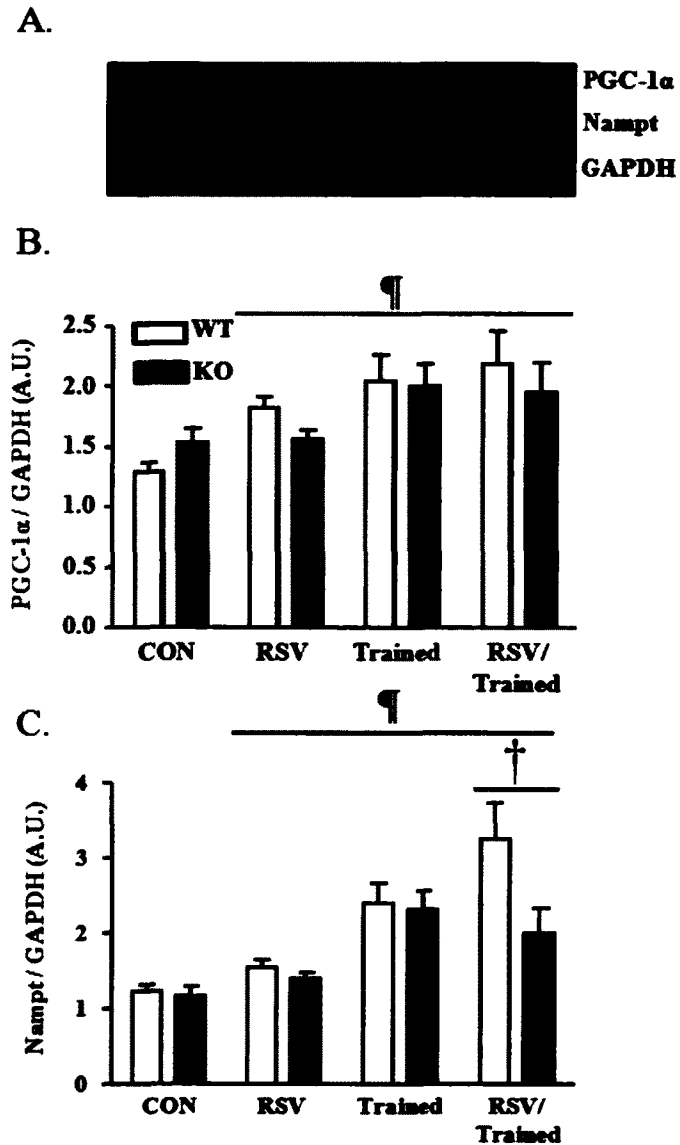


**Figure 3.** (A) PGC-1 $\alpha$  and Nampt protein expression following training, RSV and combined treatments in skeletal muscle from WT and SirT1-KO mice. (B) PGC-1 $\alpha$  and (C) Nampt protein expression is shown graphically (n=8-12, A.U., arbitrary scanner units corrected for loading using GAPDH; ‡, p<0.05, overall effect of treatment vs. control, †, p<0.05, interaction vs. Trained mice).

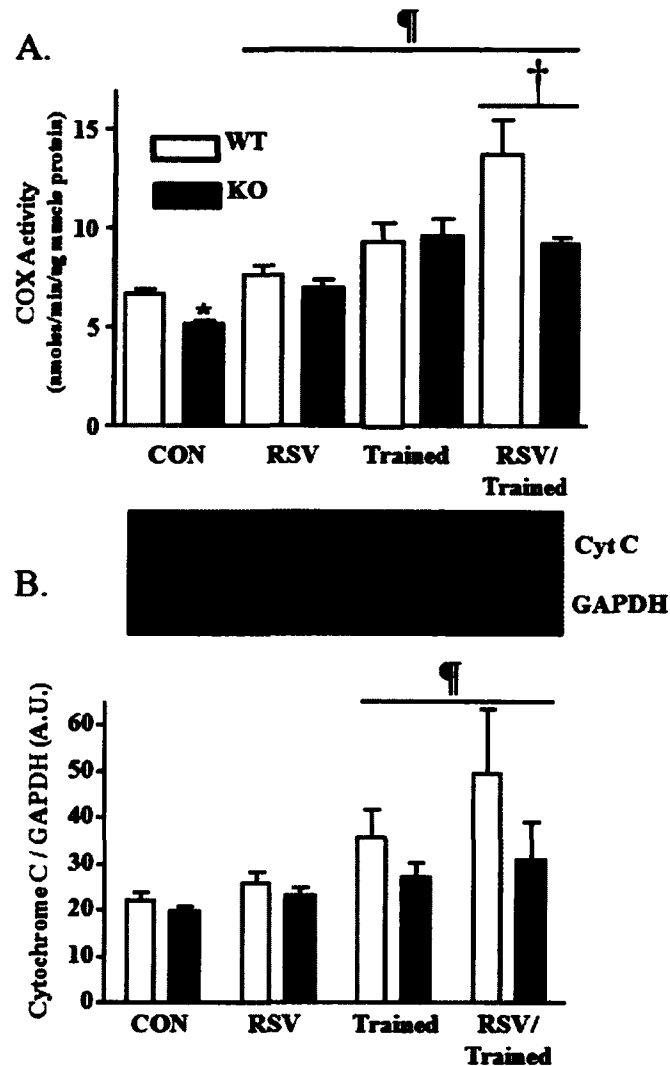


**Figure 4.** Skeletal muscle COX activity (A) and cytochrome c (Cyt C) protein (B) expression following training, RSV and combined treatments in skeletal muscle from WT and SirT1-KO mice (n=7-13, A.U., arbitrary scanner units for Cyt C are corrected for loading using GAPDH; ¶, p<0.05, overall effect of treatment vs. control, \*, p<0.05, vs. control WT mice, †, p<0.05, interaction vs. Trained mice).

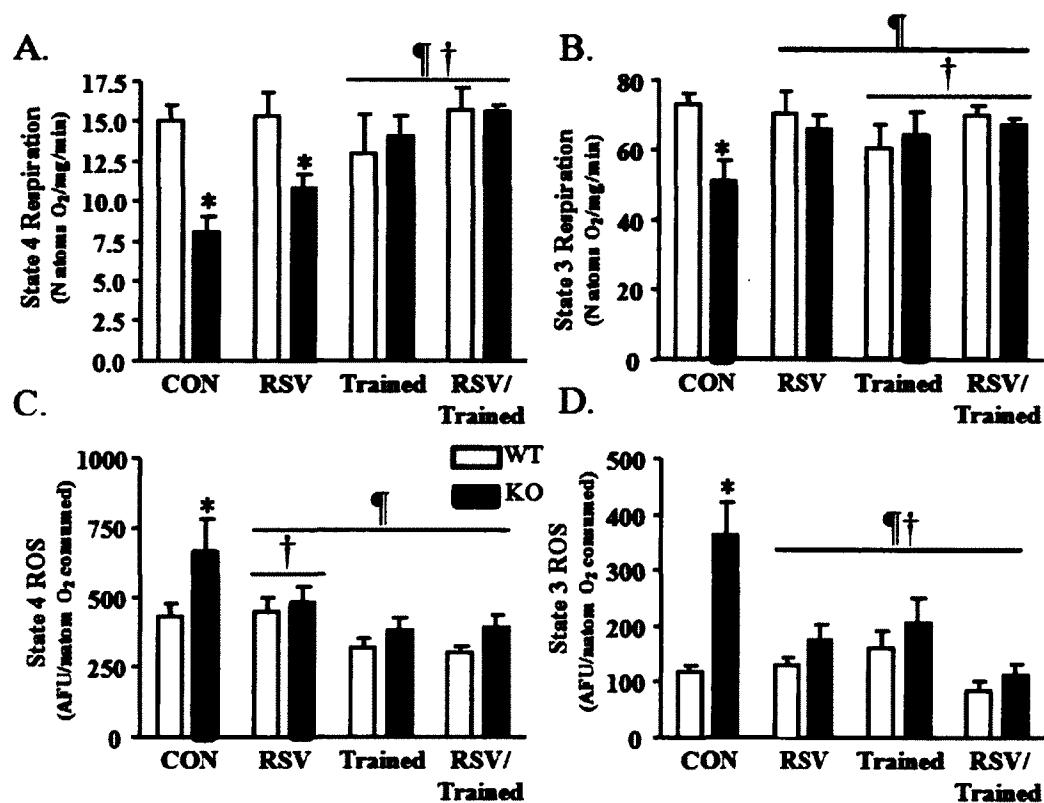


**Figure 5.** (A and B) State 4 and state 3 (basal and active) rates of oxygen consumption (VO<sub>2</sub>). (C and D) State 4 and state 3 reactive oxygen species (ROS) production per natom oxygen consumed in SS mitochondria (for each treatment condition in WT and SirT1 KO animals; n=7-14, \*, p<0.05, vs. control WT mice, ¶, p<0.05, overall effect of treatment vs. control mice, †, p<0.05, interaction vs. control mice).

## Discussion

The goal of this study was to delineate the role of SirT1 on mitochondrial function and biogenesis in both resting and exercising muscle, and the consequent effects of the lack of SirT1 on muscle performance. This is particularly relevant given the controversy surrounding the effects of acute or chronic exercise on SirT1 protein and activity (28). Here we examined the necessity of SirT1 to maintain basal muscle mitochondrial content and function, and to induce mitochondrial biogenesis following chronic voluntary endurance exercise. In addition, we provide additional insight into the SirT1-dependent and -independent effects of dietary RSV treatment on mitochondria in muscle.

First, we examined the differences in wheel running performance and fatigue in muscle-specific SirT1-KO and WT mice. SirT1-KO mice exhibited a greater rate of muscle fatigue during maximal *in situ* gastrocnemius muscle contractions compared to WT mice, during both moderate and severe contraction intensities. However, the performance of the SirT1-KO animals during the 9-week voluntary wheel running was not different from the WT animals. These experiments demonstrate that SirT1-KO animals exhibit a decreased muscle performance during a maximal *in situ* fatigue protocol, yet do not display any physiological differences *in vivo* during sub-maximal voluntary exercise. The basis of this difference likely resides in mitochondrial content and function. In addition, food consumption increased in all of the treatment groups, yet there were no differences in animal body weights suggesting that both RSV and training

increased energy expenditure. With dietary RSV this may be the result of an elevation in basal metabolic rate, as has been seen in mice and primates (16; 33), as opposed to increased physical activity.

An assessment of mitochondrial content in skeletal muscle was made using COX activity, a functional measurement for complex IV of the electron transport chain, along with cytochrome c protein expression. These measurements showed significantly less COX activity in SirT1-KO muscle compared to WT animals with a similar trend in cytochrome c protein expression. This indicates that the basal mitochondrial content of muscle relies, in part, on SirT1 expression and/or activity. However, the absence of SirT1 had a more pronounced effect on mitochondrial function, as reflected by marked decrements in both state 3 and state 4 respiration rates. Gerhart-Hines had previously demonstrated the importance of SirT1 for the induction and maintenance of fatty acid oxidation in C2C12 mouse muscle cells (19). Likewise, isolated liver mitochondria from SirT1-null mice showed reduced mitochondrial function (7). The decreases in mitochondrial function are further affirmed by the increase in ROS generation from SirT1-KO isolated muscle mitochondria during respiration compared to WT animals. Defects in respiration are known to result in an increase in ROS generation (14; 32; 45). While ROS are important signaling molecules in the cell, in large concentrations they can cause oxidative damage to proteins, DNA and other cellular macromolecules. SirT1 is therefore important for skeletal muscle oxidative stress homeostasis, as well as basal mitochondrial function and content.

As the most well known inducer of muscle mitochondrial biogenesis (23), exercise was used as a treatment for both WT and SirT1-KO mice. Voluntary wheel exercise produced an equal and substantial elevation of mitochondrial content in both the SirT1-KO animals and WT animals, along with elevated cytochrome c protein levels. This illustrates that the effects of voluntary endurance exercise do not rely on SirT1 activity to produce an increase in mitochondrial content. In addition, mitochondrial function in SirT1-KO mice following voluntary exercise was restored to normal state 3 and 4 WT levels, and ROS production was markedly reduced. As expected, exercised WT animals did not show an elevation in mitochondrial function compared to the sedentary animals. Consequently, ROS generated from mitochondria isolated from WT animals was only modestly reduced with training during state 4 but not state 3 respiration.

To examine the dependency of RSV-induced mitochondrial biogenesis on SirT1 activity, we compared WT to SirT1-KO mice following RSV treatment. A modest decrement in SirT1-KO mitochondrial content was restored back to WT levels, while RSV had no effect on content in WT animals. RSV also restored state 3 respiration and increased state 4 respiration in the direction of WT levels. However, it is evident that RSV treatment demonstrated less robust effects on mitochondrial biogenesis and function compared to voluntary wheel training in both the WT and SirT1-KO animals. The SirT1-independent effects of RSV most likely occur through the recently described activation of the CamKK $\beta$ -AMPK pathway (33).

We suspected that the effect of RSV would have a stronger influence on mitochondrial biogenesis when muscle was subject to metabolic demand, and therefore we treated our WT and SirT1-KO mice with both RSV and exercise. When RSV and exercise training treatments were combined in WT animals there was a synergistic increase in mitochondrial content that was not apparent in the SirT1-KO mice. This suggests that the effect of exercise on the AMPK-PGC-1 $\alpha$  pathway in SirT1-KO mice cannot be further enhanced by RSV treatment without the presence of SirT1 protein. The combined treatment also restored state 3 and 4 mitochondrial respiration and ROS production in SirT1-KO mitochondria back to WT levels. This would indicate that the maximal effect of RSV requires both SirT1 and a condition of energy demand in muscle which would be high in SirT1 and AMPK cofactors such as NAD<sup>+</sup> and AMP, respectively.

This study demonstrates that SirT1 protein is responsible for the partial maintenance of basal mitochondrial content and function, in addition to lowering mitochondrial ROS generation and improving muscle fatigue rates in skeletal muscle. These findings are similar, but not in total agreement, to those found previously by Philp et al. that showed no change in basal mitochondrial biogenesis and fatigue rates of the extensor digitorum longus muscle of SirT1-KO mice (34). This may be a result of the efficacy and fiber type distribution differences between their MCK- and our MLC1f-promoter driven Cre-LoxP recombination of the SirT1 gene. Nonetheless, the SirT1-independent increase in mitochondrial content with endurance exercise shown in our

study was also demonstrated by Philp et al. (34). Further, we found that RSV treatment also resulted in a SirT1-independent elevation of mitochondrial function and biogenesis, yet the effects of RSV were much less robust than those induced by endurance exercise. Since there are many reports that deacetylation is necessary for the co-activational activity of PGC-1 $\alpha$  (3; 37), the SirT1-independent effects in SirT1-KO mice during voluntary exercise may be a result of altered GCN5 acetyltransferase activity on PGC-1 $\alpha$  (26; 34). We also theorize that the reduced treatment effect of dietary RSV on mitochondrial biogenesis and function in comparison to exercise in WT animals may be a consequence of missing metabolites, specifically NAD<sup>+</sup> and AMP, that are necessary for activating AMPK and SirT1. It may be for this reason that SirT1-KO animals treated with RSV and experiencing a high energy demand, brought on by exercise, do not induce a synergistic mitochondrial response compared to WT animals. Furthermore, we previously found substantial elevations of SirT1 and PGC-1 $\alpha$  nuclear localization following electrical stimulation of C2C12 myotubes in combination with RSV treatment, when compared to RSV treatment alone, which may explain the synergistic results of the combined treatment *in vivo* (Menzies and Hood, unpublished data). The present study therefore demonstrates that RSV does not induce as robust an effect as exercise on mitochondrial biogenesis and function, but when combined with exercise may induce a SirT1-dependent synergistic response. These findings demonstrate that 1) exercise can induce mitochondrial biogenesis independent of SirT1, and 2) optimal therapeutic

**potential of RSV for the induction of mitochondrial biogenesis and function may rely on the presence of a cellular environment created by repeated energy demands.**

## **Acknowledgements**

We are grateful to Ayesha Saleem for her expert technical assistance. This work was supported by Canadian Institutes of Health Research (CIHR) grants to D. A. Hood. K. J. Menzies was a recipient of a CIHR Doctoral Award. D.A. Hood is the holder of a Canadian Research Chair in Cell Physiology.

## References

1. **Adhihetty PJ, Ljubicic V and Hood DA.** Effect of chronic contractile activity on SS and IMF mitochondrial apoptotic susceptibility in skeletal muscle. *Am J Physiol Endocrinol Metab* 292: E748-E755, 2007.
2. **Adhihetty PJ, Ljubicic V, Menzies KJ and Hood DA.** Differential susceptibility of subsarcolemmal and intermyofibrillar mitochondria to apoptotic stimuli. *Am J Physiol Cell Physiol* 289: C994-C1001, 2005.
3. **Amat R, Planavila A, Chen SL, Iglesias R, Giralt M and Villarroya F.** SIRT1 controls the transcription of the peroxisome proliferator-activated receptor-gamma Co-activator-1alpha (PGC-1alpha) gene in skeletal muscle through the PGC-1alpha autoregulatory loop and interaction with MyoD. *J Biol Chem* 284: 21872-21880, 2009.
4. **Aparicio OM, Billington BL and Gottschling DE.** Modifiers of position effect are shared between telomeric and silent mating-type loci in *S. cerevisiae*. *Cell* 66: 1279-1287, 1991.
5. **Baur JA, Pearson KJ, Price NL, Jamieson HA, Lerin C, Kalra A, Prabhu VV, Allard JS, Lopez-Lluch G, Lewis K, Pistell PJ, Poosala S, Becker KG, Boss O, Gwinn D, Wang M, Ramaswamy S, Fishbein KW, Spencer RG, Lakatta EG, Le CD, Shaw RJ, Navas P, Puigserver P, Ingram DK, de CR and Sinclair DA.** Resveratrol improves health and survival of mice on a high-

- calorie diet. *Nature* 444: 337-342, 2006.
6. **Baur JA and Sinclair DA.** Therapeutic potential of resveratrol: the in vivo evidence. *Nat Rev Drug Discov* 5: 493-506, 2006.
  7. **Boily G, Seifert EL, Bevilacqua L, He XH, Sabourin G, Estey C, Moffat C, Crawford S, Saliba S, Jardine K, Xuan J, Evans M, Harper ME and McBurney MW.** SirT1 regulates energy metabolism and response to caloric restriction in mice. *PLoS ONE* 3: e1759, 2008.
  8. **Bothe GW, Haspel JA, Smith CL, Wiener HH and Burden SJ.** Selective expression of Cre recombinase in skeletal muscle fibers. *Genesis* 26: 165-166, 2000.
  9. **Boulton SJ and Jackson SP.** Components of the Ku-dependent non-homologous end-joining pathway are involved in telomeric length maintenance and telomeric silencing. *EMBO J* 17: 1819-1828, 1998.
  10. **Breen DM, Sanli T, Giacca A and Tsiani E.** Stimulation of muscle cell glucose uptake by resveratrol through sirtuins and AMPK. *Biochem Biophys Res Commun* 374: 117-122, 2008.
  11. **Camins A, Sureda FX, Junyent F, Verdaguer E, Folch J, Pelegri C, Vilaplana J, Beas-Zarate C and Pallas M.** Sirtuin activators: Designing molecules to extend life span. *Biochim Biophys Acta* 2010.
  12. **Canto C, Jiang LQ, Deshmukh AS, Matakci C, Coste A, Lagouge M, Zierath JR and Auwerx J.** Interdependence of AMPK and SIRT1 for metabolic

- adaptation to fasting and exercise in skeletal muscle. *Cell Metab* 11: 213-219, 2010.
13. **Centeno-Baez C, Dallaire P and Marette A.** Resveratrol inhibition of inducible nitric oxide synthase in skeletal muscle involves AMPK but not SIRT1. *Am J Physiol Endocrinol Metab* 301: E922-E930, 2011.
  14. **Chen Q, Moghaddas S, Hoppel CL and Lesnefsky EJ.** Ischemic defects in the electron transport chain increase the production of reactive oxygen species from isolated rat heart mitochondria. *Am J Physiol Cell Physiol* 294: C460-C466, 2008.
  15. **Costford SR, Bajpeyi S, Pasarica M, Albarado DC, Thomas SC, Xie H, Church TS, Jubrias SA, Conley KE and Smith SR.** Skeletal muscle NAMPT is induced by exercise in humans. *Am J Physiol Endocrinol Metab* 298: E117-E126, 2010.
  16. **Dal-Pan A, Pifferi F, Marchal J, Picq JL and Aujard F.** Cognitive performances are selectively enhanced during chronic caloric restriction or resveratrol supplementation in a primate. *PLoS ONE* 6: e16581, 2011.
  17. **Finkel T and Holbrook NJ.** Oxidants, oxidative stress and the biology of ageing. *Nature* 408: 239-247, 2000.
  18. **Fulco M, Cen Y, Zhao P, Hoffman EP, McBurney MW, Sauve AA and Sartorelli V.** Glucose restriction inhibits skeletal myoblast differentiation by activating SIRT1 through AMPK-mediated regulation of Nampt. *Dev Cell* 14: 661-673, 2008.

19. **Gerhart-Hines Z, Rodgers JT, Bare O, Lerin C, Kim SH, Mostoslavsky R, Alt FW, Wu Z and Puigserver P.** Metabolic control of muscle mitochondrial function and fatty acid oxidation through SIRT1/PGC-1alpha. *EMBO J* 26: 1913-1923, 2007.
20. **Harper CE, Patel BB, Wang J, Arabshahi A, Eltoum IA and Lamartiniere CA.** Resveratrol suppresses prostate cancer progression in transgenic mice. *Carcinogenesis* 28: 1946-1953, 2007.
21. **Horn TL, Cwik MJ, Morrissey RL, Kapetanovic I, Crowell JA, Booth TD and McCormick DL.** Oncogenicity evaluation of resveratrol in p53(+/-) (p53 knockout) mice. *Food Chem Toxicol* 45: 55-63, 2007.
22. **Howitz KT, Bitterman KJ, Cohen HY, Lamming DW, Lavu S, Wood JG, Zipkin RE, Chung P, Kisielewski A, Zhang LL, Scherer B and Sinclair DA.** Small molecule activators of sirtuins extend *Saccharomyces cerevisiae* lifespan. *Nature* 425: 191-196, 2003.
23. **Irrcher I, Adhihetty PJ, Joseph AM, Ljubcic V and Hood DA.** Regulation of mitochondrial biogenesis in muscle by endurance exercise. *Sports Med* 33: 783-793, 2003.
24. **Jager S, Handschin C, St-Pierre J and Spiegelman BM.** AMP-activated protein kinase (AMPK) action in skeletal muscle via direct phosphorylation of PGC-1alpha. *Proc Natl Acad Sci U S A* 104: 12017-12022, 2007.

25. **Lagouge M, Argmann C, Gerhart-Hines Z, Meziane H, Lerin C, Daussin F, Messadeq N, Milne J, Lambert P, Elliott P, Geny B, Laakso M, Puigserver P and Auwerx J.** Resveratrol improves mitochondrial function and protects against metabolic disease by activating SIRT1 and PGC-1alpha. *Cell* 127: 1109-1122, 2006.
26. **Lerin C, Rodgers JT, Kalume DE, Kim SH, Pandey A and Puigserver P.** GCN5 acetyltransferase complex controls glucose metabolism through transcriptional repression of PGC-1alpha. *Cell Metab* 3: 429-438, 2006.
27. **Ljubicic V and Hood DA.** Kinase-specific responsiveness to incremental contractile activity in skeletal muscle with low and high mitochondrial content. *Am J Physiol Endocrinol Metab* 295: E195-E204, 2008.
28. **Menzies KJ and Hood DA.** The role of SirT1 in muscle mitochondrial turnover. *Mitochondrion* 2011.
29. **Nakahata Y, Sahar S, Astarita G, Kaluzova M and Sassone-Corsi P.** Circadian control of the NAD<sup>+</sup> salvage pathway by CLOCK-SIRT1. *Science* 324: 654-657, 2009.
30. **Narkar VA, Downes M, Yu RT, Embler E, Wang YX, Banayo E, Mihaylova MM, Nelson MC, Zou Y, Juguilon H, Kang H, Shaw RJ and Evans RM.** AMPK and PPARdelta agonists are exercise mimetics. *Cell* 134: 405-415, 2008.
31. **Nemoto S, Fergusson MM and Finkel T.** SIRT1 functionally interacts with the

- metabolic regulator and transcriptional coactivator PGC-1{alpha}. *J Biol Chem* 280: 16456-16460, 2005.
32. **O'Leary MF and Hood DA.** Effect of prior chronic contractile activity on mitochondrial function and apoptotic protein expression in denervated muscle. *J Appl Physiol* 105: 114-120, 2008.
  33. **Park SJ, Ahmad F, Philp A, Baar K, Williams T, Luo H, Ke H, Rehmann H, Taussig R, Brown AL, Kim MK, Beaven MA, Burgin AB, Manganiello V and Chung JH.** Resveratrol ameliorates aging-related metabolic phenotypes by inhibiting cAMP phosphodiesterases. *Cell* 148: 421-433, 2012.
  34. **Philp A, Chen A, Lan D, Meyer GA, Murphy AN, Knapp AE, Olfert IM, McCurdy CE, Marcotte GR, Hogan MC, Baar K and Schenk S.** Sirtuin 1 (SIRT1) deacetylase activity is not required for mitochondrial biogenesis or peroxisome proliferator-activated receptor-gamma coactivator-1alpha (PGC-1alpha) deacetylation following endurance exercise. *J Biol Chem* 286: 30561-30570, 2011.
  35. **Revollo JR, Grimm AA and Imai S.** The NAD biosynthesis pathway mediated by nicotinamide phosphoribosyltransferase regulates Sir2 activity in mammalian cells. *J Biol Chem* 279: 50754-50763, 2004.
  36. **Revollo JR, Grimm AA and Imai S.** The regulation of nicotinamide adenine dinucleotide biosynthesis by Nampt/PBEF/visfatin in mammals. *Curr Opin Gastroenterol* 23: 164-170, 2007.

37. **Rodgers JT, Lerin C, Haas W, Gygi SP, Spiegelman BM and Puigserver P.** Nutrient control of glucose homeostasis through a complex of PGC-1alpha and SIRT1. *Nature* 434: 113-118, 2005.
38. **Takahashi M and Hood DA.** Chronic stimulation-induced changes in mitochondria and performance in rat skeletal muscle. *J Appl Physiol* 74: 934-941, 1993.
39. **Timmers S, Konings E, Bilet L, Houtkooper RH, van de WT, Goossens GH, Hoeks J, van der KS, Ryu D, Kersten S, Moonen-Kornips E, Hesselink MK, Kunz I, Schrauwen-Hinderling VB, Blaak EE, Auwerx J and Schrauwen P.** Calorie Restriction-like Effects of 30 Days of Resveratrol Supplementation on Energy Metabolism and Metabolic Profile in Obese Humans. *Cell Metab* 14: 612-622, 2011.
40. **Ugucioni G and Hood DA.** The importance of PGC-1alpha in contractile activity-induced mitochondrial adaptations. *Am J Physiol Endocrinol Metab* 300: E361-E371, 2011.
41. **Valenzano DR, Terzibasi E, Genade T, Cattaneo A, Domenici L and Cellierino A.** Resveratrol prolongs lifespan and retards the onset of age-related markers in a short-lived vertebrate. *Curr Biol* 16: 296-300, 2006.
42. **Wood JG, Rogina B, Lavu S, Howitz K, Helfand SL, Tatar M and Sinclair D.** Sirtuin activators mimic caloric restriction and delay ageing in metazoans. *Nature* 430: 686-689, 2004.

43. **Zhang J.** Resveratrol inhibits insulin responses in a SirT1-independent pathway. *Biochem J* 397: 519-527, 2006.
44. **Zhang T, Berrocal JG, Frizzell KM, Gamble MJ, DuMond ME, Krishnakumar R, Yang T, Sauve AA and Kraus WL.** Enzymes in the NAD<sup>+</sup> salvage pathway regulate SIRT1 activity at target gene promoters. *J Biol Chem* 284: 20408-20417, 2009.
45. **Zuin A, Gabrielli N, Calvo IA, Garcia-Santamarina S, Hoe KL, Kim DU, Park HO, Hayles J, Ayte J and Hidalgo E.** Mitochondrial dysfunction increases oxidative stress and decreases chronological life span in fission yeast. *PLoS ONE* 3: e2842, 2008.

## **CHAPTER 4**

## **Dissertation Summary**

Both caloric restriction (1; 8) and resveratrol (RSV) (7; 9), a natural polyphenolic compound, have been shown to activate SirT1, which in turn extends lifespan and increases mitochondrial content and function (11; 12). Interestingly, the effects of RSV and those of exercise, induce many of the same physiological changes (4; 5) including mitochondrial biogenesis. For mitochondrial biogenesis to occur, the cell needs to activate nuclear genes encoding mitochondrial proteins (NUGEMPs). NUGEMPs encode up to 1500 proteins that are required for the biogenesis of new mitochondria, in addition to proteins that help to coordinate the regulation of mtDNA gene expression. Cell culture experiments have demonstrated that the  $\text{NAD}^+$ -dependent SirT1 protein regulates the activation of NUGEMPs expression through the direct deacetylation of PGC-1 $\alpha$ , an important protein for the coactivation of NUGEMP transcription (3; 10). The deacetylation of PGC-1 $\alpha$  by SirT1 depends on a dynamic equilibrium which relies on the availability of substrates and enzymes. Depending on the expression of SirT1, the metabolic status of the muscle fibre and the concentration of metabolites, such as  $\text{NAD}^+$ , there could be various outcomes on the rate of PGC-1 $\alpha$  deacetylation (13). Costford et al. demonstrated that increases in NAMPT protein, the rate limiting enzyme for the conversion of nicotinamide to  $\text{NAD}^+$ , correlated with elevations in mitochondrial content in humans (2). NAMPT expression was also found to be lower in obese or type 2 diabetic individuals and could be elevated substantially in sedentary subjects following exercise

(2). Similarly, exercise training in aged rats was shown to attenuate the age-associated shift in redox balance (6). Evidence therefore supports the involvement of SirT1 activation during exercise in skeletal muscle. Thus, using cell culture models and *in-vivo* models, we set out to examine the role of SirT1 in exercise- and resveratrol-induced mitochondrial biogenesis.

Resveratrol is known to extend lifespan and increase mitochondrial biogenesis possibly via activation of the longevity protein SIRT1. Exercise or chronic contractile activity (CCA; a cellular model of exercise) is known to induce mitochondrial biogenesis, in part, through the activation of the transcriptional coactivator PGC-1 $\alpha$ . Thus, we hypothesized that CCA and RSV would produce additive effects on mitochondrial biogenesis in excitable C2C12 myotubes by coordinating the activation of both SirT1 and PGC-1 $\alpha$ . In Chapter 2, differentiated C2C12 myotubes were treated with CCA for 3 hrs per day for up to 4 days with, or without, the addition of RSV. As hypothesized, SIRT1 protein content was elevated 2-fold following RSV treatment, but was not affected by CCA. Alternatively, CCA increased PGC-1 $\alpha$  1.6-fold in the absence of an effect of RSV. Cytochrome c oxidase (COX) activity, an indicator of mitochondrial content, increased by 1.6- and 3.1-fold with RSV treatment and CCA, respectively. Then by combining the treatments of RSV and CCA there were elevations of both SirT1 and PGC-1 $\alpha$ , which induced a synergistic 6.1-fold increase in COX activity and mitochondrial mass, along with an enhanced translocation of cytosolic PGC-1 $\alpha$  and SirT1 to the nucleus. This synergistic effect could then be blocked by the SirT1 inhibitor nicotinamide (NAM),

indicating a dependence on SirT1 activity. These results indicate that 1) CCA can induce a more robust increase in muscle mitochondrial content than RSV, 2) the combination of CCA and RSV induced a synergistic effect on mitochondrial biogenesis, and 3) the potential of RSV to be used as an ergogenic aid for skeletal muscle mitochondrial biogenesis may be limited to cellular environments in which there is a shift towards a negative energy balance within the cell, as what occurs with CCA or exercise.

To further examine the reliance between the effects exercise training or RSV on SirT1 activity, in Chapter 3 we produced a skeletal-muscle specific SirT1-deficient mouse (SirT1-KO). These mice were generated using a myosin light chain-directed Cre-loxP targeted mutation of the SirT1 gene. These mice showed no behavioural or phenotypic abnormalities and had similar body and muscle weights as wild-type (WT) animals. We used voluntary wheel-running exercise, RSV, or a combination of exercise and RSV treatments over a 9-week period to examine the reliance of these treatments on SirT1 for the induction of mitochondrial biogenesis in either WT or muscle-specific SirT1-KO animals. In comparison to WT animals under basal conditions, SirT1-KO mice exhibited similar muscle tissue expression of PGC-1 $\alpha$ , yet demonstrated a modest decline in COX activity. In addition, SirT1-KO mice demonstrated 30% and 47% reductions in rates of state 3 and state 4 mitochondrial respiration, respectively. Concurrently, there were 3.5- and 1.5-fold elevations in ROS generation for the SirT1-KO mice during both state 3 and state 4 mitochondrial respiration. With 9 weeks of voluntary running, both WT and SirT1-KO mice ran the same average and total distances, while RSV fed

animals from both groups showed elevated levels of volitional running. With exercise there were 1.4- and 1.8-fold increases in COX activity in both the WT and SirT1-KO animals, bringing them to the same absolute value of COX activity. In addition, the decrements in state 3 and 4 mitochondrial respiration, along with the increased ROS production in SirT1-KO mice, were rescued to values similar to those of the WT mice. Resveratrol did not alter COX activity or mitochondrial respiration in WT mice, but did help to restore these values back to WT levels in the KO animals. When voluntary exercise was combined with RSV feeding there was a synergistic increase in COX activity and mitochondrial respiration that was apparent in the WT, but not in the SirT1-KO animals. These experiments demonstrated that SirT1 plays a modest role in maintaining basal mitochondrial content, and a larger role in preserving mitochondrial function as reflected by respiration and ROS production. Both voluntary exercise and RSV treatment induce mitochondrial biogenesis in a SirT1-independent manner. However, when RSV and exercise are combined, there is a SirT1-dependent synergistic effect leading to the stimulation of mitochondrial biogenesis.

In closing, the results obtained from this Dissertation are important for our understanding of 1) the potency of exercise vs. RSV treatment in eliciting mitochondrial biogenesis, 2) the SirT1-independent effects of RSV and exercise training on mitochondria, and 3) the potential for a SirT1-dependent synergistic effect between RSV-treatment and chronic contractile activity or exercise. Therefore, our data not only explain the SirT1 deacetylase activity-independent and -dependent effects on skeletal muscle

mitochondrial biogenesis, but also uniquely demonstrate the synergistic therapeutic potential of RSV on mitochondrial biogenesis in a cellular environment that is exposed to repeated bouts of energy demand.

## References

1. **Cohen HY, Miller C, Bitterman KJ, Wall NR, Hekking B, Kessler B, Howitz KT, Gorospe M, de CR and Sinclair DA.** Calorie restriction promotes mammalian cell survival by inducing the SIRT1 deacetylase. *Science* 305: 390-392, 2004.
2. **Costford SR, Bajpeyi S, Pasarica M, Albarado DC, Thomas SC, Xie H, Church TS, Jubrias SA, Conley KE and Smith SR.** Skeletal muscle NAMPT is induced by exercise in humans. *Am J Physiol Endocrinol Metab* 298: E117-E126, 2010.
3. **Gerhart-Hines Z, Rodgers JT, Bare O, Lerin C, Kim SH, Mostoslavsky R, Alt FW, Wu Z and Puigserver P.** Metabolic control of muscle mitochondrial function and fatty acid oxidation through SIRT1/PGC-1alpha. *EMBO J* 26: 1913-1923, 2007.
4. **Irrcher I, Adhihetty PJ, Joseph AM, Ljubicic V and Hood DA.** Regulation of mitochondrial biogenesis in muscle by endurance exercise. *Sports Med* 33: 783-793, 2003.
5. **Joseph AM, Joanisse DR, Baillot RG and Hood DA.** Mitochondrial dysregulation in the pathogenesis of diabetes: potential for mitochondrial biogenesis-mediated interventions. *Exp Diabetes Res* 2012: 642038, 2012.
6. **Koltai E, Szabo Z, Atalay M, Boldogh I, Naito H, Goto S, Nyakas C and**

- Radak Z.** Exercise alters SIRT1, SIRT6, NAD and NAMPT levels in skeletal muscle of aged rats. *Mech Ageing Dev* 131: 21-28, 2010.
7. **Lagouge M, Argmann C, Gerhart-Hines Z, Meziane H, Lerin C, Daussin F, Messadeq N, Milne J, Lambert P, Elliott P, Geny B, Laakso M, Puigserver P and Auwerx J.** Resveratrol improves mitochondrial function and protects against metabolic disease by activating SIRT1 and PGC-1alpha. *Cell* 127: 1109-1122, 2006.
  8. **Lin SJ, Ford E, Haigis M, Liszt G and Guarente L.** Calorie restriction extends yeast life span by lowering the level of NADH. *Genes Dev* 18: 12-16, 2004.
  9. **Park SJ, Ahmad F, Philp A, Baar K, Williams T, Luo H, Ke H, Rehmann H, Taussig R, Brown AL, Kim MK, Beaven MA, Burgin AB, Manganiello V and Chung JH.** Resveratrol ameliorates aging-related metabolic phenotypes by inhibiting cAMP phosphodiesterases. *Cell* 148: 421-433, 2012.
  10. **Rodgers JT, Lerin C, Haas W, Gygi SP, Spiegelman BM and Puigserver P.** Nutrient control of glucose homeostasis through a complex of PGC-1alpha and SIRT1. *Nature* 434: 113-118, 2005.
  11. **Timmers S, Konings E, Bilet L, Houtkooper RH, van de WT, Goossens GH, Hoeks J, van der KS, Ryu D, Kersten S, Moonen-Kornips E, Hesselink MK, Kunz I, Schrauwen-Hinderling VB, Blaak EE, Auwerx J and Schrauwen P.** Calorie Restriction-like Effects of 30 Days of Resveratrol Supplementation on

Energy Metabolism and Metabolic Profile in Obese Humans. *Cell Metab* 14: 612-622, 2011.

12. **Viswanathan M and Guarente L.** Regulation of *Caenorhabditis elegans* lifespan by sir-2.1 transgenes. *Nature* 477: E1-E2, 2011.
13. **Zhang T, Berrocal JG, Frizzell KM, Gamble MJ, DuMond ME, Krishnakumar R, Yang T, Sauve AA and Kraus WL.** Enzymes in the NAD<sup>+</sup> salvage pathway regulate SIRT1 activity at target gene promoters. *J Biol Chem* 284: 20408-20417, 2009.

## **CHAPTER 5: APPENDICIES**

**APPENDIX I: ADDITIONAL DATA**

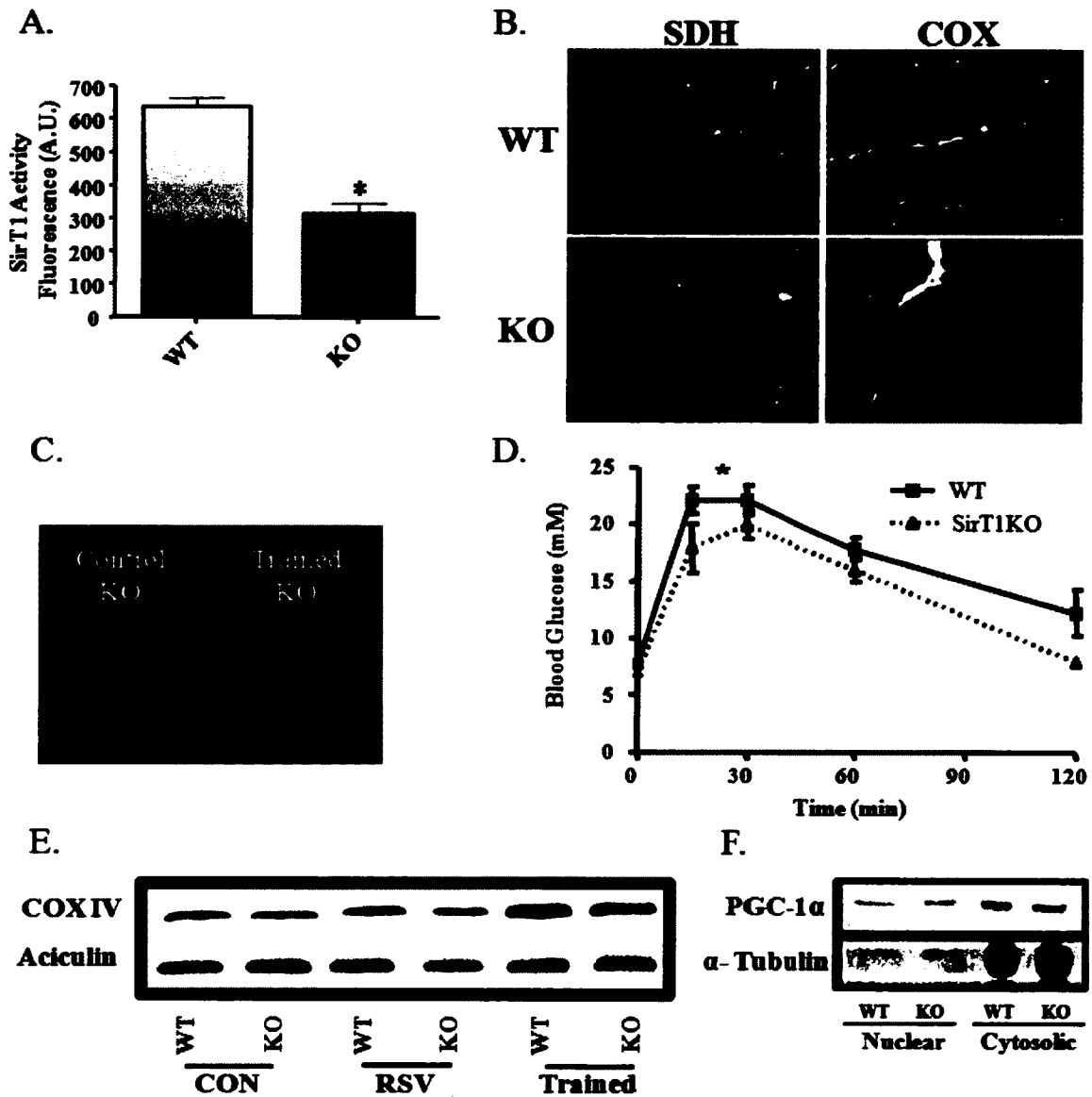


**Figure 1.** (A) SirT1 activity in WT and SirT1-KO muscle enzyme extracts (n=4). (B) Cytochrome c oxidase (COX) and succinate dehydrogenase (SDH) histochemical staining of serial sections from WT and SirT1-KO mice. (C) Muscle homogenates from SirT1 KO mice before and after training. (D) Intraperitoneal glucose tolerance test was performed on WT and SirT1-KO animals. Mice were given an intraperitoneal injection of D-glucose (2g/kg of body weight) following 6 hours of fasting. (E) Immunoblot of COXIV protein expression. Treatments with RSV do not appear to alter COX IV protein expression, however, training increases expression for both SirT1KO and WT animals (n=8). (F) PGC-1 $\alpha$  expression in nuclear and cytosolic fractions of control WT and SirT1-KO mice (n=4). (\*,  $p < 0.05$ , vs. WT mice).

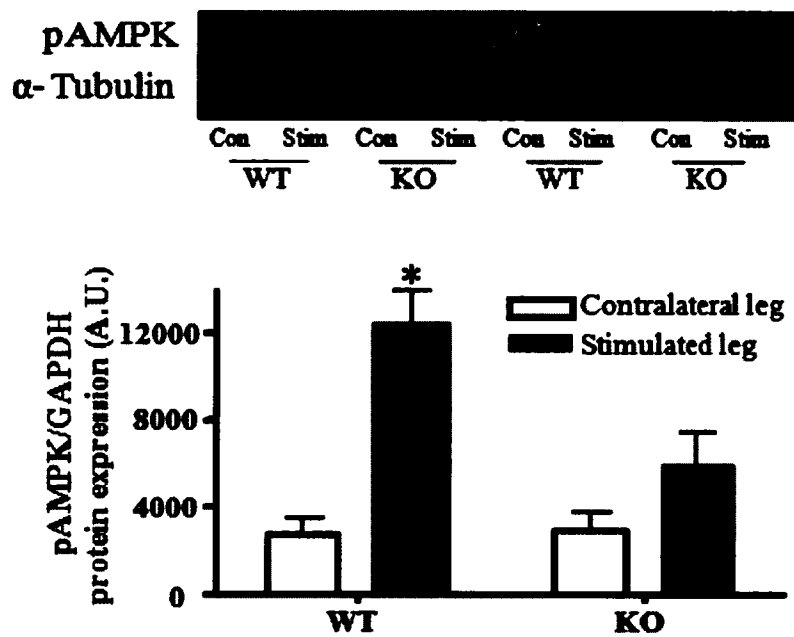


**Figure 2.** pAMPK expression in gastrocnemius muscle that was immediately frozen following stimulation at 1 tetanic contraction per second (TPS) and 3 TPS for 2 min. Muscle from the stimulated leg is compared to the contralateral leg for both WT and SirT1-KO mice (n=8) (\*,  $p < 0.05$ , vs. WT Con mice).

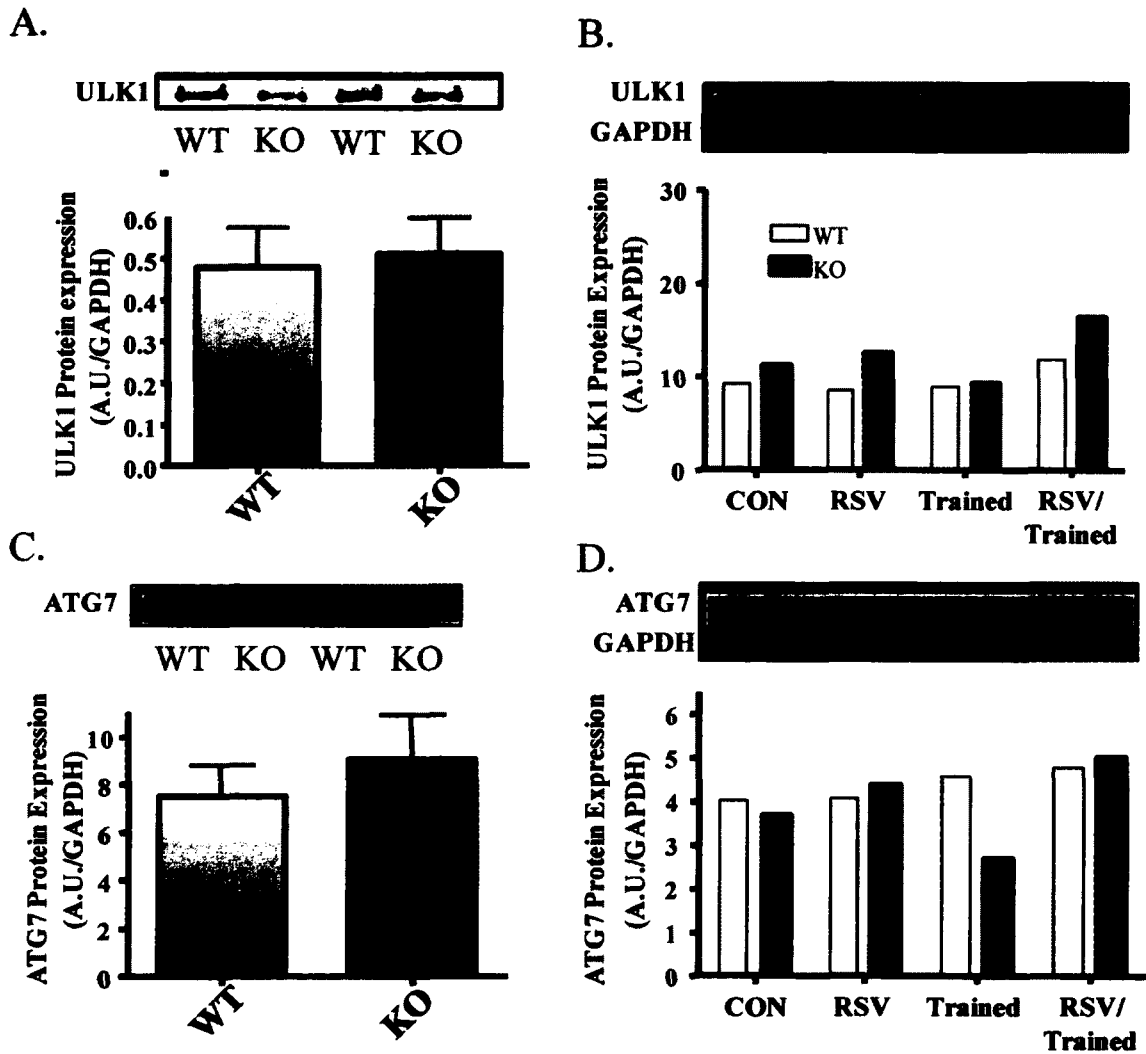


**Figure 3.** Measurements for general autophagy in whole muscle extracts from WT and SirT1-KO mice. (A) ULK1 expression (n=8) and (C) ATG7 expression (n=4) in muscle from WT and SirT1 KO animals. ULK1 (B) and ATG7 (D) protein expression in muscle from WT and SirT1 KO animals fed control or RSV diets, and/or treated with voluntary wheel running (n=2).

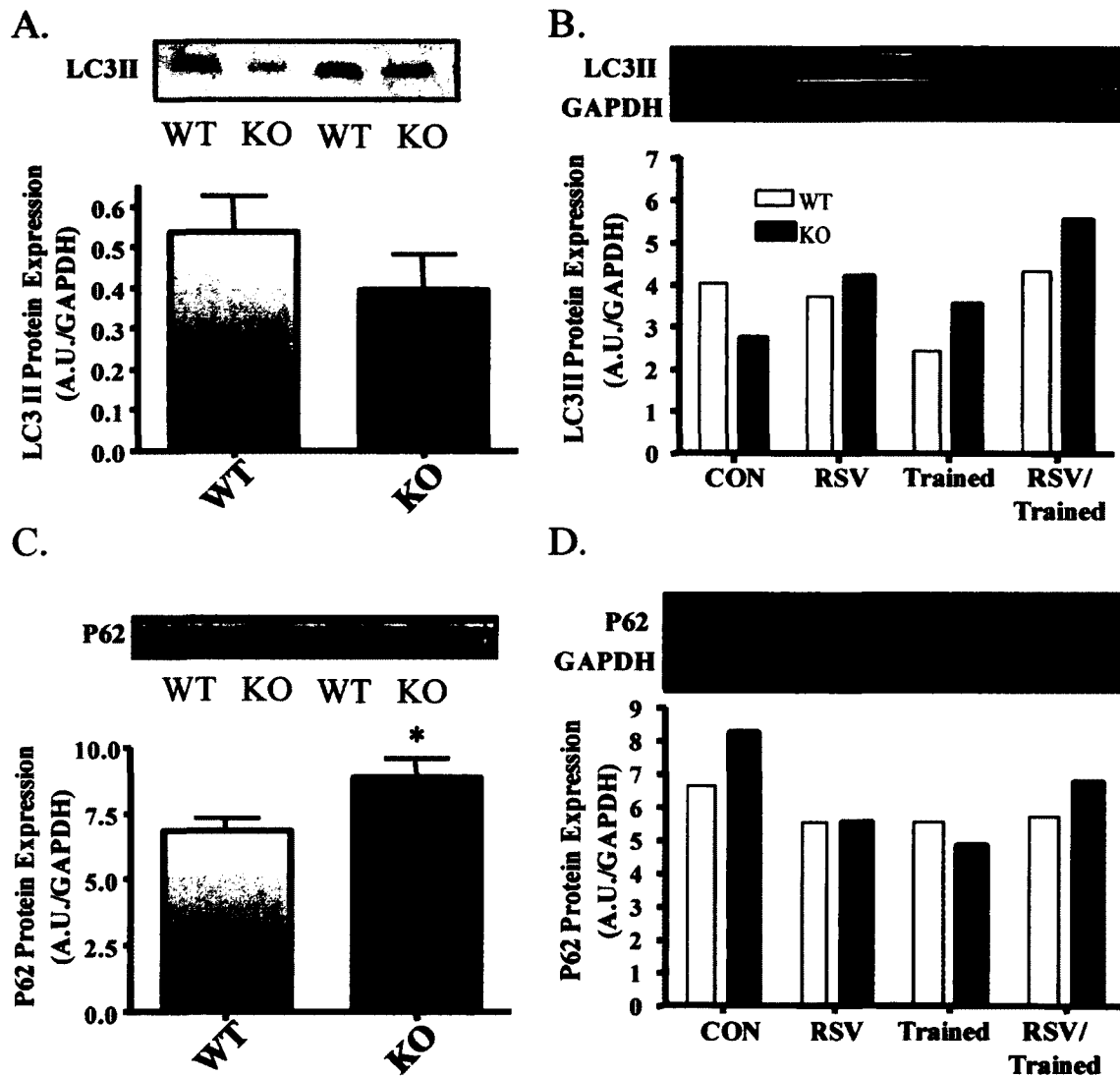


**Figure 4.** Indicators for mitophagy measured in whole muscle extracts from WT and SirT1-KO mice. (A) LC3II expression (n=10) and (C) P62 expression (n=12) in muscle from WT and SirT1 KO animals. LC3II (B) and P62 (D) protein expression in muscle from WT and SirT1 KO animals fed control or RSV diets, and/or treated with voluntary wheel running (n=2) (\*, p<0.05, vs. WT mice).

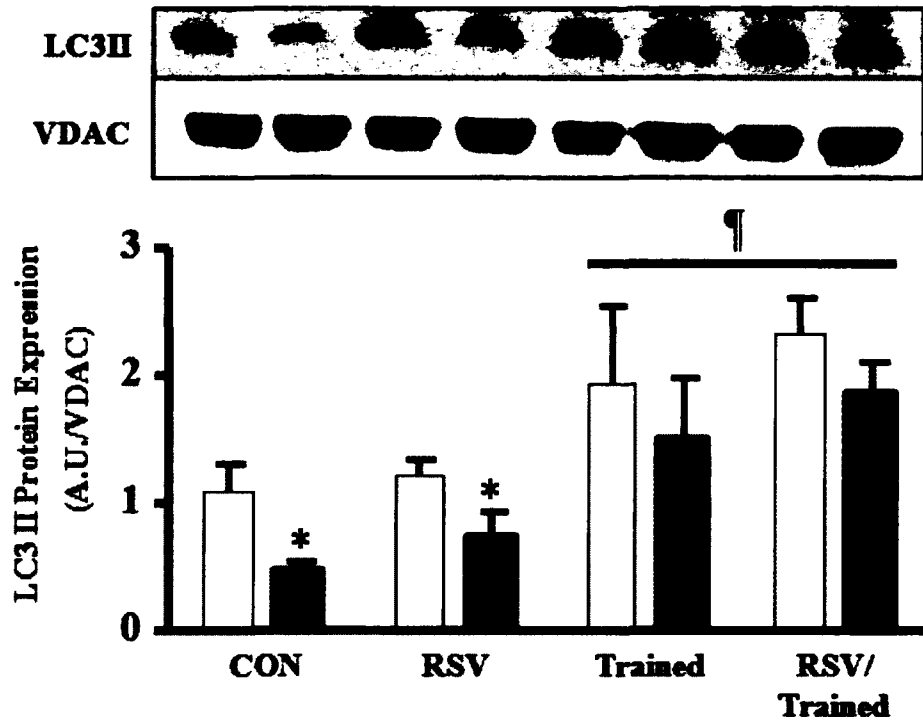


**Figure 5.** LC3II protein expression from isolated mitochondria was measured as an indicator for the activation of mitophagy. Measurements were made in muscle mitochondria from WT and SirT1-KO animals fed control or RSV diets, with or without voluntary wheel running (n=8, \*, p<0.05, vs. WT mice, §, p<0.05, overall effect of Training vs. control mice).

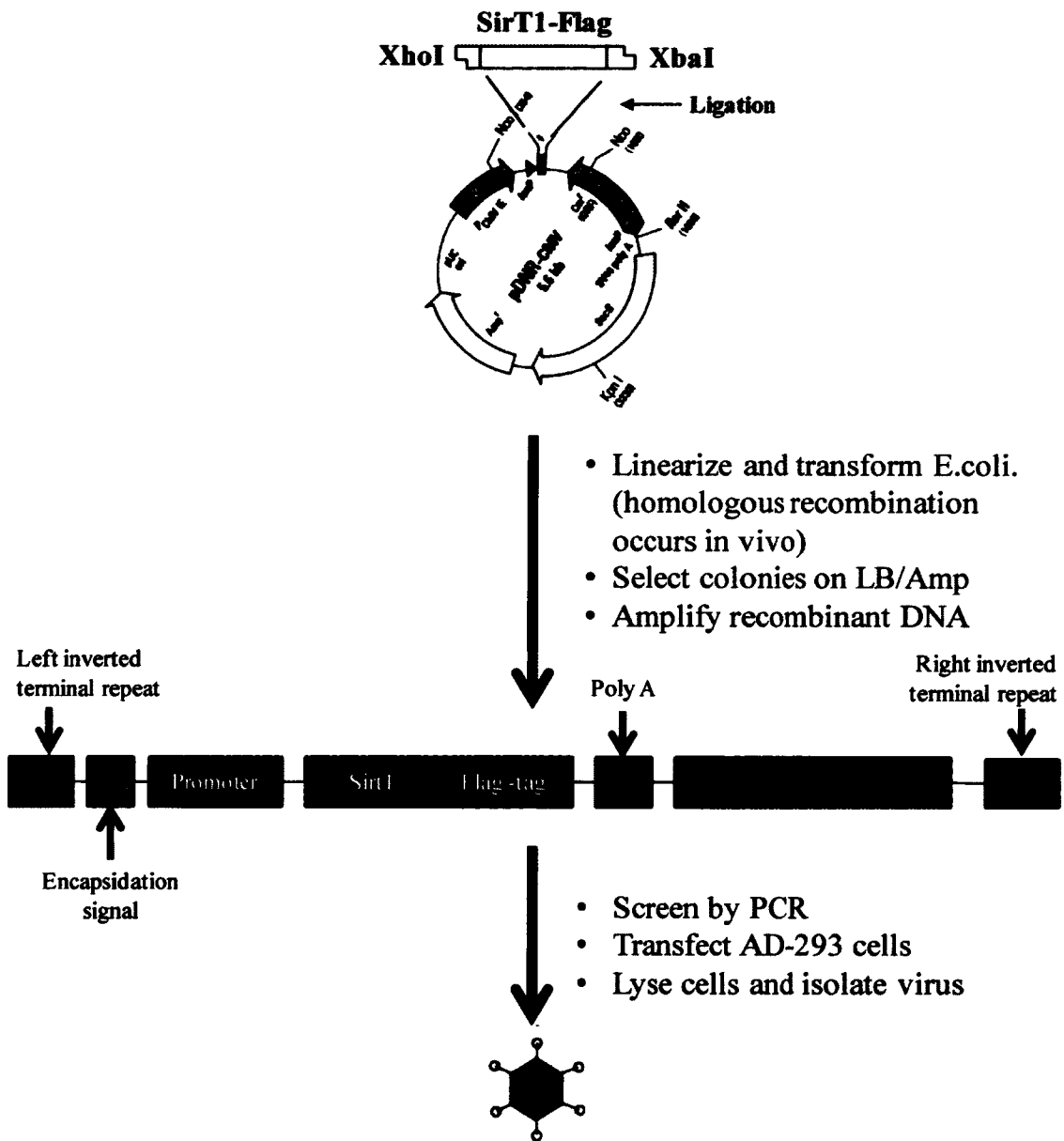


**Figure 6.** Schematic shows a summary of steps required for the creation of the SirT1-Flag (Flag-tagged) adenovirus. Also shown is the final version of the linearized recombinant adenoviral plasmid that was transfected into AD-293 cells to produce virus.

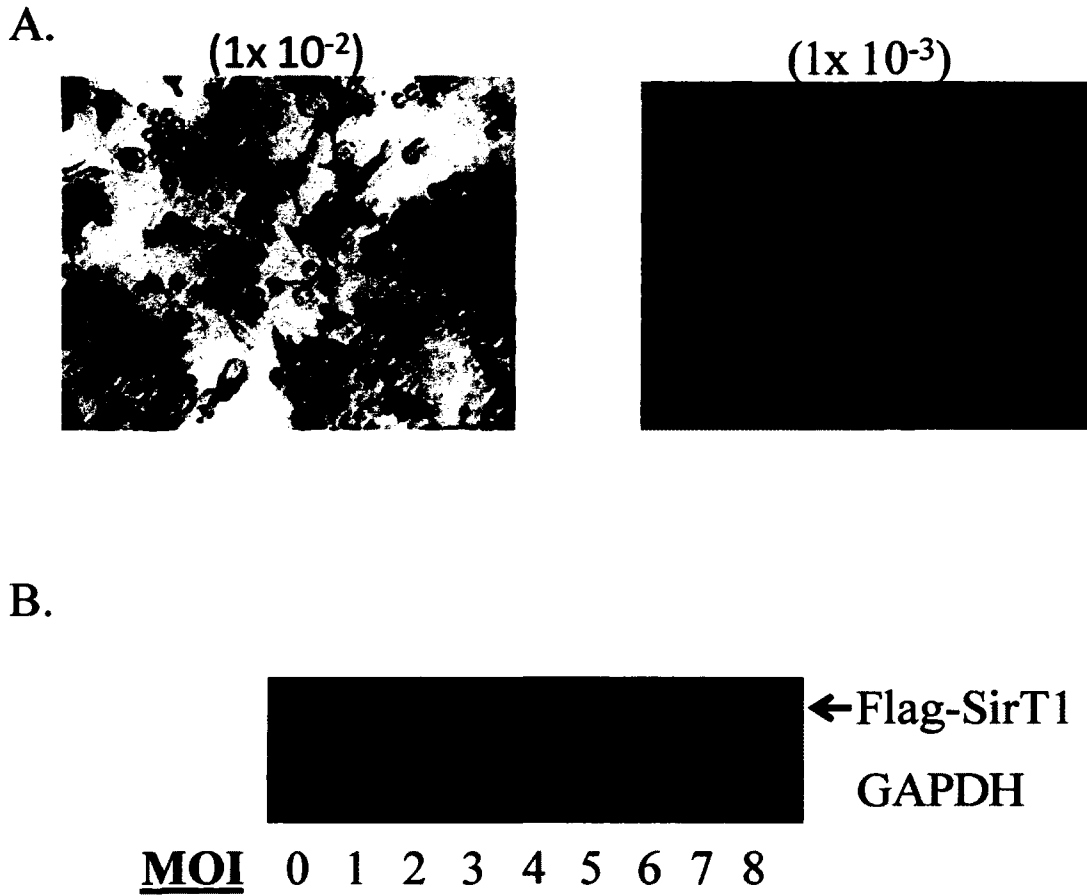


**Figure 7.** Bright field images (A) of SirT1-Flag adenovirus infected AD-293 cells that were immunohistochemically stained with an anti-hexon antibody with dilutions of  $1 \times 10^{-2}$  to  $1 \times 10^{-3}$  of the viral stock. (B) Immunoblot of Flag tagged SirT1 protein in C2C12 myotube extracts with different MOIs of infection using SirT1 adenovirus. No protein was detectable at these low MOIs.

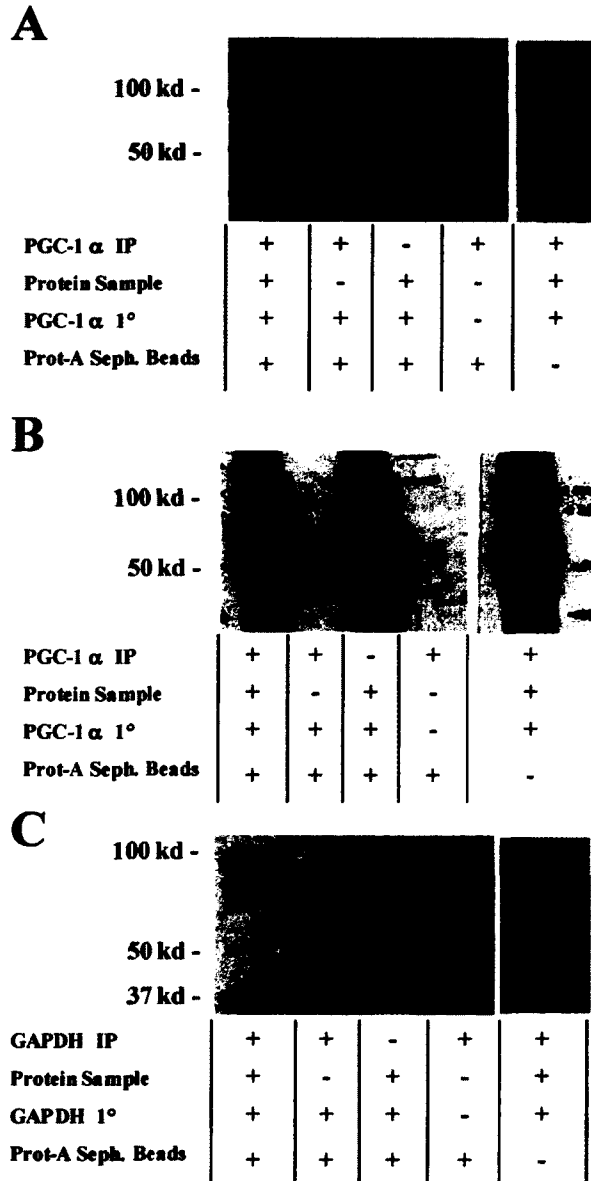
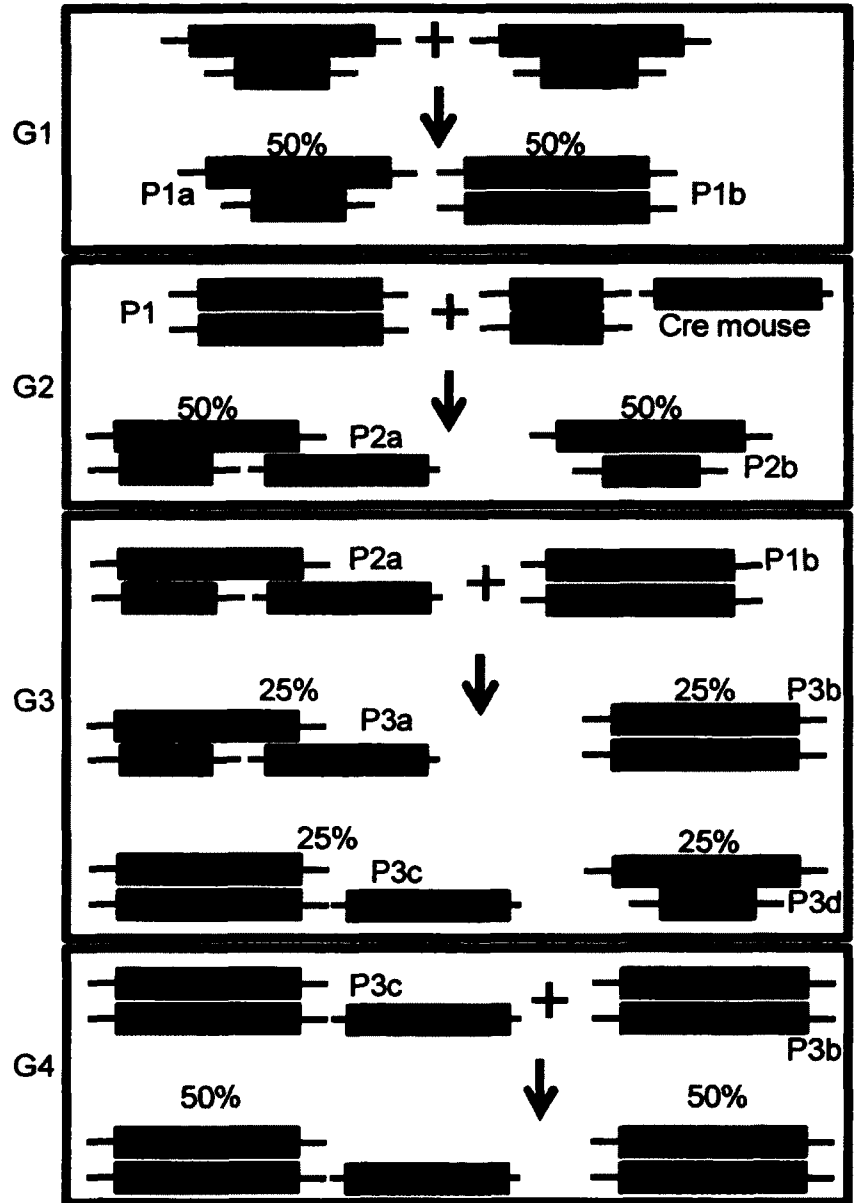


**Figure 8.** Development of immunoprecipitation protocol to examine PGC-1 $\alpha$  acetylation as a potential measure of SirT1 deacetylase activity. (A) Immunoblot of PGC-1 $\alpha$  (~105 kD) using the same antibody as was used for the immunoprecipitation (IP, PGC-1 $\alpha$ -Calbiochem; 1°, PGC-1 $\alpha$ -Calbiochem). PGC-1 $\alpha$  normally has an molecular weight of 105kD on an immunoblot. (B) Immunoblot of PGC-1 $\alpha$  using a different antibody than that of which was used for the immunoprecipitation (IP, PGC-1 $\alpha$ -Santa Cruz Biotechnologies; 1°, PGC-1 $\alpha$ -Calbiochem). (C) Immunoblot of GAPDH (~37 kD) using the same antibody as was used for the immunoprecipitation.

## **APPENDIX II: PROTOCOLS**

## BREEDING STRATEGY TO CREATE MUSCLE-SPECIFIC SIRT1-KO MICE

**Figure 1.** Breeding strategy for creating muscle-specific SirT1-KO mice. Alleles for either loxP or Cre genes are grouped by mouse in this schematic. Four generations of mice were required to create the Cre<sup>+</sup>-SirT1<sup>loxP/loxP</sup> mice and are labeled G1 to G4. Progeny (P1 to P3) from each generation were used for breeding in G2, G3 and G4. Mice received from Jackson Laboratory were heterozygous SirT1<sup>loxP/-</sup> animals however homozygous SirT1<sup>loxP/loxP</sup> mice are now available. If creating Cre<sup>+</sup>-SirT1<sup>loxP/loxP</sup> mice with homozygous SirT1<sup>loxP/loxP</sup> mice then start at generation 2 (G2).



### Breeding Regimen to Maintain SirT1-KO Mice:

SirT1<sup>tm1Ygu</sup> (sirtuin 1 (silent mating type information regulation 2, homolog) 1 (*S. cerevisiae*); targeted mutation 1, Yansong Gu) mice also known as SirT1<sup>co</sup> or SirT<sup>loxP</sup> mice were purchased from Jackson Laboratories. SirT1<sup>co/co</sup> (homozygous for SirT1

loxP) mice must breed with SirT1<sup>co/co</sup>/Cre<sup>+/-</sup> (homozygous for SirT1 loxP and heterozygous for Cre) mice to maintain Cre-recombinase heterozygosity. If SirT1<sup>co/co</sup>/Cre<sup>+/-</sup> mice breed with SirT1<sup>co/co</sup>/Cre<sup>+/-</sup> mice the resulting SirT1<sup>co/co</sup>/Cre<sup>+/+</sup> mice may lead to an increasing number of Cre gene alleles with future breeding. This would result in the elevation of Cre-recombinase expression in the skeletal muscle of future generations. Each generation of SirT1<sup>co/co</sup>/Cre<sup>+/-</sup> mice should only be compared to the same generation of SirT1<sup>co/co</sup> control mice in order to properly account for changes in genetic background with each generation.

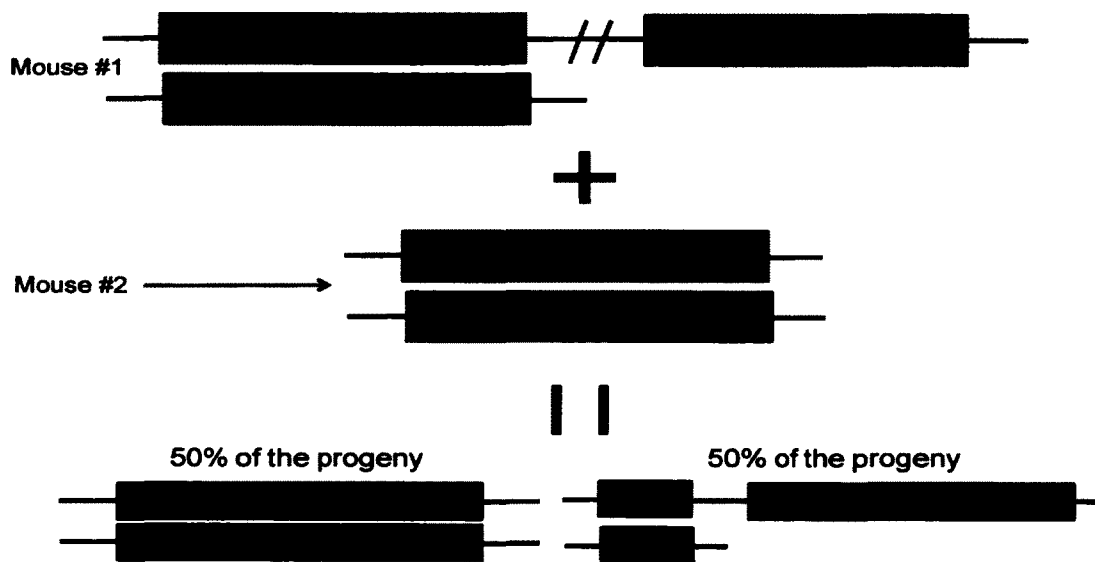


**Figure 2.** Schematic demonstrating the breeding regimen to obtain SirT1<sup>co/co</sup>/Cre<sup>+/-</sup> mice (muscle-specific SirT1-KO mice). This schematic demonstrates that within muscle tissue 50% of the progeny will contain SirT1 loxP genes while the other 50% will have no SirT1 as a result of loxP recombination.

## GENOTYPING MUSCLE-SPECIFIC SIRT1-KO MICE

**Background:** This protocol is designed to detect sequences in the murine genome that differ between wild-type and muscle-specific SirT1-Floxed animals using polymerase chain reaction amplification. PCR is a rapid, inexpensive and simple way of copying specific DNA fragments from minute quantities of source DNA material. There are basically 3 procedural steps involved in PCR:

1) **Denaturation:** DNA is heated to high temperature to separate the DNA double helix to single strands making them accessible to primers. During denaturation (94° C, 30sec), the DNA strands separate to form single strands.

2) **Annealing:** The reaction mixture is cooled down. Primers anneal to the complementary regions in the DNA template strands, and double strands are formed again between primers and complementary sequences. During annealing (60°C, 30sec) one primer binds to one DNA strand and another binds to the complementary strand. The annealing sites of the primers are chosen so that they will prime DNA synthesis in the region of interest during extension.

3) **Extension:** The DNA polymerase synthesizes a complementary strand. The enzyme reads the opposing strand sequence and extends the primers by adding nucleotides in the order in which they can pair. During extension (72°C, 45sec), DNA synthesis proceeds through the target region and for variable distances into the flanking region, giving rise to long fragments of variable lengths. The whole process is repeated over and over.

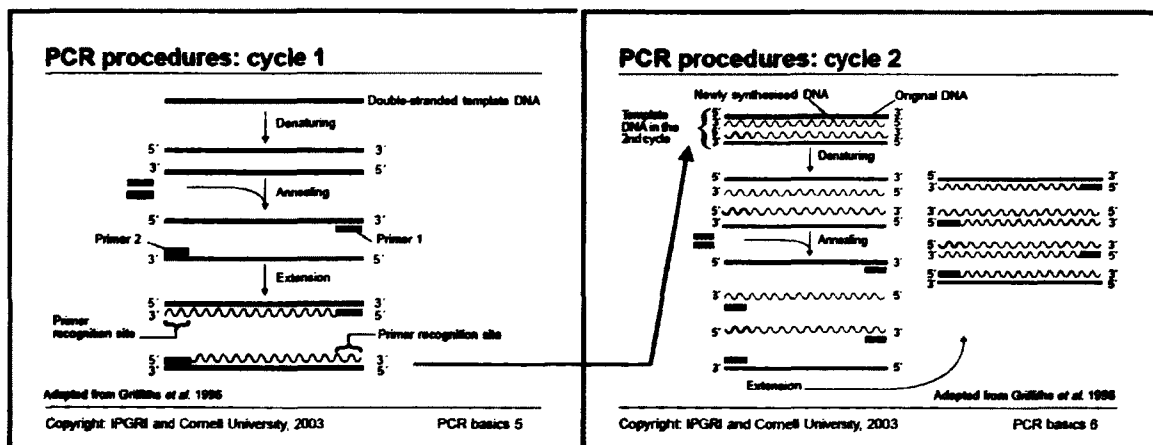


**Fig.1:** Schematic of basic PCR procedures.

The DNA polymerase, known as Taq polymerase, is named after the hot-spring bacterium *Thermus aquaticus* from which it was originally isolated. The enzyme can withstand the high temperature needed for DNA-strand separation. The cycle of heating and cooling is repeated over and over, stimulating the primers to bind to the original sequences and to newly synthesized sequences. The enzyme will continue to extend primer sequences. This cycling of temperatures results in copying and then copying of copies, leading to an exponential increase in the number of copies of specific sequences. Because the amount of DNA placed in the tube at the beginning is very small, almost all the DNA at the end of the reaction cycles are copied sequences.

The reaction products are then separated by gel electrophoresis and visualized with the use of ethidium bromide.

### **Reagents**

#### **Lysis Buffer (pH=8.0)**

10 mM Tris HCl (0.121g/100ml)

150 mM NaCl (0.8766g/100ml)

20 mM EDTA (0.744g/100ml)

Autoclave for 30min and store at room temperature.

#### **Super mix**

Sigma Jumpstart REDtaq Ready Mix PCR Reaction Mix (P0982)

Product contains 20 mM Tris-HCl, pH 8.3, 100mM KCl, 4 mM MgCl<sub>2</sub>, 0.002% gelatin, 0.4 mM each dNTP (dATP, dCTP, dGTP, TTP), inert dye, stabilizers, 0.06 unit/μl Taq DNA polymerase, JumpStart Taq antibody.

#### **Primers**

Forward and Reverse for KO and Floxed Stock Concentration 500 pmol/μl

Working Concentration of Primers (10X dilution): 50 pmol/ul

To make up 50 pmol/μl: use 5 μl of 500 pmol/μl stock and add 45μl of sterile water

#### **Proteinase K**

ProK- concentration of 1mg/ml

#### **Reagents for Agarose Gel Electrophoresis of PCR product**

Agarose

50XTAE

50 X TAE

242 g TRIS

1X TAE (dilute 50X TAE with stH<sub>2</sub>O)

500ml dH<sub>2</sub>O

10mg/ml EtBr

100ml 0.5M EDTA (pH 8.0)

Sterile water

57.1ml Glacial Acetic Acid

Make up to 1L and autoclave

### **DNA Extraction from ear clippings**

1. Make (**fresh**) 10:1 mixture of lysis buffer to ProK (@concentration of 1mg/ml-**fresh**)
2. Add 20 μl of this mixture to a 1.5 ml sterile eppendorf tube.
3. Obtain ear clipping from animal, add to tube and vortex (ensure ear clipping is immersed in solution).

4. Incubate in a 55 °C water bath (no higher than 60 °C) for 30min, vortexing every 15 minutes.
5. Add 180 µl sterile distilled water.
6. Place in boiling water for 5 minutes (use hot plate) and then vortex.
7. Store at -20°C, or use immediately for PCR

### **PCR method**

1. Make mastermix for each of the primers you will be using. Mastermix contains: 25 µl of Supermix sample
  - 1 µl of Forward Primer per sample
  - 1 µl of Reverse Primer per sample
  - Enough sterile distilled water for a volume per sample of 50 µl.
2. For each sample use 48 µl of master mix and 2 µl of template DNA extracted from procedure described above. Add 1 drop of mineral oil to each PCR tube to prevent evaporation of sample during cycling.
3. Cycling times:
 

Initial Denaturation	94°C	3min
35 cycles: Denaturation	94°C	30sec
Annealing	56°C	1min
Extension	72°C	1min
Final Extension	72°C	2min
Hold	4°C	

### **Running PCR product on gel**

1. Loading buffer is already included in Supermix.
2. Preparation of a 1.2% agarose gel. **For large gel system:** 3.6g Agarose, 6 ml 50X TAE and volume up to 300 ml with sterile H<sub>2</sub>O. Mix solution and note weight followed by boiling in microwave. Remove periodically to mix during boiling procedure in microwave. Upon complete dissolving of agarose and a homogenous and relatively clear agarose solution, weigh solution and replace lost amount of evaporated H<sub>2</sub>O. Add 25µl of EtBr (10mg/ml), slightly cool solution in room temperature (5-10min), then pour into caster.

**For small gel system:** 1.92g Agarose, 3.2 ml 50X TAE, and 156.8ml st H<sub>2</sub>O; follow same procedure as noted above. Only add 8 µl of EtBr (10mg/ml).

**Electrophoresis Running Buffer:** 1X TAE: 40 ml of 50X TAE made up to 2L with H<sub>2</sub>O.

3. Run 10 µl of PCR product reaction on either a small or large 1.2% agarose gel for 1hr @ approximately 90V.

### **Example of Experimental Setup/Procedure for PCR Genotyping (15 mice)**

1. Make up master mix for both KO- and Floxed-primers for the number of animals required for genotyping.
2. Forward Floxed Primer: oIMR7909F -GGTTGACTTAGGTCTTGTCTG  
Reverse Floxed Primer: oIMR7910R -CGTCCCTTGTAATGTTTCCC  
Forward KO Primer: oIMR7911WTF -AGGCGGATTTCTGAGTTCGA  
Reverse KO Primer: oIMR7912WTR -CGTCCCTTGTAATGTTTCCC

#### **Master mix (proportions)**

##### **A) Floxed Master mix**

25µl Super mix  
1µl Forward Floxed Primer  
1µl Reverse Floxed Primer  
23µl Sterile Water  
50µl Total

##### **B) KO Master mix**

25µl Super mix  
1µl Forward KO Primer  
1µl Reverse KO Primer  
23µl Sterile Water  
50µl Total

**X 17 reactions** (over estimate, since 15 animals required)

#### **Total Master mix**

##### **A) Floxed Master mix**

425µl Super mix  
17µl Forward Floxed Primer  
17µl Reverse Floxed Primer  
391µl Sterile Water  
850µl Total

##### **B) KO Master mix**

425µl Super mix  
17µl Forward KO Primer  
17µl Reverse KO Primer  
391µl Sterile Water  
850µl Total

1. Label PCR tubes with 1K and 1F to represent each animal and each master mix, respectively.
2. Place 48 µl of KO master mix in PCR tubes with K designation and 48 µl of Floxed master mix in PCR tubes with F designation.
3. Add 2µl of DNA template from animals into the appropriate PCR tubes i.e. DNA isolated from animal #1 into 1K and 1F.
4. Include negative controls using dH<sub>2</sub>O instead of DNA template with both KO and Floxed master mix i.e. 2 µl of dH<sub>2</sub>O into PCR tubes with 48 µl of Floxed master mix and 2 µl of dH<sub>2</sub>O into PCR tubes with 48 µl of KO master mix.
5. Add 1 drop of mineral oil to each tube and place tubes into thermocycler for 35 cycles. Use file # 29 on thermocycler for the initial 2 min denaturation then STOP this program. Use file # 30 for repeated cycles. Scroll through the settings in File # 29 and change the settings to achieve:

Denaturation 94°C 30sec  
 Annealing 56°C 1min  
 Extension 72 °C 1min

Then link this file (#29) to file #33 which is the final extension of 72°C for 2min. This will be followed by a hold cycle at 4°C. Samples can be left holding overnight if necessary.

6. Prepare either large gel or small gel or both depending on number of samples. Load PCR products onto gel and run for 1-1.5 hours.
7. Visualize PCR products using UV lightbox in the molecular core facility.

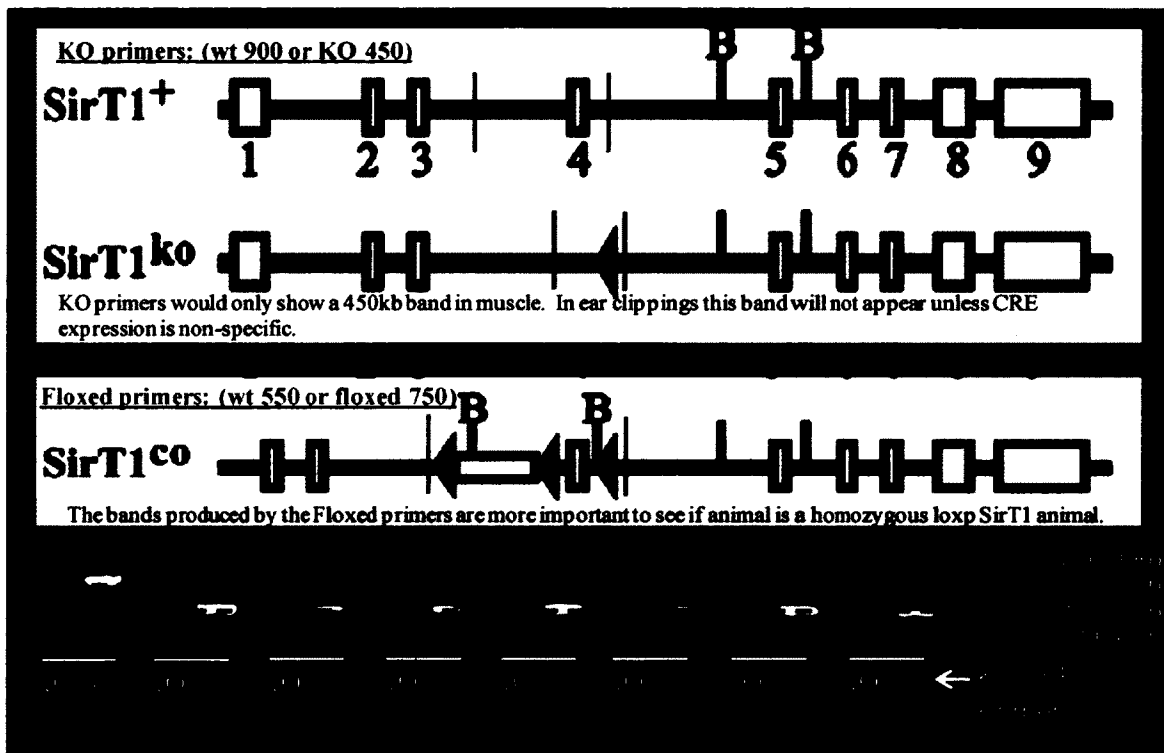


**Fig.2:** Typical agarose gel displaying PCR products and animal genotypes. KO primer will only show evidence of a KO (450kb band) if it is performed in the tissue that expresses CRE recombinase (muscle in the SirT1-KO animals). The KO primers therefore act as a control to examine the specificity of CRE expression. In this example of a gel there is 1 floxed, 3 WT, 4 heterozygotes and 0 KO animals (DNA taken from ear clippings) shown in gel image. Each animal is examined by the PCR product of the KO primers (first lane for each animal) and the Floxed primers (F1; second lane for each animal).

### **Genotyping for Cre-recombinase Mice**

Using the same PCR protocol we were able to assess which mice expressed Cre-recombinase x SirT1<sup>co/co</sup> (SirT1-KO mouse) versus those that just expressed SirT1<sup>co/co</sup>, which are defined as the control mice.

### **Example of Experimental Setup/Procedure for PCR Genotyping (15 mice)**

1. Make up master mix for Cre-primers for the number of animals required for genotyping.
2. Cre 5' Primer: ATGTCCAATTTACTGACCG  
Cre 3' Primer: CGCCGCATAACCAGTGAAAC  
BAND SIZE IS 300BP

#### **Master mix (proportions)**

##### **A) WT Master mix**

25µl Super mix

1µl Forward Primer Cre-recombinase

1µl Reverse Primer Cre-recombinase

23µl Sterile Water

50µl Total

**X 17 reactions** (over estimate, since 15 animals required)

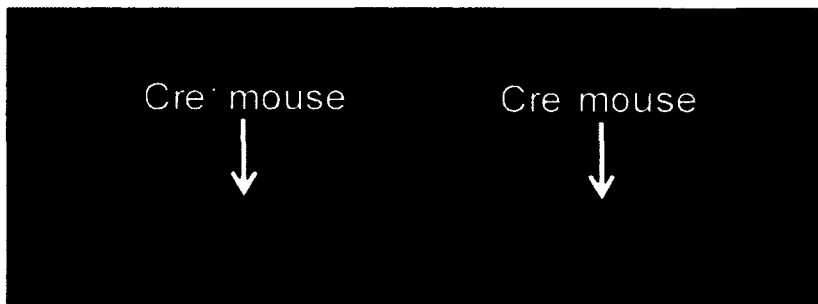


Fig. 3. Typical agarose gel displaying the PCR product for Cre recombinase primers. Mice that are positive for Cre-recombinase have one band at ~400bp. Mice that are negative for Cre-recombinase have no band.

## **IMMUNOFLUORESCENCE EXPERIMENTS WITH C2C12 MYOTUBES**

Grow cells on coverslips to 70% confluence in 6-well dishes using 1 coverslip/dish. Coverslips should be dipped in 70% ethanol (with sterile tweezers) and dried in a covered culture dish under the UV lamp **24 hours before**.

**\*\*\*\*All following steps can be performed outside the hood\*\*\*\***

- 1) Remove the media from the culture dish and wash the plate 2X with 3 mls PBS.
- 2) Fix the cells with 3mls of fixing solution for 7 minutes at room temperature (RT).
- 3) Transfer the coverslips to 65mm culture dishes using tweezers and wash the coverslips 3 X 5 minutes with 3 mls PBS using a rotator at RT.
- 4) Remove the PBS and permeabilize the coverslips in permeabilizing solution for 5 minutes at 4°C.
- 5) Wash the coverslips 3 X 5 minutes with 3 mls PBS at RT.
- 6) Remove the PBS and block with 3 mls of blocking buffer for 1 hour at RT on a rotator.
- 7) Incubate the coverslips overnight with the 1<sup>o</sup> antibody dissolved in blocking buffer at 4°C. The antibody solution is placed onto a glass plate covered in parafilm and the coverslips are placed face down onto the solution. Use 250-400 µl of the antibody solution per coverslip.
- 8) Remove the coverslips from the antibody solution and place back into culture dishes and wash 3 X 5 minutes with 3 mls PBS at RT.

**\*\*\*\*ALL FOLLOWING STEPS ARE CARRIED OUT IN THE DARK\*\*\*\***

- 9) Incubate the coverslips with the appropriate 2<sup>o</sup> antibody for 1 hour at RT. The coverslips are placed face up onto a glass plate covered in parafilm and the antibody solution is placed onto the coverslips.
- 10) Pick up one coverslip using tweezers and remove any excess antibody by dipping the coverslip into PBS 3X.
- 11) Carefully remove any excess blocking buffer from the coverslip by dabbing the corners with a kimwipe.
- 12) Immediately place the coverslip face down onto a microscope slide using ~100-150µl of the anti-bleaching/mounting medium – **it is important to perform steps 12, 13, and 14 for one coverslip at a time to avoid drying of the coverslip.**
- 13) Wait a few minutes (~2-5) for the mounting medium and the coverslip to adhere properly.
- 14) Seal the coverslip to the slide using nailpolish around the edges of the coverslip.

- 15) Transfer the slides from the dark room to the confocal microscope in a black bag to avoid any exposure to light.
- 16) Slides that are stored at 4°C in a small box and then placed into a black bag can be viewed for a few months.

## **SOLUTIONS**

**Fixing Reagent** – \*\*\*\*must be made fresh the day of the experiment\*\*\*\*

**For 20 mls:**

- 3% Paraformaldehyde - 0.6g
- 2% Sucrose - 0.4g
- dissolve into 20 mls of PBS;
- add 7 drops of 0.01M NaOH;
- heat tube to 70°C (The paraformaldehyde will slowly dissolve - takes about 1 hour);
- cool the solution to room temperature and check pH=7.4.

**Blocking buffer**

**For 50mls:**

- 10% goat serum (GIBCO #16210-064) – 5 mls
- 2% BSA (Sigma A-2153) – 1g
- 10mM HEPES pH=7.4 – 0.5mls of 1M stock
- 1mM CaCl<sub>2</sub> – 5.5mg
- 1mM MgCl<sub>2</sub> – 4.8mg
- dissolve into Hanks buffered saline solution;
- store at 4°C;
- good for about 2 weeks.

**Anti-bleaching/mounting reagent**

**For 10mls:**

- 2.5% DABCO (Sigma D-2522) – 250mg (in fridge)
- 10% Polyvinyl alcohol (Sigma P-8136) – 1g
- 5% Glycerol – 1ml of 50% stock
- 25mM Tris (pH=9.0) – 250µl of 1M stock solution
- dissolve into 10 mls of ddH<sub>2</sub>O;
- microwave for 10 seconds ONLY, shake to dissolve. Repeat if necessary;
- store at 4°C in a tube wrapped in foil;
- solution is good for 7-10 days.

### **Permeabilizing Solution**

#### **For 100mls:**

0.1% Triton X-100           – 0.1mls  
200mM Sucrose             – 6.9g  
50mM Tris-HCl (pH 7.4) – 5mls  
5mM MgCl<sub>2</sub>                 – 48mg

- dissolve into ddH<sub>2</sub>O;
- store at 4°C;
- solution is good for a few weeks.

## MITOCHONDRIAL ISOLATION PROCEDURE FROM SKELETAL MUSCLE

REFERENCES: Krieger et al., J. Appl. Physiol. **48**: 23-28, 1980  
Cogswell et al. Am. J. Physiol. **264**: C383-C389, 1993

### SOLUTIONS:

1. Buffer 1: pH 7.4 (store at 0-4°C)

100 mM KCl	1.862 g / 250 mL
5 mM MgSO <sub>4</sub>	0.15 g / 250 mL
5 mM EDTA	0.465 g / 250 mL
50 mM Tris-HCl	1.97 g / 250 mL

2. Buffer 1 + ATP: pH 7.4 (store at 0-4°C)

Buffer 1 + 1 mM ATP	0.151 g / 250 mL
---------------------	------------------

3. Buffer 2: pH 7.4 (store at 0-4°C)

100 mM KCl	3.725 g / 500 mL
5 mM MgSO <sub>4</sub>	0.30 g / 500 mL
5 mM EGTA	0.951 g / 500 mL
1 mM ATP	0.3025 g / 500 mL
50 mM Tris-HCl	3.94 g / 500 mL

4. Resuspension Medium: pH 7.4 (store at 0-4°C)

10 mM HEPES	0.2383 g / 100 mL
0.25 M sucrose	8.56 g / 100 mL
10 mM Na succinate	0.2701 g / 100 mL
2.5 mM K <sub>2</sub> HPO <sub>4</sub>	0.0435 g / 100 mL
0.21 mM ADP	0.009 g / 100 mL
1 mM DTT	0.0154 g / 100 ml

5. Nagarse: (\*\* make fresh daily\*\*)  
concentration = 10 mg/mL in Buffer 2  
use : 0.025 ml Nagarse/g tissue

### ISOLATION PROCEDURE:

This final isolation procedure has been determined to be an optimal method for the isolation of pure and intact IMF and SS mitochondria through differential centrifugation. The entire procedure is done at 4°C (everything to be kept on ice).

- 1:** Set out materials (get 2 buckets of ice and put centrifuge tubes, scissors, watchglass, forceps, and four beakers with 10-20 ml of Buffer 1 on ice).
- 2:** Remove the muscle sample from the rat, and put it immediately in a beaker containing 10-20 ml Buffer 1 (no ATP), on ice. Repeat this for 3 subsequent rinse steps using Buffer 1.
- 3:** Quickly blot the excess Buffer 1 from the muscle tissue on gauze and trim away fat or connective tissue. Place it on a watchglass that is also on ice. Proceed to thoroughly mince the complete muscle sample with forceps and scissors, until the tissue is well mixed and no large pieces are remaining.
- 4:** For each centrifuge tube, take between 1.0 g and 1.5 g of the minced tissue and record the exact weight. Place the sample in a capped 50 ml plastic centrifuge tube (on ice).

---Repeat this step for each sample---

- 5:** Add a 10-fold dilution of Buffer 1 + ATP to each tube.

(tissue weight \* 10 -tissue weight= ml of solution to add for a 10-fold dilution).

- 6:** Homogenize the samples using the Ultra-Turrax polytron (7mm probe) with 40% power output and 10 second exposure time. During the time the samples are being polytroned, move the plastic tube vigorously in a circular motion. Shaft can be rinsed with 0.5 mL of buffer 1 + ATP to help minimize loss.
- 7:** At a centrifuge setting of 800 g, with Beckman JA25.50 rotor, spin homogenate samples for 10 min. This is the step that divides the IMF and SS mitochondrial fractions. The supernate will contain the SS mitochondria and the pellet will contain the IMF mitochondria. To differentiate between the two fractions, the SS fraction will be labelled with step numbers ending in "-SS" and the IMF fraction will be labelled with step numbers ending in "-IMF".

**SS mitochondrial isolation:**

- 8-SS:** Filter the supernate through a single layer of cheesecloth into a second set of 50 ml plastic centrifuge tubes.
- 9-SS:** Spin tubes at 9000 g for 10 minutes. Upon completion of the spin discard the supernate and gently resuspend the pellet using a 1000  $\mu$ l pipette in 3.5 ml of Buffer 1 + ATP. This is called the "wash step". Since the mitochondria are easily damaged, it is important that the resuspension of the pellet is done carefully. Cytosol can be isolated from the supernate by spinning for 60 min. at 100 000 g (Takahashi et.al. *Am. J. Physiol.* 274 (Cell Physiol. 43): C1380-1387, 1998.).
- 10-SS:** Repeat the centrifugation of the previous step (9000 g for 10 minutes) and discard the supernate.
- 11-SS:** Resuspend the pellet in a small volume of Resuspension Medium. The volume of medium to use depends on the amount of SS pellet isolated, however, an approximate volume would be 0.4 ml. This resuspension is done using a 1000  $\mu$ l pipette, being gentle so as to prevent damage to the SS mitochondria. Some extra time is needed during this final resuspension to ensure the SS pellet is completely resuspended.
- 12-SS:** Measure and record the final volume of the resuspended SS mitochondrial sample, and store in labelled eppendorf tubes. Labels should include sample identification, isolation date and final volume. Keep the samples on ice while proceeding to isolate the IMF fraction.

**IMF mitochondrial isolation :**

- 8-IMF:** Gently resuspend the pellet (from step 9) in at least a 10 fold dilution of Buffer 1 + ATP using a Teflon pestle.
- 9-IMF:** Using an Ultra-Turrax polytron set at 40 % power output, polytron the resuspended pellet for 10 seconds. Rinse the shaft with 0.5 ml of Buffer 1 + ATP to help minimize sample loss.
- 10-IMF:** Spin at 800 g for 10 minutes and discard the resulting supernate.

- 11-IMF:** Resuspend the pellet in a 10-fold dilution (this is the minimum volume) of Buffer 2 using a Teflon pestle.
- 12-IMF:** Add the appropriate amount of nagarse. The calculation for the appropriate volume is 0.025 mL / g of tissue. Mix gently let stand exactly 5 minutes. The protease nagarse, serves to release the IMF mitochondria from the myofibrils.
- 13-IMF:** Dilute the nagarse by adding 20 ml of Buffer 2
- 14-IMF:** Spin the diluted samples at 5000 g for 5 minutes and discard the resulting supernate.
- 15-IMF:** Resuspend the pellet in Buffer 2 (again a 10-fold dilution). Gentle resuspension is with a Teflon pestle.
- 16-IMF:** Spin the samples at 800 g for 10 minutes. This spin allows the IMF mitochondria to remain in the supernate. This time, upon the completion of the spin, the supernate is poured into another set of 50 ml plastic tubes (on ice), and the pellet is discarded.
- 17-IMF:** Spin the supernate at 9000 g for 10 minutes. The supernate is discarded and the pellet is resuspended in 3.5 ml of Buffer 2 using a 1000  $\mu$ l pipette. This is the "wash step" for the IMF mitochondria.
- 18-IMF:** Spin samples at 9000 g for 10 minutes and discard the supernate.
- 19-IMF:** Resuspend the pellet in a small volume Resuspension Medium. As with the SS mitochondrial pellet, the volume depends on the size of the resulting pellet, however, an approximate volume is 0.45 ml of Resuspension Medium. Gently resuspend the pellet using a 1000  $\mu$ l pipette.
- 20-IMF:** Using a 1000  $\mu$ l pipette, measure and record the final volume of the resuspended IMF sample and store in labelled eppendorf tubes. Labels should include identification of the sample, the isolation date and the final volume.

## MITOCHONDRIAL RESPIRATION

(Muscle) Estabrook, R.W., Meth. Enzymol., **10**: 41-47 (1967)

### THEORY:

The rate of mitochondrial respiration is an important consideration in the biochemical analysis of mitochondria. There are three phases of interest in analyzing the respiratory ability of mitochondria. Mitochondria produce ATP in the presence of oxygen. The respiratory ability of the freshly isolated IMF and SS mitochondrial fractions and the homogenates can be illustrated by measuring the rate of oxygen consumption using a Clark oxygen electrode in the presence of a) the substrate alone (e.g. glutamate for state 4 or resting respiration); b) ADP, (state 3 or active respiration); and c)  $\text{NADH}^+$ , which is used to measure the amount of damage that has occurred to the mitochondria, since the inner membrane is impermeable to  $\text{NADH}^+$ .

### SOLUTIONS:

#### $\text{VO}_2$ Buffer for muscle mitochondria:

250 mM Sucrose (FW=342.30)	42.8 g/500 ml
50 mM KCl (FW=74.55)	1.86 g/500ml
25 mM Tris-HCl *	1.97 g/500ml
10 mM $\text{K}_2\text{HPO}_4$ (FW=174.18)	0.871 g/500ml

\* In place of 25mM Tris-HCl you can use 25 mM Tris (aka Tris (hydroxymethyl) methylamine). This works out to 1.5125 g/500ml (FW=121.4). Using Tris in place of Tris-HCl means that you will have to add more HCl to get the pH down to 7.4.

#### Substrates for Muscle (Assume 2.25 ml total vol.):

1. **Glutamate** - final conc. of 11.1 mM.....**2.0 M initial conc.** (406.4 mg/ml)
2. **ADP** (FW = 427.2 g/mol) - Final conc. of 0.44 mM for muscle, 0.88 mM for heart..... **20 mM initial conc.** (8.54 mg/ml)
3. **NADH** (FW = 709.4 g/mol). Final conc.: 2.8 mM.....**0.5 M initial conc.** ( 354.7 mg/ml)

## **PROCEDURE:**

1. Set water bath at 30°C -- clean out chambers (Strathkelvin instruments oxygen meter model 782 and mitocell MT200) and stir bars.
2. Add 2.0 ml of VO<sub>2</sub> Buffer to each chamber.
3. Insert electrode # 2 into the chamber.
4. Remove all bubbles in the chamber and allow it to reach equilibrium temperature (30°C) while spinning.
5. Set monitor and recorder to 100 %.
6. Remove electrode. Put in the volume of mitochondria as follows:
  - a. Muscle (SS): 0.3 ml (approximately 1-1.5 mg protein by Lowry assay).
  - b. Muscle (IMF): 0.2 ml (approximately 1-1.5 mg protein by Lowry assay).
7. Allow a steady state to be reached.
8. Add 12.5 µl glutamate (muscle).
9. Wait approximately 3 minutes then add ADP: 50 µl for muscle, 100 µl for heart.
10. Wait (about 2-3 minutes) for a steady rate of state 3 respiration before adding 12.5 µl of NADH. Prepare the next chamber while the respiration recordings are being made.
11. Clean out the chamber in the following manner: Remove the electrode and aspirate, remove the magnetic stir bar and aspirate, and finally, clean the electrode by rinsing with distilled water and pat dry.
12. Put electrode in the next chamber (which should already have the buffer and sample in it).
13. Prepare the next chamber while the measuring the respiration of the current chamber (i.e. add 2 ml of VO<sub>2</sub> Buffer and allow to equilibrate).
14. Calculate the state 4, state 3 and NADH<sup>+</sup> rates for each sample. (slope=rate)
15. Calculate the rates of state 3 and state 4 respiration per mg of mitochondrial protein by dividing the state 3 and 4 rates by the amount of protein (mg) added to the VO<sub>2</sub> Buffer.

Calculate the Respiratory Control Ratio (RCR) :

$$\text{RCR} = \text{state 3 rate} / \text{state 4 rate}$$

Calculate the % of intact mitochondria :

$$\% \text{ intact} = \text{RCR} / (\text{NADH}^+ \text{ rate} / \text{state 4 rate}) \times 100$$

For the above ratios you need only use slopes from the graph. However, for exact calculations of the state 3 and state 4 rates follow the method below:

References: Biological Oxygen Monitor Instruction Manual (table 1, p.13).

Chappel, J.B. Biochem. J. (1964) 90:225-237

- Assume a barometric pressure of 1 atm. (760 mmHg). At 1 atm. the amount of oxygen dissolved in medium equals 5.47  $\mu\text{l O}_2/\text{ml}$  (value taken from Biological Oxygen Monitor Instruction Manual). Since 2 ml are being used in the chamber, total  $\text{O}_2$  is equal to  $2 \times 5.47 = 10.94 \mu\text{l}$ . The rate of change from 100%  $\text{O}_2$  can then be used to calculate the amount of  $\text{O}_2$  consumed per unit time:

$$\frac{\text{State 3 or 4} / \text{mg protein} \times 10.94 \mu\text{l O}_2}{100\%}$$

- But the units of  $\text{O}_2$  consumed are now typically expressed in units of natoms  $\text{O}_2$ . Thus,

$$\underline{\text{State 3 or 4} / \text{mg prot.} \times 968 \text{ natoms O}_2} = x \text{ natoms O}_2/\text{mg}$$

## ASSESSMENT OF ROS PRODUCTION FROM ISOLATED MITOCHONDRIA

**Background:** Mitochondria are the primary source of reactive oxygen species (ROS) to the cell. It is estimated that about 2% of total cellular oxygen is converted ROS by the inappropriate reduction of molecular oxygen by intermediate members of the electron transport chain (ETC). ROS are damaging molecules that are capable of compromising the integrity of macromolecules within the mitochondria and may lead to overall organelle dysfunction. In particular, mtDNA may be prone to attack by ROS because 1) mtDNA is located in close proximity to the ETC, 2) mtDNA lacks the protective sheath of histones compared to nuclear DNA and, 3) mitochondria have an insufficient repair system for mtDNA mutations. ROS can exist in a variety of molecular permutations such as superoxide ( $O_2^-$ ), hydroxyl radical ( $OH^\cdot$ ) and hydrogen peroxide ( $H_2O_2$ ).

DCF (2,7-dichloro-fluorescein; Fig.1) is a reagent that is non-fluorescent until the acetate groups are removed by intracellular esterases and oxidation occurs within the mitochondria (Fig.1). DCF is oxidized by all of the different forms of ROS and this can be detected by monitoring the increase in fluorescence with a fluorometric plate reader. The appropriate plate reader filter settings for fluorescein are the following: **Excitation 485/20** and **Emission 528/20** (Fig.2).

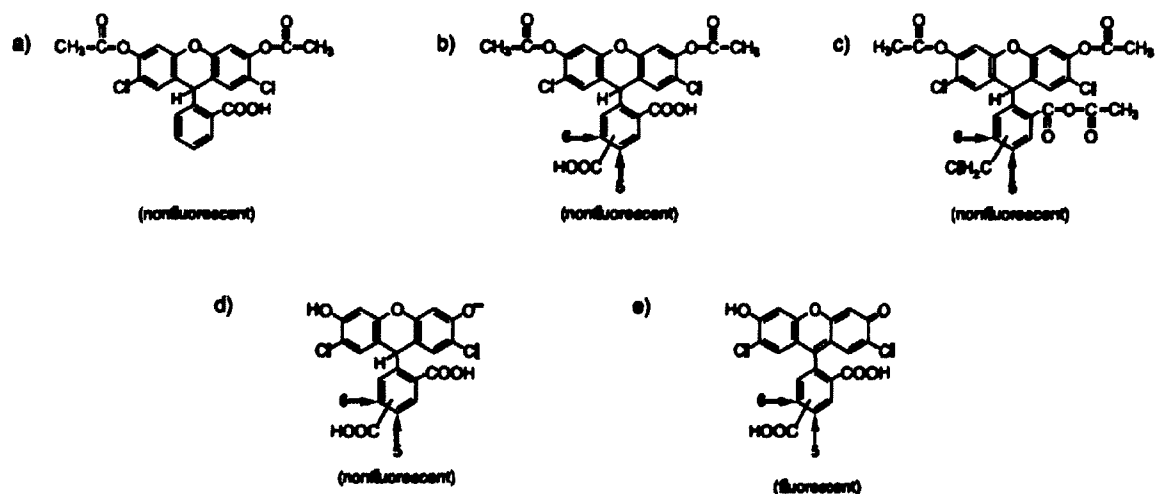


Fig.1-DCF molecule and oxidation of DCF resulting in fluorescence

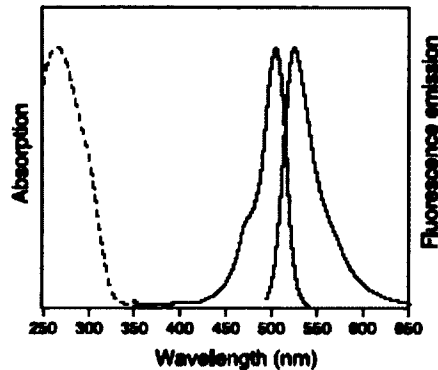


Fig.2-Absorption spectrum of reduced dye (---) and absorption/emission spectra of oxidized dye (—).

**KC4 Software Settings:** The Settings icon in the upper left corner allows the alteration of various parameters. Once clicked, another window appears, click on the Wizard Icon. In this window there will be a variety of components that can be altered. The following are the parameters that need to be changed in order to utilize the DCF and measure time-dependent ROS production from isolated mitochondria:

- 1) Top Middle Panel- Absorbance, Fluorescence, Luminescence- choose **Fluorescence**
- 2) Top Left Panel- End Point, Kinetic, Spectrum- choose **Kinetic**
- 3) Top Middle Panel- Click on larger box labeled Kinetic to set parameters- **Run Time 1:20:00, Interval 5:00 (takes a measure every 5 minutes)**, click on box labeled **Allow Well Zoom during Read**, and also click on box labeled **Individual Well Auto Scaling**- The Well Zoom and Auto scaling allows for monitoring each individual well during the experiment and scales it appropriately.
- 4) Middle Panel-**Filter Set**- Choose #1, then set the **excitation to 485/20**, and **emission to 528/20** as described above. The optics position should be set to the **TOP** (i.e. readings are taken from the top of the well) and the sensitivity is set at **50** (depending upon the amount and/or nature of the sample).
- 5) Plate-Type-choose **96-well plate**, choose which wells are to be read i.e. **A1-C12**.
- 6) Shaking-**Intensity** set at **1**, **Duration** set at **15s** and then click the box that is labeled **before every reading** (it shakes the samples for 15 s before every reading).

7) Temperature Control- Click on the box indicating **YES** , also click on box labeled pre-heating, and put 37°C into the temperature box.

### **DCF Reagent and VO<sub>2</sub> Buffer**

DCF (2,7,-dichlorodihydrofluorescein diacetate) reagent MW=487.29 (Molecular Probes D-399/ 100mg)

**1°STOCK-** Make up **50mM** Stock Solution in EtOH- 24 mg/ml- only make about 500µl i.e. 14 mg per 500µl EtOH. Wrap stock solution in aluminum foil and limit exposure to light since DCF is light-sensitive.

**Working Stock Solution- 2° STOCK-** Dilute 50mM by 100-fold by taking 10µl and adding 990 µl of EtOH to attain a **500uM DCF Stock Solution**. This will be the DCF concentration used to add to the reaction mixture.

VO<sub>2</sub> Buffer- refer to mitochondrial respiration protocol

### **Procedure**

1. SS and IMF mitochondria are isolated as described in the mitochondrial isolation protocol. Alternatively, frozen mitochondrial extracts can also be used.
2. Determine the volume necessary for 50µg of mitochondria. Typical volumes should range between 5-40µl depending upon concentration of mitochondrial extracts.
3. Final concentration of DCF is 50µM. The total volume of the reaction mixture is 250µl. Thus, 25ul of DCF is used in the reaction mixture since this represents a 10-fold dilution. Set up table (*as shown below*) and determine the amount of VO<sub>2</sub> buffer necessary to make each of the reaction mixtures equal to 250 µl. (Remember to include a *control* with only VO<sub>2</sub> buffer and DCF reagent as in Well #1 shown below)

	SS			
	Control	Mar.23	Mar.25	Mar.29
	Well #1	Well #2	Well #3	Well #4
$\mu\text{g}$ mito	0	50	50	50
$\mu\text{l}$ mito	0.00	11.77	9.80	17.24
VO <sub>2</sub> Buff	225.00	213.23	215.20	207.76
DCF (50 $\mu\text{M}$ )	25	25	25	25
Total Volume	250	250	250	250

4. Once table is complete and volumes for all samples have been determined, place the frozen (already thawed) or fresh mitochondria, VO<sub>2</sub> buffer and DCF (500 $\mu\text{M}$ ) into a 37°C circulating water bath for 5-10 min.
5. Pipette the volume of VO<sub>2</sub> buffer required for each of the samples followed by the mitochondrial samples into the appropriate wells of a 96-well plate. In addition, include a well (usually in the corner well) with only 250  $\mu\text{l}$  of VO<sub>2</sub> buffer to monitor temperature (see below). Place the 96-well plate with the VO<sub>2</sub> buffer and mitochondria into a 37°C incubator. Using the YSI temperature probe, place the recording electrode into the well with buffer only and monitor the temperature until 37°C is reached. During this time, be sure that the KC4 software is set up and that the Biotek plate reader is pre-heating to 37°C.
6. Once mitochondria and buffer have reached temperature (37°C), take the DCF out of the circulating water bath (37°C) and quickly add the DCF to each of the reaction mixtures. Following addition of DCF, promptly place the plate into the Biotek plate reader for fluorescence measurement and start the KC4 program by pressing **READ** plate on the upper left portion of the computer screen. Kinetic program will operate for 1 h and 20 min.

## SIRT1 ACTIVITY ASSAY

Using SIRT 1 fluorimetric Drug Discovery Kit – AK 555 – BIOMOL

### THEORY

Tissue or cell extracts containing SIRT1 are added to the Fluor de Lys–SIRT1 and  $\text{NAD}^+$  substrates. The fluorophore is sensitized during the reaction, and it emits light in presence of Developer II when excited at 360 nm. Fluorescence is detected at 460 nm and is proportional to SIRT1 activity.

### REAGENTS

- Fluor de Lys–SIRT1, Deacetylase Substrate 5 mM (K1–177)
- Fluor de Lys Developer II Concentrate (5x) (K1–176)
- $\text{NAD}^+$  50mM (K1–282)
- Nicotinamide (NAM) (Sigma; N3376 – 100g)
- Trichostatin A (TSA) (GR–309) 1 mg dissolved in DMSO to 2 mM
- Assay buffer (K1–286)

### PREPARING REAGENTS FOR ASSAY

- Dilute  $\text{NAD}^+$  to 0.5 mM in Assay Buffer, and keep stock at  $-20^\circ\text{C}$  until used.
- Dilute Fluor de Lys–SIRT1 substrate to 0.5 mM in assay buffer, volume sufficient for 2 (n+1) samples.
- Weigh 12.21 mg and 30.52 mg of Nicotinamide (NAM) and resuspend in 1 ml Assay buffer to get concentrations of 100 and 250 mM.
- Dilute Trichostatin A in Assay buffer to 100  $\mu\text{M}$  (35 $\mu\text{l}$  TSA 2mM + 475  $\mu\text{l}$  Assay buffer).

### PROCEDURE

Prepare substrates mix according the number of samples to assay:

For 25 $\mu\text{l}$ :	10 $\mu\text{l}$ Fluor de Lys–SIRT1 0.5 mM	} 2 x (n+1)
	10 $\mu\text{l}$ $\text{NAD}^+$ 0.5 mM	
	5 $\mu\text{l}$ of Assay buffer	

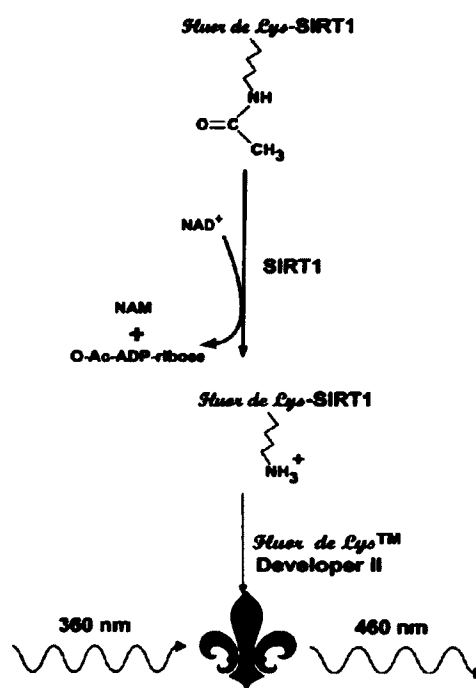


Figure 1. Reaction Scheme of the SIRT1 Fluorescent Activity Assay.  $\text{NAD}^+$ -dependent deacetylation of the substrate by recombinant human SIRT1 sensitizes it to Developer II, which then generates a fluorophore (symbol). The fluorophore is excited with 360 nm light and the emitted light (460 nm) is detected on a fluorometric plate reader.  $\text{NAD}^+$  is consumed in the reaction to produce nicotinamide (NAM) and O-acetyl-ADP-ribose.

In white microplate: add solutions according to the following table

	Extracts	Assay Buffer	Nicotinamide 250 mM
Blank	-	25 µl	-
Sample 1	25 µg to 100 µg prot	Volume up to 25 µl	0
Sample + NAM	25 µg to 100 µg prot	Volume up to 15 µl	10 µl

Activity of each sample has to be measured with and without NAM. Take white microplate and add first the assay buffer, NAM if required and the sample. Mix by pipetting.

Incubate the plate and substrate mix at 37°C and monitor temperature with probe in a well containing assay buffer. When the temperature reaches 37°C, add 25 µl of the substrates mix in each well and mix by pipetting. Incubate 30 minutes at 37°C.

During this time, prepare Developer mix for 2x [n+1 tubes]

For 50 µl:	Developer 5 x - 10 µl	final concentration	1x
	NAM 100 mM - 5 µl		10 mM
	TSA 100 µM - 5 µl		10 µM
	Assay Buffer - 30 µl		

When the incubation is done, add 50 µl of Developer mix in each well, mix by pipetting. Monitor fluorescence kinetics at 360 nm (excitation) and 460 nm (emission) at 37°C for 1 hour with measures every 5 minutes.

### CALCULATIONS

$$\text{SIRT 1 activity} = \frac{[\text{fluorescence @ 1h - blk}] - [\text{fluorescence + NAM @ 1h - blk}]}{(30\text{minutes}) \times (\mu\text{g protein})}$$

$$= \text{SIRT1 activity (AFU/min mg protein)}$$

For cells, use common cells extracts

For tissues, make a 10-fold extract in extraction buffer or Sakamoto buffer with only one spin.

## CYTOCHROME C OXIDASE ASSAY FOR MICROPLATE READER

*J. Biol. Chem.* 189:665, 1951,  
*Meth. Biochem. Anal.* 2:427, 1955,  
*Meth. Enzymol.* 10:245, 1967.

### THEORY:

Tissue extract containing cytochrome c oxidase is added to the test solution containing fully reduced cytochrome c. The rate of cytochrome c oxidation is measured over time as a reduction in absorbance at 550 nm. The reaction is carried out at 30° C.

### REAGENTS:

1. 20 mM KCN; MW= 65.12, 13.02 mg/10 ml dH<sub>2</sub>O
2. 100 mM K-Phosphate Buffer
  - make up 0.1 M KH<sub>2</sub>PO<sub>4</sub>; MW= 136.09  
= 13.6 g/1000 ml  
(pH approx. 5)  
(rm. temp)
  - make up 0.1 M K<sub>2</sub>HPO<sub>4</sub>·3H<sub>2</sub>O; MW= 174.18  
= 17.4 g/1000 ml  
(pH approx. 8)  
(rm. temp)
  - mix in equal proportions, pH to 7.0
3. 10 mM K-Phosphate Buffer
  - dilute 0.1 M KPO<sub>4</sub> Buffer prepared above 1:10 with ddH<sub>2</sub>O (e.g. 10 ml buffer + 90 ml ddH<sub>2</sub>O)
4. Extraction Buffer (100 mM Na-K-Phosphate, 2 mM EDTA; pH 7.2)
  - 500 ml 0.1 M Na<sub>2</sub>HPO<sub>4</sub>·2H<sub>2</sub>O;  
Combine 8.9 g sodium phosphate with 0.372 g EDTA up to 500 ml.
  - 200 ml 0.1 M KH<sub>2</sub>PO<sub>4</sub>;  
Combine 2.7 g potassium phosphate with 0.149 g EDTA up to 200 ml.
  - combine both solutions and pH to 7.2
5. Test Solution (reduced cytochrome c, 2 mg/ml), for 10 ml (enough for 36 microplate wells);

- weigh out 20 mg of horse heart cytochrome c (Sigma, C-2506) in a scintillation vial
- add 1 ml of 10 mM KPO<sub>4</sub> buffer and dissolve cytochrome c
- make up a small volume of 10 mg/ml sodium dithionite-10 mM KPO<sub>4</sub> stock solution (make fresh each experiment and use within twenty minutes)
- add 40 µl of the dithionite stock solution to the test solution and observe red-orange colour change
- add 8 ml of ddH<sub>2</sub>O
- add 1 ml of 100 mM KPO<sub>4</sub> buffer.

#### PROCEDURE:

1. Place powdered muscle samples in liquid N<sub>2</sub>.
2. Add 50 µl of extraction Buffer to 1.5 ml Eppendorf tubes in the aluminium block on ice. (One Eppendorf per sample).
3. Add 5-7.5 mg tissue to each tube, recording exact tissue mass. Mix by tapping.
4. Add the volume of Extraction Buffer required to obtain a 20-fold dilution.
5. Add a stir bar and mix for 15 min. Make up Test Solution during this time and wrap in foil.
6. Sonicate each tube 3 x 3 seconds, cleaning the probe between samples.
7. Pipette some of 20-fold sample extract into new Eppendorf tube and add volume of Extraction Buffer required to obtain an 80-fold dilution. (e.g. 50 µl of 20-fold extract + 150 µl Ext. Buffer = 200 µl of 80-fold sample extract). Keep 80-fold sample extract tube on ice for duration of experiment
8. Add 270 µl of Test Solution into 4-8 wells of 96-well microplate and incubate at 30°C for 10 minutes to stabilize the temperature and absorbance.
9. Open KC4 plate reader program (on Triton). Select CONTROL icon, then PRE-HEATING tab, enter 30°C and select ON. (Do not run assay until KC4 temperature has reached 30°C.)
10. Select WIZARD icon, then READING PARAMETERS icon.
  - Select Kinetic for Reading Type.
  - Select Absorbance for Reader and 550 nm for wavelength (drop-down menu).
  - Select Sweep for Read Mode.
  - Select 96 Well Plate (default) for Plate Type.
  - Enter first and last well to be read (e.g. A1 and A4 if reading 4 samples simultaneously).
  - Select Yes and Pre-heating and enter 30 for Temperature Control.
  - For Shaking enter 0 for both intensity and duration (shaking is not necessary and it will delay the first reading).
  - Do not select either of the two options for Pre-reading.
  - Click on the KINETIC... rectangular tile to open the Kinetic window.
  - Enter run time (1 minute is recommended) and select MINIMUM for

Interval time (under these conditions the minimum Interval time should be 3 seconds).

- Select Allow Well Zoom During Read to see data in real time (optional).
- Under Scales, checkmarks should appear for both Auto check boxes. Do not select Individual Well Auto Scaling.
- Press OK to return to Reading Parameters window. Press OK to return to Wizard window. Press OK. Do not save the protocol.

11. Set the multipipette to 250  $\mu$ l and secure 4-8 yellow tips on the white projections (make sure they are on tight and all at the same height).
12. In a second, clean 96 well plate, pipette samples into 4-8 empty wells (start with A1). Recommended volumes: 30  $\mu$ l of 80-fold extract for Mixed Gastroc, 10  $\mu$ l for Heart. Adjust volumes according to oxidative capacity of the tissue. (e.g. 25  $\mu$ l for Red Gastrocnemius and 35  $\mu$ l for White Gastrocnemius).
13. Remove microplate with Test Solution in 4-8 wells from the incubator (as long as it has been incubating for 10 minutes). Place this plate beside the plate with the sample extracts in it.
14. On KC4 program, select the READ icon and press the START READING icon, then press the READ PLATE button. A box will appear that says, "Insert plate and start reading". Do not press OK yet, but move the mouse so that the cursor hovers over the OK button.
15. Using the multipipette (set to 250  $\mu$ l) carefully draw up the Test Solution. Make sure the volume is equal in all the pipette tips, and that no significant air bubbles have entered any of the tips.
16. Pipette the Test Solution into the wells with the sample extracts (the second plate). As soon as all the Test Solution has been expelled from the tips (do not wait for the second push from the multipipette), place the plate onto the tray of the plate reader and with the other hand on the mouse, press the OK button. (Speed at this point is paramount, as there is an unavoidable latency period between the time of pressing the OK button and the time of the first reading.)
17. If desired, add 5  $\mu$ l KCN to one of the wells to measure any absorbance changes in the presence of the CYTOX inhibitor.
18. Once reading is complete, hold the CTRL key on the keyboard, and use the mouse to click once on each of the squares corresponding to a well that had sample in it. Once all the desired wells have been highlighted by a black square (up to a maximum of 8 wells), let go of the CTRL key and a large graph will appear with lines on it representing each sample.

19. To obtain the rate of change of absorbance over different time periods, select Options and enter the amount of time for which you would like a rate of change of absorbance to be calculated. The graph, along with one rate (at whichever time interval is selected) for each sample can be printed on a single sheet of paper, and the results can be saved
20. The delta absorbance will appear in units of mOD/min and the number given will be negative. Convert this to OD/min by dividing by 1000 and omit the negative sign in the calculation. (e.g. if Mean V: -394.8 mOD/mn, then use 0.395 OD/min)

CALCULATION: CYTOX activity ( $\mu\text{mole}/\text{min}/\text{g}$  tissue)

$$= \frac{\text{delta absorbance}/\text{min} \times \text{total volume (ml)} \times 80 \text{ (dilution)}}{18.5 (\mu\text{mol}/\text{ml extinction coeff.)} \times \text{sample vol (ml)}}$$

$$18.5 (\mu\text{mol}/\text{ml extinction coeff.)} \times \text{sample vol (ml)}$$

Example Calculation:

30  $\mu\text{l}$  of 80-fold sample extract  
 250  $\mu\text{l}$  of Test Solution  
 Mean V: -284.2 mOD/mn

$$\text{COX activity} = \frac{(.284)(.280)(80)}{(18.5)(.030)}$$

$$= 11.5 \mu\text{mol}/\text{min}/\text{g tissue}$$

$$= 11.5 \text{ U}/\text{g tissue}$$

Tissue	Heart	Mixed Gastroc
Weight (mg)	5 mg	7.5 mg
Vol. for 20-fold	100 $\mu\text{l}$	150 $\mu\text{l}$
Remove, put in new Eppendorf	50 $\mu\text{l}$	75 $\mu\text{l}$
Vol. needed for 80-fold	Add 150 $\mu\text{l}$ of extract. buffer	Add 225 $\mu\text{l}$ of extract. buffer
Final Volume of 80-fold	200 $\mu\text{l}$	300 $\mu\text{l}$
Vol. of 80-fold per well	10 $\mu\text{l}$	30 $\mu\text{l}$

## WESTERN BLOT

### PROCEDURE: SDS POLYACRYLAMIDE GEL ELECTROPHORESIS (SDS-PAGE) PROTEAN BIO-RAD SYSTEM

#### Reagents

1. Polyacrylamide Solution  
30 % (w/v) Acrylamide  
0.8 % (w/v) Bisacrylamide  
Filter using 15 cm Whatman circular filter paper.  
Store at 4°C  
For 400 ml: Using gloves, measure out 120 g of acrylamide and 3.2 g of bisacrylamide and volume up to 400 ml with dH<sub>2</sub>O. Suction filter.
2. Under Tris Buffer  
1 M Tris-HCl pH 8.8 (60.5g / 500 ml)
3. Over Tris Buffer  
1 M Tris-HCl, pH 6.8 (12.1 g / 100 ml)  
Bromphenol Blue (for colour) Store at 4°C
4. Ammonium Persulfate (APS)  
10% (w/v) APS in ddH<sub>2</sub>O (1g/10ml)  
store at 4°C
5. Sodium Dodecyl Sulfate (SDS)  
10% (w/v) in ddH<sub>2</sub>O (1g/10ml)  
Store at room temperature.
6. TEMED (Sigma)
7. Electrophoresis Buffer pH=8.3 (10.0L)

25.0 mM Tris	30.34g
192.0 mM Glycine	144 g
0.1% (w/v) SDS	10 g
8. 6X SDS Sample Dye (10ml ; store in 1ml aliquots @-20°C)

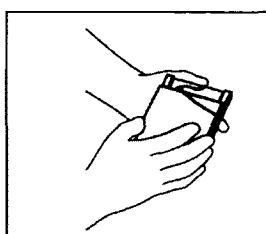
1M Tris (pH 6.8)	3ml
DTT	0.926g
Bromophenol Blue	0.06g
100 % glycerol	6ml
SDS	1.2g
dH <sub>2</sub> O	1ml

9. *tert*-Amyl alcohol, 99%

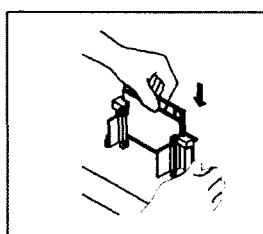
**Procedure**

1. Prepare electrophoresis rack:

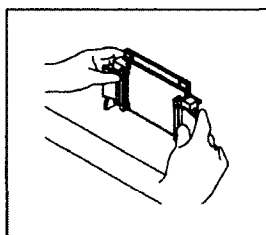
- A) Clean glass plates thoroughly with soap followed by acetone, and then distilled water.
- B) Dry carefully with paper towel without touching surface.
- C) Clean combs and glass plates
- D) Assemble glass plates as shown:



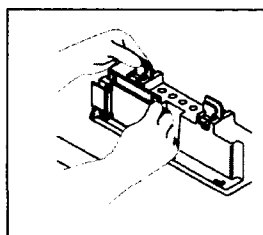
4a. Place a Short Plate on top of the Spacer Plate.



4b. Slide the two plates into the Casting Frame keeping the Short Plate facing front.



4c. Lock the pressure cam to secure the glass plates.



4d. Secure the Casting Frame in the Casting Stand by engaging the spring loaded lever.

- F) Check the seal by adding a small volume of dH<sub>2</sub>O, then pour this off and let dry.

2. Prepare Separating Gels:

A) Mini PROTEAN 3 BIO-RAD SYSTEM

	<u>8 %</u>	<u>10 %</u>	<u>12 %</u>	<u>15 %</u>	<u>18 %</u>
Acrylamide	2.7 ml	3.3 ml	4.0 ml	5.0 ml	6.0 ml
Water	4.1 ml	3.5 ml	2.8 mL	1.8 ml	0.8 ml
Under Tris	3.0 ml	3.0 ml	3.0 ml	3.0 ml	3.0 ml
SDS	100 µl	100 µl	100 µl	100 µl	100 µl
APS	100 µl	100 µl	100 µl	100 µl	100 µl
TEMED	10 µl	10 µl	10 µl	10 µl	10 µl

- B) Mix the contents of the separating gel as described in 2 without adding APS or TEMED, stir.
- C) Add APS and TEMED, stir.
- D) Slowly pour the entire volume from the beaker into the slot between the plates, keeping the plates tilted on an angle to prevent bubbles from forming.
- E) Add *tert*-Amyl alcohol to cover the top of the gel.
- F) Allow ~30 minutes for polymerization.
- G) Remove *tert*-Amyl by pouring it off quickly, and remove the remainder with a kimwipe. Rinse thoroughly with dH<sub>2</sub>O.

**Prepare stacking gel:**

A)

	<b><u>Mini Gel</u></b> (Volume/Gel)
Acrylamide	500 $\mu$ l
Above Tris buffer	625 $\mu$ l
ddH <sub>2</sub> O	3.75 ml
SDS	50 $\mu$ l
APS	50 $\mu$ l
TEMED	7.5 $\mu$ l

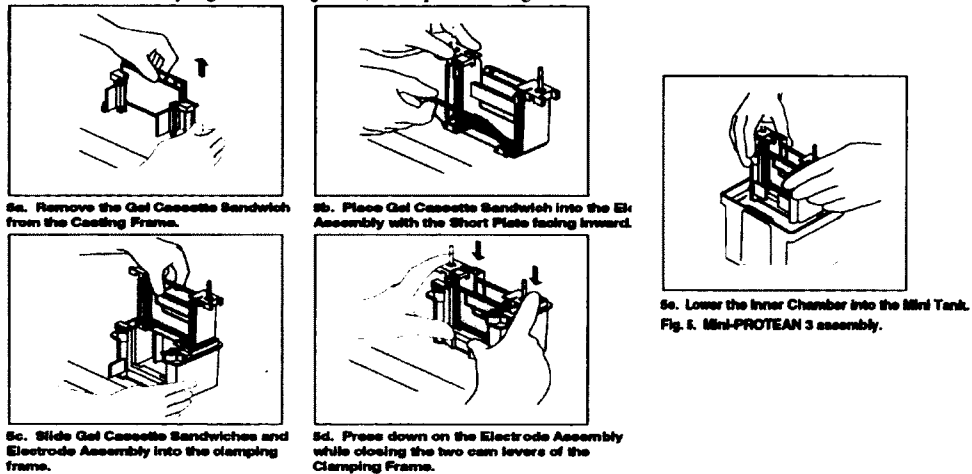
- B) Mix the contents of the stacking gel without adding APS or TEMED, stir.
- C) Add APS and TEMED, stir.
- D) Using a pasteur pipette slowly pour the entire volume from the beaker into the side of the plates.
- E) Add combs.
- F) Allow 30 minutes for polymerization.

**Prepare samples:**

- A) Turn on block heater to 95°C.
- B) Mix each sample with 6X Sample Buffer (6 volumes of sample dye to 1 vol sample).
- C) Briefly spin each sample to bring the volume to bottom of tube.
- D) Incubate each sample at 95°C for 5 minutes in a heating block to denature the proteins.
- E) Briefly spin again to bring the volume to the bottom of the tube, quick cool on ice.

## Sample Application:

Assemble Mini-protean 3 as shown:



- A) Add electrophoresis buffer ensuring that bottom of plates is well covered.
- B) Place the gel inside the chamber on bottom support of electrophoresis chamber.
- C) Clamp the gel plates to the electrophoresis chamber. If you are only running 1 gel, a rectangular plastic plate must be clamped on the side of the chamber opposite to the gel side.
- D) Remove air bubbles using a 5ml syringe.
- E) Add electrophoresis buffer in the top of the rack.
- F) Remove the comb slowly and evenly using 2 hands from both sides and fix any lanes, which have been deformed using a small spatula.
- G) With a kimwipe remove debris from the top of the plates, and clean out wells using a pipette.
- H) Withdraw the entire volume of the sample into the pipette tip. Add it slowly into the well, injecting the sample.

## Gel electrophoresis:

**\*Immediately following sample application:**

- A) Put the cover(s) on gel chamber.
- B) Turn on power supply (Indicator should be set to measure Voltage not current)  
For small gels: Use 80-120 volts
- C) When the Bromphenol Blue has run to the bottom of the gel, the run is over.  
Turn off the power supply and remove the electrodes.
- D) Remove the plates carefully from the gel and cut off a corner of the gel to

remember the gel orientation. The gel is now ready for electrotransfer of proteins.

Note: Maximum sample volume/well.

# wells	Well width	0.5 mm	0.75 mm	1.0 mm	1.5 mm
5	12.7 mm	—	70 $\mu$ l	105 $\mu$ l	160 $\mu$ l
9	5.08 mm	—	33 $\mu$ l	44 $\mu$ l	66 $\mu$ l
10	5.08 mm	22 $\mu$ l	33 $\mu$ l	44 $\mu$ l	66 $\mu$ l
15	3.35 mm	13 $\mu$ l	20 $\mu$ l	26 $\mu$ l	40 $\mu$ l

### **PROCEDURE: ELECTROTRANSFER OF PROTEIN AND IMMUNODECORATION**

#### **References:**

Towbin, H.H. et al. PNAS 76:4350, 1979.

Slater, R.J. Chapter 19-3, p.311

Electroblotter Instructions

#### **Purpose:**

- to test antibody specificity when more than one protein isoform exists
- to compare the level of specific protein isoform in a tissue extract subject to an experimental treatment

#### **General supplies required:**

- staining and destaining solution of gels (cf.SDS-gel)
- SDS-PAGE gel, unfixed and ready to transfer
- plastic gloves
- electroblotter
- Hybond nitrocellulose sheets (Amersham Life Science)
- filter paper (Mandel # S-31520)
- Ponceau S (red) stain (Sigma # P7767)
- skim milk powder
- Horse serum (Sigma H1270)
- Tween 20 (Sigma P-1379): Polyoxyethelene-Sorbitan Monolaurate
- PBS (1X)
- trays for washing filters (min volume used=50ml)
- glass plate covered with parafilm
- antisera or purified Ab
- peroxidase-coupled IgG (e.g. rabbit anti-mouse)
- saran wrap

**A. Assembly of Components for Electrotransfer (for a single gel)**

**Transfer Protocol for Biorad MiniProtean 3 System**

- 1) Make up 1L of transfer buffer and put in the fridge.
- 2) Fill western ice holder with water and freeze.
- 3) Cut 6 squares of Whatman paper (8.5 x 7.5 cm) and 1 square of nitrocellulose (8.5 x 7.5 cm).
- 4) Open the plastic sandwich BLACK side down in a casserole dish and place a scrubbie on top. Fill the dish with cold transfer buffer until you just cover the scrubbie.
- 5) Place 3-4 squares of Whatman paper wetted in transfer buffer on top of the scrubbie. Roll the stack with a test tube to make sure that it is flat.
- 6) Then place 1 square of nitrocellulose membrane wetted in transfer buffer onto the Whatman paper. Roll the membrane with a test tube.
- 7) Then take your gel and cover the membrane. Roll your gel with a test tube to ensure that there are no bubbles between the gel and the membrane.
- 8) Cover your gel with 3-4 squares of Whatman paper wetted in transfer buffer. Roll the Whatman paper with a test tube.
- 9) Cover the stack with a scrubbie soaked in transfer buffer and roll the scrubbie with a test tube.
- 10) Close the sandwich and put into the red/black holder BLACK AWAY FROM BLACK.
- 11) Add the ice block and fill the gel box with transfer buffer from the casserole dish and from the bottle.
- 12) Put the gel box into the casserole dish and put the lid on.
- 13) Transfer the gel for 1.5 hours at 120V.

**B. Nitrocellulose Sheet**

- 1) Place the membrane in dH<sub>2</sub>O water to rinse.
- 2) Lie in Ponceau stain and rotate gently for 5 minutes. Save the Ponceau for reuse.
- 3) Rinse each blot thoroughly with dH<sub>2</sub>O water to decrease the red background. If the membrane is to be cut, it should be done now while protein bands are visible.
- 4) Wash with 1X PBS (10 min) to remove more Ponceau stain (protein bands disappear now).
- 5) Incubate with rotation in 5% skim milk powder with 1.25% Horse serum in 1X PBS for 1 hour at RT. A total volume of 50ml is normally used for a regular-sized blot (9cm x 5cm).
- 6) Wash the blot in 1X PBS for 20 minutes.
- 7) Incubate with antiserum or antibody for at least 2 hours at RT, or overnight in a 4°C fridge. At RT, this incubation is done by placing the blot on a glass plate covered with stretched parafilm and applying the antibody directly to the surface. When

the incubation is carried out overnight, the antibody is applied to the glass plate and the blot is placed face down into the solution. To maintain a moist environment during an overnight incubation, wet a small Kimwipe and form it into a ball. This is placed on any corner of the plate. For both incubation procedures, the plate is covered over with a heavy object over a plastic container. A minimum of 2ml solution is used for a 9cm x 5cm blot.

- 8) Wash 2X with 1X PBS/Tween (2 x 5 min). This removes non-specific binding.
- 9) Wash 1X with 1X PBS (20 min).
- 10) Incubate with enzyme coupled 2<sup>nd</sup> antibody raised against the animal in which the antisera or antibody was produced (e.g. rabbit anti-sheep-IgG/PO). Incubate as in step 7 at RT.
- 11) Wash 2X with 1X PBS/Tween (2 x 5 min).
- 12) Wash 1X with 1X PBS (20 min).

#### **C. Staining using Enhanced Chemiluminescence Detection**

1. Mix ECL fluids 1:1 for a total volume of 2ml.
2. Apply fluid to blot and leave for 1 minute.
3. Drip off the excess and place the blot in saran wrap.
4. Develop while clipped to metal film holder (max 2 minutes).
5. Fix for 2 minutes.

#### **D. Stripping blots and re-probing**

1. Pre-heat the rotating incubator to 60°C
2. Place one previously probed membrane in a small hybridization tube with 20 mL of Stripping Solution
3. Wash in rotating incubator for 30 minutes at 60°C
4. Wash membrane 2 x 10 minutes in PBS. The membrane is now ready to be blocked and re-probed.

### **SOLUTIONS FOR WESTERN BLOT**

#### **Transfer buffer**

0.025M TrisCl, pH 8.3	(3.0285g)
0.15M Glycine	(11.26g)
20% MeOH	(200ml)

make up to 1L with ddH<sub>2</sub>O

#### **10X PBS**

320 g NaCl  
8 g KH<sub>2</sub>PO<sub>4</sub>, pH 7.4, make up to 4 liters, dilute 10X  
140 g Na<sub>2</sub>HPO<sub>4</sub> to make 1X PBS

8 g KCl

PBS/0.05% Tween

500 ul Tween/ 1 liter 1XPBS

PBS/Milk Powder (make fresh- no clumps)

for 5% (w/v) 5 g Skim milk powder with 100 ml 1X PBS

for 1% (w/v) 1 g Skim milk powder with 100 ml 1X PBS

1.25% Horse Serum in PBS

1.25 ml Horse Serum per 100 ml 1X PBS

Antibody Preparation

for dilution of 1:1000:

2 ml of 1% milk powder in 1X PBS

2  $\mu$ l antibody

(can be reused approx. 6 times); label the Ab with each use and store at 4°C

antiserum can be diluted 1:50 or 1:100 in 1% milk powder in 1X PBS

Enzyme Coupled 2nd Antibody Preparation

same dilution as primary antibody

use secondary horseradish peroxidase-coupled antibody corresponding to your primary antibody

(make fresh each day)

Stripping Solution (for 20 mL)

100  $\mu$ l of 1M NaH<sub>2</sub>PO<sub>4</sub>, pH=7.5 (0.005M)

2.8  $\mu$ l of beta-mercaptoethanol (0.002M)

4.0 ml of 10% SDS (2%)

volume up to 20 ml with distilled water

## **SUMMARY OF SIRT1 ADENOVIRAL WORK**

Infectious adenovirus is produced by transfecting recombinant adenoviral vector into AD293 cells (ATC; cat#240085), and E1 trans-complementing cell line used for the production and propagations of E1/E3 adenoviruses, using AdEasy XL Adenoviral Vector System and protocol (cal#240010). AD293 cells are considered biosafety level 2 because they contain adenoviruses. The constructed adenoviruses will also be biosafety level 2. Although they are infectious, they are replication-deficient.

### **PURPOSE OF RECOMBINANT ADENOVIRUSES:**

To study the overexpression of genes of interest in cell lines that are otherwise difficult to transfect.

### **DECONTAMINATION:**

Regular lab safety procedures are sufficient. Bleach, 70% ethanol, and autoclave will be used for decontamination, as well as after work with viruses (with spill or not).

For example, the BSC, equipment used and gloves will be wiped down with bleach. Large pipettes must be bleached overnight (in a beaker with bleach, run bleach up and down pipette first, then leave overnight to soak). Small pipette tips must be disposed in a biohazardous sharps container. All gloves must be cleaned with bleach and then disposed of in autoclave garbage.

### **MODE OF INFECTION:**

Aerosol

### **CENTRIFUGATION:**

Always spin cells in 15mL/50ml falcon with cap tightened, and use rotor aerosol tight lids.

## **IN SITU MUSCLE STIMULATION (FATIGUE ASSAY)**

Animals are anesthetized and prepared for in situ stimulation according to the following procedure:

### **A. Exposing hindlimb Muscles (for bilateral sampling of tissues):**

1. Both hindlimbs are skinned, and either the right or left leg is prepared for electrical stimulation.
2. A hole is made with forceps under the achilles tendon. This is used to start the incision for the removal of the hamstring muscles medially and laterally. Vessels are cauterized to prevent blood loss.
3. The sciatic nerve is carefully isolated to prevent irritation. It is tied off and cut proximally, leaving a nerve stump 2-3 cm long for stimulation.
4. The muscles on either side of the knee joint are cauterized before drilling a hole through the thickest part of the femur. A pin is inserted through the femur and used to stabilize the leg during stimulation.
5. A string is tied around the achilles tendon through the hole (step 2) and used to secure a pin attaching the cut achilles (and thus the gastrocnemius-plantaris-soleus muscle group) to a strain gauge. The soleus muscle can be detached from the contracting muscle group at its tendon.
6. Both limbs can be prepared in the same manner.

### **B. Stimulation:**

1. The animal is placed ventral side down in the in situ preparation with the stabilization pin positioned in a brass block, and the achilles tendon attached to the strain gauge via the metal pin.
2. Body temperature is maintained using a heating pad. Muscle temperature is maintained at 37°C with a heat lamp, and monitored with a surface thermometer (Yellow Springs Instrument Co., Inc. Ohio). The muscle belly is covered with Saran wrap over the temperature probe to prevent tissue dehydration. It is periodically squirted with 0.9% NaCl.

3. In chronically denervated muscle, general observations are made regarding the relative muscle mass of the denervated and contralateral hindlimbs, the degree to which a sheath had formed between the severed nerve ends, and the condition of the denervated foot.
4. The appropriate resting tension of the muscle is established by generating a length-tension curve. This value should approximate 150g (for a 350 g rat).
5. The voltage required to produce maximum tension can be determined with either indirect nerve stimulation or direct muscle stimulation. Muscles are stimulated directly with platinum wire electrodes inserted parallel to the long axis of muscle fibers, or indirectly by attaching the nerve to the coiled platinum electrodes being careful not to stretch it.
6. The time to peak tension and 1/2 relaxation time can be determined at high paper speeds (500 cm/sec) from single twitches, elicited using supramaximal voltage.
7. Muscle endurance performance is evaluated using continuous stimulation of the muscle over 5-15 minutes at, for example, 1 Hz stimulation frequency, using supramaximal voltage and 0.1 ms duration.
8. The leg is then wrapped in cellophane while the same stimulation procedures outlined above are carried out on the other leg.

## **NUCLEAR AND CYTOSOLIC FRACTIONATION FROM TISSUE**

### **Reagents:**

- NE-PER® Nuclear and Cytoplasmic Extraction Kit (Fisher Scientific PI78833)
  - Contains three buffers CER I, CER II and NER
- PBS (Sigma D-8537)

### **Method:**

#### **Tissue Preparation**

1. Cut 20-100mg of tissue into small pieces and place in a microcentrifuge tube.
2. Wash tissue with PBS. Centrifuge tissue at  $500 \times g$  for 5 minutes.
3. Using a pipette, carefully remove and discard the supernatant, leaving cell pellet as dry as possible.
4. Homogenize tissue using a Dounce homogenizer or a tissue grinder in the appropriate volume of CER I (Table 2). Proceed Cytoplasmic and Nuclear Protein Extraction, using the reagent volumes indicated in Table 2.

**Table 1. Reagent volumes for different packed cell volumes.**

<b>Tissue Weight (mg)</b>	<b>CER I (<math>\mu</math>l)</b>	<b>CER II (<math>\mu</math>l)</b>	<b>NER (<math>\mu</math>l)</b>
20	200	11	100
40	400	22	200
80	800	44	400
100	1,000	55	500

## **Cytoplasmic and Nuclear Protein Extraction**

**Note:** Scale this protocol depending on the cell pellet volume (Table 1). Maintain the volume ratio of CER I: CER II: NER reagents at 200:11:100  $\mu$ l, respectively.

1. Vortex the tube vigorously on the highest setting for 15 seconds to fully suspend the cell pellet. Incubate the tube on ice for 10 minutes.
2. Add ice-cold CER II to the tube.
3. Vortex the tube for 5 seconds on the highest setting. Incubate tube on ice for 1 minute.
4. Vortex the tube for 5 seconds on the highest setting. Centrifuge the tube for 10 minutes at maximum speed in a microcentrifuge ( $\sim$ 16,000 x g).
5. Immediately transfer the supernatant (cytoplasmic extract) to a clean pre-chilled pre-labelled eppendorf tube. Place this tube on ice until use or storage.
6. Wash remaining pellet (DO NOT RESUSPEND) with PBS 3X and remove PBS with a pipette after brief centrifugation to sediment the pellet.
7. Suspend the insoluble (pellet) fraction produced in Step 4, which contains nuclei, in ice-cold NER.
8. Vortex on the highest setting for 15 seconds. Place the sample on ice and continue vortexing for 15 seconds every 10 minutes, for a total of 40 minutes.
9. Centrifuge the tube at maximum speed ( $\sim$ 16,000 x g) in a microcentrifuge for 10 minutes.
10. Immediately transfer the supernatant (nuclear extract) fraction to a clean pre-chilled tube. Place on ice.
11. Store extracts at  $-80^{\circ}\text{C}$  until use.

**APPENDIX III: OTHER PROGRESS DURING PHD CANDIDACY**

## **PUBLICATIONS IN PEER-REVIEWED JOURNALS**

12. O'Leary MO, Vainshtein A, Iqbal S, **Menzies KJ**, Ostojic O, Hood DA. The effect of chronic contractile activity on young and aged skeletal muscle. 2012 March [In preparation].
11. **Menzies KJ**, Schenk S, Braga VA, Chabi B, Hood DA, Philip A and DD Guimaraes. Commentaries on Viewpoint: Does SIRT1 determine exercise-induced skeletal muscle mitochondrial biogenesis: differences between in vitro and in vivo experiments? J Appl Physiol. 112:929-930, 2012.
10. **Menzies KJ** and DA Hood. The role of SirT1 in muscle mitochondrial turnover. Mitochondrion. March 12 2011. [In Press].
9. Ljubicic V, **Menzies KJ**, Hood DA. Mitochondrial dysfunction is associated with a pro-apoptotic cellular environment in senescent cardiac muscle. Mech Ageing Dev. 131(2):79-88, February 2010.
8. Chabi B, Adihetty PJ, O'Leary MF, **Menzies KJ**, Hood DA. Relationship between SirT1 expression and mitochondrial proteins during conditions of chronic muscle use and disuse. J Appl Physiol. 107(6):1730-5, December 2009.
7. **Menzies KJ**, Robinson BH, Hood DA. Effect of thyroid hormone on mitochondrial properties and oxidative stress in cells from patients with mtDNA defects. Am J Physiol Cell Physiol. 296(2):C355-62, February 2009.
6. Chabi B, Ljubicic V, **Menzies KJ**, Huang JH, Saleem A, Hood DA. Mitochondrial function and apoptotic susceptibility in aging skeletal muscle. Aging Cell. 7(1):2-12, January 2008.

## **CHAPTERS IN BOOKS**

2. Joseph, A.-M. V. Ljubicic, **K.J. Menzies**, L. Kazak, G. Ugucconi, and D.A. Hood Mitochondrial biogenesis in health and disease-influence of stress stimuli. In: J. Magalhaes and A. Ascensao (Eds.) *Muscle Plasticity: Advances in Physiological and Biochemical Research*. Kerala: The Research Signpost / Transworld Research Network, pp. 151-171, 2009.
1. Hood, D.A., B. Chabi, **K.J. Menzies**, M. O'Leary and D. Walkinshaw. Exercise-induced mitochondrial biogenesis in skeletal muscle. In: Stocchi, V., P. DeFeo and D.A. Hood (Editors). *Role of Physical Exercise in Preventing Disease and Improving the Quality of Life*. Milan: Springer-Verlag Italia, pp. 37-60, 2007.

## **ORAL PRESENTATIONS**

8. **Menzies, K.J. (presenter)**, D.A. Hood. The role of SirT1 in muscle mitochondrial biogenesis. *Muscle Health Research Centre Colloquium Series*, Toronto, Canada, Oct. 12, 2011.
7. **Menzies, K.J. (presenter)**, Singh K and D.A. Hood. Attenuation of Mitochondrial Dysfunction in SirT1-Deficient Muscle by Resveratrol or Voluntary Running. *Canadian Society for Exercise Physiology*. Toronto, Canada, Nov. 3-6, 2010.
6. **Menzies, K.J. (presenter)** and D.A. Hood. Muscle-specific disruption of SirT1 reduces mitochondrial function and increases reactive oxygen species production. *FASEB J.* 24:987.6, 2010.
5. Hood D.A. (Presenter), Chabi B., Connor M.K., Irrcher I., Joseph A-M., Ljubicic V., Adhihetty P.J., Huang J., Saleem A., Uguccioni G., and **K.J. Menzies**. Mechanisms of mitochondrial biogenesis in muscle: effect of exercise and age. *Proceedings of the Asian Society for Mitochondrial Research and Medicine*. Tianjin, China, Nov.7-9, 2008.

## **POSTERS**

18. **Menzies, K.J.**, Singh K and D.A. Hood. SirT1 is required for the ergogenic effect of resveratrol on exercise. *Diversity matters: Variations in science*, York University, Toronto, Canada, March 9, 2012.
17. Green, A.E., **Menzies K.J.**, D.A. Hood. Thyroid hormone (T<sub>3</sub>) as a potential mediator of mitophagy in cells containing mtDNA mutations. *Ontario Exercise and Physiology Conference*, Barrie, Ontario, January 28-30, 2012.
16. Zhang, Y., M.F.N. O'Leary, **K.J. Menzies**, A. Saleem and D.A. Hood. Non-apoptotic functions of Bax and/or Bak: Role in mitochondrial protein import in skeletal muscle. *Ontario Exercise and Physiology Conference*, Barrie, Ontario, January 28-30, 2012.
15. Zhang, Y., M.F.N. O'Leary, **K.J. Menzies** and D.A. Hood. Novel role for Bax/Bak in mitochondrial protein import in skeletal muscle. *Canadian Society for Exercise Physiology*. Quebec City, Canada, Nov. 3-6, 2010.
14. **Menzies, K.J.**, Singh K and D.A. Hood. SirT1 is not required for exercise-216

induced mitochondrial biogenesis, but maintains basal organelle content and function. *FASEB J.* 25:1105.2, 2011.

13. **Menzies K.J.** and D.A. Hood. Resveratrol and Voluntary Running both Attenuate the Reduced Mitochondrial Function in Muscle-Specific SirT1-KO Animals. *Muscle Health Research Centre; Muscle Health Awareness Day, May 28, 2010.*
12. **Menzies, K.J.** and D.A. Hood. Combined effects of resveratrol and chronic contractile activity on muscle mitochondrial biogenesis. *Appl. Physiol. Nutr. Metab.* Vol. 34: 1144, 2009.
11. Ljubicic V., Adihetty P.J., Joseph A-M, Huang J.H., Saleem A, Ugucioni G, **Menzies K.J.** and David A. Hood. Plasticity of aged skeletal muscle: chronic contractile activity-induced adaptations in muscle and mitochondrial function. *FASEB J.* 22: 754.9, 2008.